Postsynaptic mechanisms of plasticity at developing mossy fiber-CA3 pyramidal cell synapses

Ho Tsz Wan

A Thesis Submitted in Partial Fulfillment of the Requirements for the Degree of Doctor of Philosophy

in

Biochemistry

The Chinese University of Hong Kong

June 2009

ProQuest LLC.
789 East Eisenhower Parkway
P.O. Box 1346
Ann Arbor, MI 48106 - 1346

Thesis/Assessment Committee

Dr. Chris McBain	(Thesis Supervisor)
Professor Shaw, Pang-Chui	(Thesis Supervisor)
Professor Wan, Chi Cheong	(Committee Member)
Professor Huang, Yu	(Committee Member)
Dr. John Isaac	(External Examiner)
Dr. Yung, Ken Kin Lam	(External Examiner)

Acknowledgements

First of all, I would like to send my gratitude to my supervisors, Dr.Chris McBain and Dr. Pang Chui Shaw for granting me the chance to work under their supervision. Chris, who has been the core scientific advisor in this thesis research, I will always be indebted to all the resources and efforts that he has put in to nurture me these 5 years. Dr. Pang Chui Shaw, who has been my supervisor for almost 8 years, his encouragement is always the positive push that endures me through these years. I would also like to send my grateful thanks to postdoctoral fellow Dr. Kenneth A. Pelkey, in co-supervising me these years. He was the one who diligently worked with me, taught me all the techniques and knowledge required to survive in this field. I will not forget the support he gave me at time when I wanted to give up. Thanks Xiaoqing Yuan for providing excellent research support on this research, as well as her motherly comfort during my difficult times. My thanks also go to other members of the McBain lab, especially Dr. Josh Lawrence, Dr. Christine Torborg, Mr. Brian Jeffreys, Dr. Michael Daw, Mr. Christian Andres Cea-Del Rio and Dr. Ludovic Tricoire. They have provided numerous support in my research and have colored my laboratory life.

I want to show my appreciation to Dr. Jean Claude Lacaille and Dr. Ronald S. Petralia, for their collaboration on this research, and for all their kind and practical comments.

My thanks also go to Dr. Queenie Vong, Dr. Leung Wai Hang, Mr. Matthew Chu, Mr. Roman Cheung, Dr. Edmund Tung, Dr. Mabel Yu, Dr. Winnie Chung, Mr. Tony Chan, Dr. Annie Chan, Ms Eva Chen, Fr. Eric de la Peña and Fr. Nick Hien Nguyen. They are the

people who have encouraged and comforted me when I feel that I am so insufficient and powerless over everything.

I would like to thank my mother, for all her care over the phone during these 5 years. I am also amazed by how independent she can be, and is proud of her for being certified as a Chinese medicine doctor during the time when I was away. My love and memories also go to my grandfather, who passed away during my stay here in the US, while I was not able to be with him at his last moments.

Thank you Lord for having me baptist on 2006. It was one of the most significant blessings for me during these 5 years. His love has carried me through all the good times and bad times.

Finally, I want to dedicate this piece of work to my father in heaven. I know he will always appreciate my hard work.

Abstract

At birth many central circuits contain mixtures of synapses in various stages of maturation making it difficult to monitor early development of receptor function in defined neuronal pathways. As a characterized central synapse that matures almost entirely postnatally, hippocampal mossy fiber (MF) to CA3 pyramid (PYR) connections initiate contact with their postsynaptic PYR targets during the first postnatal week and reach a fully mature state by the end of the third postnatal week. This late development of MF-PYR synapses provides an attractive model to probe for potential changes in receptor properties during synapse maturation. The majority of central excitatory synaptic maturation and development involves alterations in both the molecular and biophysical characteristics of postsynaptic ionotropic and metabotropic glutamate receptors often due to changes in subunit composition. For AMPA receptors (AMPARs) the GluR2 subunit dominates properties of channel permeability and mediates distinct protein-protein interactions, making it an important determinant of synaptic function and plasticity. While GluR2-containing, Ca^{2+}-impermeable AMPARs (CI-AMPARs) prevail at synapses between mature principal neurons, accumulating evidence indicates that GuR2-lacking, Ca^{2+}- permeable AMPARs (CP-AMPARs) contribute at many synapses early in development. In the first part of this thesis, I report that transmission at nascent MF-PYR synapses is mediated by a mixed population of CP- and CI-AMPARs. CP-AMPAR expression at MF-PYR synapses is transient, being limited to the first three postnatal weeks and is regulated by PICK1. Of interest, transmission via CP-AMPARs is selectively depressed during depolarization-induced long-term depression (DiLTD) of synaptic transmission. DiLTD induction and expression is postsynaptic, independent of

NMDAR activation, requires activation of L-type voltage gated Ca^{2+} channels (L-VGCCs), and is developmentally regulated. My findings indicate that the developmental profile for DiLTD expression is dictated by CP-AMPAR expression utilizing a PICK1 dependent mechanism.

The period of MF development and DiLTD expression is concomitant with a time when PYRs exhibit intense burst firing (BF) – a naturally occurring phenomenon that can lead to alteration of synaptic properties in both mature and developing hippocampal PYRs. Thus, in the second part of this thesis, I examined whether physiologically relevant phasic action potential (AP) patterns of PYR neuron activity can activate L-VGCCs and trigger DiLTD. I demonstrate that a brief period of PYR BF, produced by direct current injection or elevation of $[K^+]_o$, induces LTD that is dependent on L-VGCC activation. The NMDAR-independent BF induced LTD, just like DiLTD, is specific for developing MF-PYR synapses, is PICK1 dependent and is expressed postsynaptically.

In conclusion, the developmental window in which we observe DiLTD is dictated by the transient participation of CP-AMPARs which is regulated by PICK1 at young MF-PYR synapses. Futhermore, DiLTD can be induced by phasic L-VGCC activation driven by PYR BF suggesting the engagement of natural PYR activity patterns for synapse maturation, indicating a previously unsuspected role for PYR BF in MF-PYR synapse plasticity and development.

摘要

神經突觸在發展的各個階段，都是由不同特性的突觸及受體所組成，而在已定義的神經通路監測受體之早期發展亦有一定的難度。作為特點中央突觸， 海馬苔蘚纖維 (Mossy fiber, MF) 跟 CA3 區錐體細胞 (Pyramidal cell, PYR) 的突觸發展是完全後天的， MF-PYR 突觸形成於出生後的第一週， 並於第三週才發展完全。 這種完全後天的神經突觸發展提供了一個吸引的平台讓我們去探索早期受體潛在的變化在突觸發展中的角色。大多數的興奮性突觸的成熟和發展都涉及分子和生物物理特徵的改變， 當中包括後突觸離子型谷氨酸受體的組合變化。在谷氨酸受體（AMPARs）中， 谷氨酸受體 2 亞基 (GluR2 subunit) 在通道之滲透和介導不同蛋白質中佔主導的地位， 成為決定突觸功能和其可塑性上一項重要的條件。載有 GluR2， 鈣防滲 (Calcium impermeable, CI) - AMPARs 的 AMPARs 多出現於成熟的神經突觸，而越來越多的證據表明，缺乏 GluR2，鈣滲透 (Calcium permeable, CP) - AMPARs 對突觸的早期發展有直接的影響。在這部論文當中， 我報告了新生的 MF-PYR 突觸是由混居的 CI 和 CP - AMPARs 而介導的， CP -AMPARs 只會在出生後的首三星期表達， 並由 PICK1 蛋白所控制。 重要的是， CP-AMPARs 會在突觸之去極化長期抑壓 (Depolarization induced long-term depression, DiLTD) 中被選擇性地抑壓。 DiLTD 的表達並不需要 NMDA 受體的激活， 過程發生在後突觸， 並且需要 L 型電壓門控性鈣通道 (L-type voltage gated calcium channels, L-VGCCs) 的激活。 我的調查結果表明，CP - AMPARs 的表達跟 DiLTD 的表達時間是重疊的。

與此同時， 海馬苔蘚纖維的發育時間和 DiLTD 的表達時間， 剛好跟 CA3 PYRs 產生由動作電位(Action potential, AP) 所組成的激烈發射 (Burst firing, BF) 的時間相若， BF 是 CA3-PYRs 自然發生的現象， 其活動能令成熟和發展中的 MF-PYRs 突觸產生變化。 在這部論文中， 我亦就海馬區錐體細胞生理相關之 AP 模式能否激活 L-VGCCs， 從而表達出 DiLTD 作出研究。 我發現，錐體細胞在經歷由直接的電流注入， 或是因為提高鉀之濃度而產生之短暫 BF, 都能激活 L-VGCCs 而引發出 DiLTD 的表達。 這種同樣不需要 NMDA 受體激活的 BF-LTD， 跟 DiLTD 一樣，只能在 MF-PYR 突觸中表達， 並且同樣是由 PICK1 蛋白所控制。

總括來說，觀察 DiLTD 之表達取決於由 PICK1 蛋白所控制的 CP – AMPARs 之瞬態參與。 另一方面， DiLTD 亦可由 BF 引發之 L-VGCC 激活而產生， 研究結果顯示 CA3 PYRs 之自然活動在突觸早期發展中有重要的作用。

Table of Contents

List of Figures

List of Scientific Abbreviations

5-HT……...……serotonin

ABP……AMPAR binding protein

ACSF…….artificial cerebrospinal fluid

AMPA……..……α-amino-3-hydroxy-5methylisoxazole-4-propionic acid

AMPARs…….AMPA receptors

AP……..……action potential

AP-4…….....4-aminopyridine

BAPTA……1,2-bis(o-aminophenoxy)ethane-N,N,N',N,-tetraacetic acid

BAR…….…….. bin/amphiphysin/Rvs

BF……....burst firing

CAR……....C-terminal acidic region

CaMKII……....calcium/calmodulin-dependent protein kinase II

CaTs……..calcium transients

CV…….....coefficient Of variation

cDNA……complementary deoxyribonucleic acid

CNS…….…..central nervous system

CP-AMPARs……...calcium permeable – AMPARs

CI-AMPARs…….... calcium impermeable – AMPARs

D-APV……D-2-amino-5-phosphono-valeric acid

DCGIV…….……(2S,2'R,3'R)-2-(2',3'-dicarboxycyclopropyl)glycine

DG……..……..dentate gyrus

DiLTD……depolarization induced long term depression

DL-APV……..DL-2-amino-5-phosphono-valeric acid

EGTA……ethyleneglycol-bis-(-aminoethyl)-N,N,N',N'-tetraacetic acid

EM…….……electron microscopy

EPSC…….....excitatory postsynaptic current

GABA……..…… γ-Aminobutyric acid

$GABA_AR$……..…GABAA receptor

GCs……granule cells

GDPs……....giant depolarizing potentials

GluR..…….....glutamate receptor

GRIP…….glutamate receptor interacting protein

GYKI-53655…1-(4-aminophenyl)-4-methyl-7,8-methylenedioxy-5H-2,3-benzodiazepine

HEK……..……. Human Embryonic Kidney 293

HEPES…….……N-2-hydroxyethylpiperazine-N'-2-ethanesulfonic acid

HFS…….high frequency stimulation

HPP……..N-(4-hydroxyphenylpropanoyl)

iGluRs……..……..…ionotropic glutamate receptors

I-V……..current-voltage

KA……...…...……kainate

KARs……...……KA receptors

KCC2……K^+-Cl^- cotransporter

KO……..knock-out

L-AP4……..…… L-(+)-2-Amino-4-phosphonobutyric acid

LFS……..….low frequency stimulation

LTD……..long term depression

LTP…….long term potentiation

L-VGCCs……L-type voltage gated calcium channels

MF……..……mossy fiber

mGluR…… metabotropic GluR

mRNA……..…… messenger ribonucleic acid

NAR……...N-terminal acidic region

NGS…….normal goat serum

NKCC1…….…….…… Na^+, K^+, 2Cl- type I cotransporter

NMDA…….....N-methyl-D-aspartic acid

NMDARs……..……NMDA receptors

NR2B……..… NMDA receptor 2B

NTD……..……..N-terminal ligand binding domain

OGB-1…….……..……Oregon-Green-BAPTA-1

PDZ ….....Postsynaptic density protein-Drosophila disc large tumor suppressor- Zonula occludens-1 protein

PhTx……...philanthotoxin-433

PICK1……protein interacting with C-kinase-1

PKA…….……protein kinase A

PKC…….…….protein kinase C

PPF……..…….paired-pulse facilitation

PPR……paired-pulse ratio

PSD-95…….postsynaptic density-95

PYRs……..……pyramidal cells

QX-314……..……N-(2,6-Dimethylphenylcarbamoylmethyl)triethylammonium chloride

RI……..……..…….……rectification index

RIM1α…….…. Rab3-interacting molecule 1α

RNA……...……..ribonucleic acid

Ser…….serine

TARPs……transmembrane AMPAR-regulatory proteins

TBST……..…Triton X-100

TTX…….. tetrodotoxin

VTA……...ventral tegmental area

V_h……..holding voltage

WT……..wild type

ΔF…….……change in fluorescence

Chapter 1:

General Introduction and Background

1.1 General Background on AMPARs

1.1.1 Structure of AMPA Receptors

Ionotropic glutamate receptors (iGluRs) are found throughout the mammalian central nervous system, contributing to almost all fast excitatory synaptic transmission. Three main families of glutamate-gated ion channel can be found throughout the central nervous system (CNS): AMPA-(α-amino-3-hydroxy-5-methyl-4-isoxazole-propionic acid), kainate (KA) - and NMDA (N-methyl-D-aspartate)-receptors. Of these three, fast excitatory synaptic transmission is mediated primarily by AMPA receptors (AMPARs). AMPAR subunits exist in four varieties (GluR1-GluR4 or GluRA-GluRD) (Hollmann & Heinemann, 1994; Dingledine *et al.*, 1999). Each of them consists of an extracellular N-terminal ligand binding domain (NTD), four transmembrane domains (M1-4) (of which M2 forms a special re-entrant loop facing the cytoplasm) and an intracellular C-terminal domain (Gasic & Hollmann, 1992; Molnar *et al.*, 1994; Bennett & Dingledine, 1995) (Fig. 1.1). Functional AMPARs are tetramerically assembled as homo- or heterotetramers (Rosenmund et al., 1998), with a maximum of two subtypes present in each AMPAR receptors (AMPARs) (Ayalon & Stern-Bach, 2001; Mansour *et al.*, 2001). Their functional properties are determined by the subunit composition, as well as by the presence of non-pore-forming, auxiliary transmembrane AMPAR-regulatory proteins (TARPs) (Chen et al., 2000; Tomita et al., 2003).

1.1.2 AMPAR Posttranscriptional Modification and Receptor Kinetics

Since the cloning of the first functional ionotropic glutamate receptor in 1989 (Hollmann et al., 1989), the subsequent cloning of various ionotropic glutamate receptors rapidly followed (Bettler *et al.*, 1990; Keinanen *et al.*, 1990; Moriyoshi *et al.*, 1991; Lomeli *et al.*, 1992). Expression of heterooligomeric GluR1-4 subunits in Xenopus oocytes determined that the presence of GluR2 subunit critically regulated many biophysical properties (Boulter et al., 1990; Keinanen et al., 1990). GluR2 lacking AMPARs possess a rectifying current-voltage (I-V) relationship, while those containing GluR2 subunit possessed linear I-Vs (Hollmann *et al.*, 1991; Verdoorn *et al.*, 1991; Burnashev *et al.*, 1992a; McBain & Dingledine, 1993; Kamboj *et al.*, 1995). This effect of GluR2 subunit incorporation on AMPAR properties resulted from selective GluR2 mRNA editing at the "Q/R site" located at position 607 (Hollmann *et al.*, 1991; Sommer *et al.*, 1991; Verdoorn *et al.*, 1991; Burnashev *et al.*, 1992a; Seeburg *et al.*, 1998). During post transcriptional modification, the M2 re-entrant loop region (Fig. 1.1) changes the adenosine at position 607 within the ion channel pore, to an inosine through oxidative deamination. This modification results in a codon change from glutamine(Q) to arginine (R) (Sommer *et al.*, 1991; Higuchi *et al.*, 1993; Melcher *et al.*, 1995; Rueter *et al.*, 1995; Yang *et al.*, 1995) - a process that is 99% efficient (Burnashev et al., 1992b). The incorporation of edited GluR2 subunits into AMPARs results in a channel with a low-conductance, and importantly prevents the passage of divalent cations through the channel pore. Consequently GluR2-containing AMPARs have a relatively linear I–V relationship (Hollmann & Heinemann, 1994; Seeburg, 1996). In contrast, AMPARs lacking edited GluR2 have higher conductance, are readily Ca^{2+} permeable (CP), and

exhibit inwardly rectifying I–V relationships caused by voltage-dependent channel block by intracellular polyamines (Bowie & Mayer, 1995; Donevan & Rogawski, 1995; Kamboj *et al.*, 1995; Koh *et al.*, 1995). Interestingly, Q/R editing is not only restricted to AMPAR subunits, but is also observed in the mRNA encoding GluR5 and GluR6 subunits of kainate receptor (Sommer et al., 1991). The Q/R editing was also reported to alter the tetramerization of AMPAR assembly, where edited GluR2 subunits tend to be retained in the ER, ensuring their widespread incorporation with other unedited GluR subunits (Greger *et al.*, 2002; Greger *et al.*, 2003; Cull-Candy *et al.*, 2006). In the mature CNS the majority of AMPARs are GluR2 containing (Wenthold et al., 1996), however, increasing examples of the early expression of GluR2 lacking AMPARs have been reported at numerous immature synapses (Burnashev *et al.*, 1992a; Muller *et al.*, 1992; Aizenman *et al.*, 2002; Kumar *et al.*, 2002; Eybalin *et al.*, 2004), consistent with the low GluR2 mRNA expression observed early in development (Monyer et al., 1991; Pellegrini-Giampietro et al., 1992a). AMPAR subunits also undergo a developmentally and regionally regulated alternative splicing resulting in distinct "flip" and "flop" versions in the region preceding the predicted M4 transmembrane of the subunits (Sommer et al., 1990) (Fig.1). "Flip" versions of AMPARs desensitize 4 times more slowly than the "flop" version (Mosbacher et al., 1994; Tomita et al., 2005). Additionally, AMPARs interact with TARP family members (Tomita et al., 2003), and such interactions can specifically stabilize AMPAR expression in synapses (Chen et al., 2000; Chen et al., 2003), reduce AMPAR desensitization, increase channel conductance (Priel *et al.*, 2005; Tomita *et al.*, 2005; Kott *et al.*, 2007) and reduce polyamine block in CP-AMPARs (Soto et al., 2007).

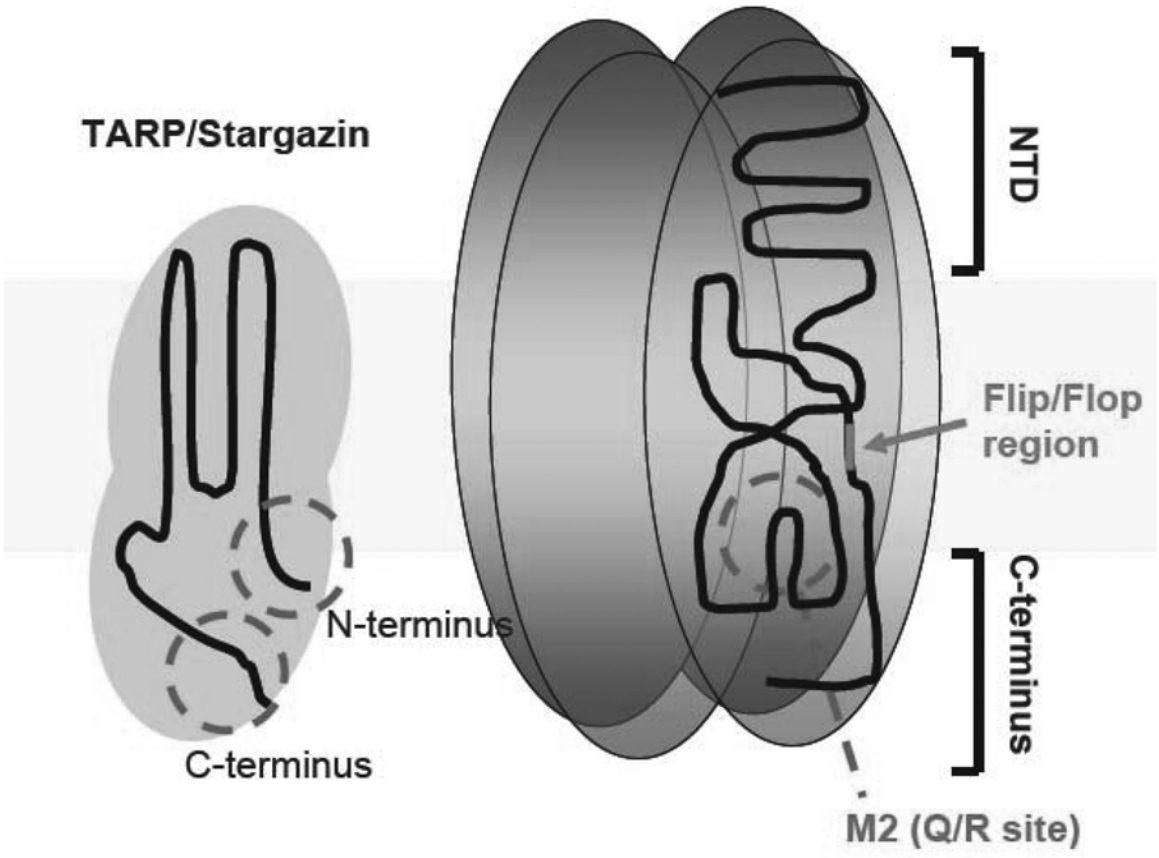

Figure 1.1 General structure of tetrameric AMPAR complex. Each AMPAR is composed of 4 transmembrane subunits (green) while each subunit consists of an extracellular N-terminal ligand binding domain (NTD) and an intracellular domain processing the C-terminal domain. Posttranscriptional modification takes place at the re-entrant loop of the M2 region (pink circle). Flip/flop region and the auxiliary subunit TARP are also shown.

(Priel *et al.*, 2005; Tomita *et al.*, 2005; Kott *et al.*, 2007) and reduce polyamine block in CP-AMPARs (Soto et al., 2007).

1.1.3 Association of PDZ Domain Containing Proteins and GluR2 Subunits of AMPA Receptors

AMPARs are responsible for the majority of fast excitatory synaptic transmission. Trafficking of receptors into and out of the synapse can result in profound changes in synaptic strength; a mechanism thought to underlie NMDAR dependent plasticity at most cortical synapses. Interactions with various trafficking proteins are required for the efficient trafficking of AMPARs. The most important of which will be discussed below.

1.1.3.1 GRIP/ABP

GRIP (glutamate receptor interacting protein) was first identified using yeast-two hybrid screening as a PDZ-domain-containing protein that can interact with the c termini of AMPARs (Dong et al., 1997). Expression of GRIP was found in olfactory bulb, cerebral cortex, hippocampus, cerebellum and spinal cord. The GRIP cDNA encodes 7 PDZ domains, however, only the forth and fifth PDZ domain were shown to interact with the c-terminus of GluR2 in yeast, where the last 7 amino acids of GluR2 c-termini is crucial for such interactions (Dong *et al.*, 1997; Burette *et al.*, 1999). Mutation in Ser880 of GluR2 c-termini eliminates the GRIP-GluR2 interaction (Dong et al., 1997). Due to the similarity between GluR2 and GluR3 c-termini tail, GluR3 can also interact with GRIP in coimmunoprecipitation experiment. Interestingly, GRIP proteins not only interact with AMPARs (Wyszynski et al., 1998). A large amount of GRIP proteins were found to be located at non-synaptic regions (Wyszynski et al., 1998). Expression of GRIP is neither enriched in the PSD as seen for other prototypical scaffolding protein, such as PSD-95 (Wyszynski et al., 1998) nor is it restricted to excitatory pyramidal cells, being found

highly expressed in the cytoplasm and proximal dendrites of non-pyramidal neurons, such as GABAergic interneurons (Wyszynski *et al.*, 1998; Burette *et al.*, 1999). In the absence of an obvious catalytic domain, GRIP was proposed to act as an adaptor or scaffolding protein to attach AMPAR to other proteins (Dong et al., 1997). GRIP1 knockout mice develop abnormalities of the dermo-epidermal junction, which results in extensive blistering, and early death due to massive blood loss, indicating an important role for GRIP in the development of dermo-epidermal junction (Bladt et al., 2002). Interestingly, ABP (AMPA receptor–binding protein) can also interact selectively with GluR2/3 c-termini tail. The cDNAs of ABP encode 5 PDZ domain fragments (PDZ2-6) with only the third, fifth and sixth domains interacting with the c termini of GluR2/3 (Srivastava & Ziff, 1999). ABP mRNA expression is found in hippocampus, striatum, thalamus, hypothalamus, cerebellum and brainstem, and unlike GRIP, it is specifically found in neuronal tissues (Srivastava & Ziff, 1999) and was found highly enriched at the postsynaptic density (PSD). ABP can either dimerize with itself, or dimerize with GRIP to form larger scaffold/aggregates, and result in redistribution into larger plaquelike aggregates (Srivastava & Ziff, 1999).

1.1.3.2 PICK1

Another protein that can interact with the c-terminal domains of GluR2/3 is the protein interacting with C kinase 1 (PICK1) protein (Wyszynski *et al.*, 1998; Dev *et al.*, 1999). PICK1 was first identified as an interacting partner with GluR2/3 in a yeast two hybrid screen (Staudinger et al., 1995). PICK1 is a PKCα binding protein, utilizing its single PDZ domain at its NH_2 terminus to interact with the COOH terminus of

PKCα (Staudinger et al., 1997). Structurally, PICK1 protein contains a PDZ domain, flanked by two acidic regions NAR and CAR. PICK1 also possess a Bin/Amphiphysin/Rvs (BAR) domain. The name Bin/Amphiphysin/Rvs comes from the closest domain homologue of amphiphysin in human (Bin3) and yeast (Rvs) (Lombardi & Riezman, 2001). BAR domain is a banana shaped α-helix dimer that can sense membrane curvature (Peter *et al.*, 2004; Dawson *et al.*, 2006). It is also a lipid binding domain serves as a molecular scaffold to bring along protein complex and AMPARs cannot be clustered in PICK1 BAR domain mutant (Jin *et al.*, 2006). The PICK1 PDZ domain binds GluR2 and GluR3 subunits at their c-termini (Xu & Xia, 2006). PICK1 is widely expressed in tissues like heart, liver, lung, spleen, kidney and muscle, especially in brain and testis where high levels of PICK1 expression can be found (Xia *et al.*, 1999; Xu & Xia, 2006). Expression of PICK1 gradually increases from embryonic day 14-15 and plateaus at postnatal 2 weeks (Xia *et al.*, 1999; Xu & Xia, 2006). The binding of PICK1 to GluR2/3 plays an important role in synaptic trafficking and targeting, in which the PICK1 BAR domain regulates surface expression of GluR2-containing AMPARs (Jin et al., 2006). Overexpression of PICK1 results in a PKC and calcium/calmodulin-dependent protein kinase II dependent increase of a polyamine sensitive AMPAR mediated current in CA1 hippocampal slices, while the surface expression of GluR2 content is significantly decreased (Terashima et al., 2004). In addition, PICK1 is a calcium sensor with its N-terminal acidic domain responsible for the binding of Ca^{2+} (Henley and Hanley, 2005). The PICK1-GluR2 interaction is bimodial and optimal in 15μM Ca^{2+} (Hanley & Henley, 2005).

1.1.4 Synaptic Receptor Trafficking Regulated by AMPA Receptor Phosphorylation and Interaction with PDZ Domain Containing Trafficking Proteins

The c-terminal cytoplasmic tail of AMPARs is the point of interaction for many trafficking proteins, with phosphorylation playing a major role in regulating these protein interactions. Phosphorylation of Ser845 by PKA and Ser831 sites by both PKC and CaMKII in the GluR1 C-terminus alters synaptic transmission (Roche *et al.*, 1996; Barria *et al.*, 1997a; Barria *et al.*, 1997b; Mammen *et al.*, 1997). Ser845 phosphorylation results in a 40% potentiation of the peak current through GluR1 homomers in whole cell patch recording (Roche et al., 1996) while phosphorylation of Ser831 also results in long term potentiation of Schaffer collateral in a mechanism thought to arise from facilitating channel conductance (Derkach et al., 1999). However, suppression of AMPAR current by the same phosphorylation in cortical pyramidal neurons through a calpain-induced proteolytic cleavage from GluR1 c-termini has also been reported (Yuen et al., 2007a; Yuen et al., 2007b). Phosphorylation of the c-termini of GluR2 subunits is also important in regulating synaptic transmission. PKC phosphorylation of Ser880 site at the GluR2 c-termini occurs both in vitro and in vivo (Dong *et al.*, 1997; Matsuda *et al.*, 1999; Chung *et al.*, 2000), which can drastically reduce the interaction between GRIP and GluR2 in HEK cells (Matsuda et al., 1999). Interestingly, stimulation induced cerebellar LTD causes phosphorylation of Ser880 site at GluR2 c-termini, leading to dissociation of GluR2-GRIP clusters. GluR2 released from GRIP can be internalized and result in cerebellar LTD (Matsuda et al., 2000), as well as hippcampal LTD, (Kim et al., 2001). Additionally, activation of PKC results in the internalization of GluR2 protein (Chung et

al., 2000; Matsuda et al., 2000), further emphasizing the importance of Ser 880 phosphorylation in LTD induction.

Since the PDZ domain containing c-termini of GluR2/GluR3 can interact with various trafficking proteins, the use of inhibitory peptides has become a popular tool for the study of the role of different trafficking proteins involved in AMPAR trafficking (Li *et al.*, 1999; Xia *et al.*, 2000; Dev *et al.*, 2004). GluR2 and GluR3 share a common cytoplasmic c-terminal sequence in their last four amino acid sequences – SVKI. These regions interact with GRIP, ABP and PICK1 (Dong *et al.*, 1997) (Srivastava *et al.*, 1998); (Wyszynski *et al.*, 1998; Dev *et al.*, 1999; Xia *et al.*, 1999). The first direct physiological evidence for the binding of GluR2/3 cytoplasmic tails to the PDZ domain containing proteins GRIP/ABP in the recruitment of AMPARs was found in the silent sensory synapses in spinal cord slices (Li et al., 1999). Serotonin (5-HT), a transmitter that can facilitate synaptic transmission between sensory afferent fibers and dorsal horn neurons, probably acts via the functional recruitment of AMPARs into the postsynaptic area, resulting in subsequent activation of silent glutamatergic synapses (Li & Zhuo, 1998). Li et al. (1998) made use of a series of synthetic peptides to mimic the last 10 amino acid of GluR2 (i.e. NVYGIESVKI; referred to subsequently as SVKI) to disrupt the corresponding GluR2-GRIP/ABP interaction. They found that following disruption of the GluR2-GRIP/ABP interaction, the original facilitating effect by 5-HT application was abolished. However, application of SVKI not only inhibits GluR2-GRIP/ABP interactions, it can inhibit all other GluR2-PDZ interactions (Li & Zhuo, 1998; Xia *et al.*, 2000; Gardner *et al.*, 2005; Liu & Cull-Candy, 2005). In contrast a peptide sequence

(KKEGYNVYGIEEVKI; referred to subsequently as EVKI) specifically disrupts the interaction between PICK1 and GluR2 (Xia *et al.*, 1999; Gardner *et al.*, 2005; Liu & Cull-Candy, 2005). This Intracellular application of EVKI was found not to abolish the enhancement of synaptic transmission by 5-HT, further highlighting the importance of GluR2-GRIP/ABP interaction for this type of synaptic plasticity. Subsequent discoveries on the importance of GluR2-PDZ protein interactions using inhibitory peptides include using inhibitory peptides SVKI and EVKI, Xia et al. (1999) found that the binding of GluR2-PICK1 is essential for the expression of cerebellar LTD in cultured Purkinje cells (Xia et al., 1999) while GluR2-PDZ interaction is essential for hippocampal LTD maintenance (Daw et al., 2000).

1.2 General Background on Hippocampal Mossy Fiber (MF) Structure and Development

1.2.1 Characteristics of Hippocampal MF Synapses

The axons of the dentate granule cells (GCs), the so-called "mossy fibers (MFs)" form the primary connection between the dentate gyrus and the CA3 hippocampus. GCs receive extrinsic input from the entorhinal cortex and relay this information to all CA3 pyramidal cells (PYRs) and inhibitory interneurons via the MF pathway. Even though PYRs also receive monosynaptic glutametergic input from the entorhinal cortex (Yeckel & Berger, 1990; Berzhanskaya *et al.*, 1998), MF-PYR synapses are a major focus of research in numerous labs because of their characteristic anatomy, physiological properties as well as their target specific expression of synaptic plasticity (Maccaferri *et al.*, 1998; Toth & McBain, 2000; McBain, 2008; Pelkey & McBain, 2008).

The MF axon was described and named after their filamentous extensive structure reminiscent of "moss" (Blackstad et al., 1970; Claiborne et al., 1986). The mossy fiber axons project to CA3 PYRs and run parallel to their cell body. At light microscopic level, they formed a clear layer which is called the "stratum lucidum". A small number of fibers also form an infrapyramidal projection into the CA3c subfield (Blackstad *et al.*, 1970; Claiborne *et al.*, 1986; Acsady *et al.*, 1998). MFs are unmylinated, and have a diameter of ~ 0.2-1μm. Each mossy fiber can give rise to 7-12 boutons into the hilus and 11-18 boutons in the CA3, where 120-150 filapodial extensions can be formed at the hilus and 40-50 of which in CA3 region (Acsady *et al.*, 1998). The large MF boutons

make contact with specialized spines or "thorny excrescences" of CA3 PYRs, while the smaller en passant terminals or filopodial extensions of the mossy fiber boutons synapse preferentially to inhibitory interneurons in the dentate hilus and stratum lucidum (Acsady et al., 1998). This anatomical specialization of MFs, suggested that MFs may also be functionally specialized, depending on their postsynaptic targets. A single CA3 dendrite contains about up to 18 thorny excrescences. Most thorny excrescences are connected to one MF bouton, however, very large thorny excrescences may contacted by multiple boutons (Chicurel & Harris, 1992; Acsady *et al.*, 1998; Gonzales *et al.*, 2001). Since mossy fiber boutons are spaced from ~160-280μm apart along the axon (Claiborne *et al.*, 1986; Acsady *et al.*, 1998) and thorny excrescences are spaced from 30-140μm along the CA3 dendrites, it is unlikely that a thorny excrescence of a given CA3 PYR will be contacted by more than one MF bouton of a single MF (Acsady *et al.*, 1998; Gonzales *et al.*, 2001). This implies that each mossy fiber axon synapses with ~10-18 CA3 PYRs and with 40-50 GABAergic interneurons at the CA3 region (Acsady et al., 1998; Henze et al., 2000; McBain, 2008) (Fig. 1.2). However, the larger numbers of mossy fiber-interneuron synapses does not necessarily mean that a net inhibition will result in the active hippocampal network (Henze et al., 2000). Each mossy fiber bouton typically has a diameter of 4-10μm and contains up to 35 individual release sites (Chicurel & Harris, 1992). The total number of release sites on postsynaptic PYRs therefore approximates 350-630 inputs, surpassing the number of interneurons that are typically innervated by MF filopodia with a single release site. However, individual release sites in the MF bouton have low release probability (0.01/site) , contrasting with the much higher release probability of MF filopodial synapse onto interneurons (0.5-0.7) (Jonas et al., 1993;

Lawrence et al., 2004). These differences in structure and synapse properties between MF-PYRs and MF-interneurons endow them with the ability to generate a variety of complex mechanisms of synaptic plasticity which will be further discussed in 1.3.3.

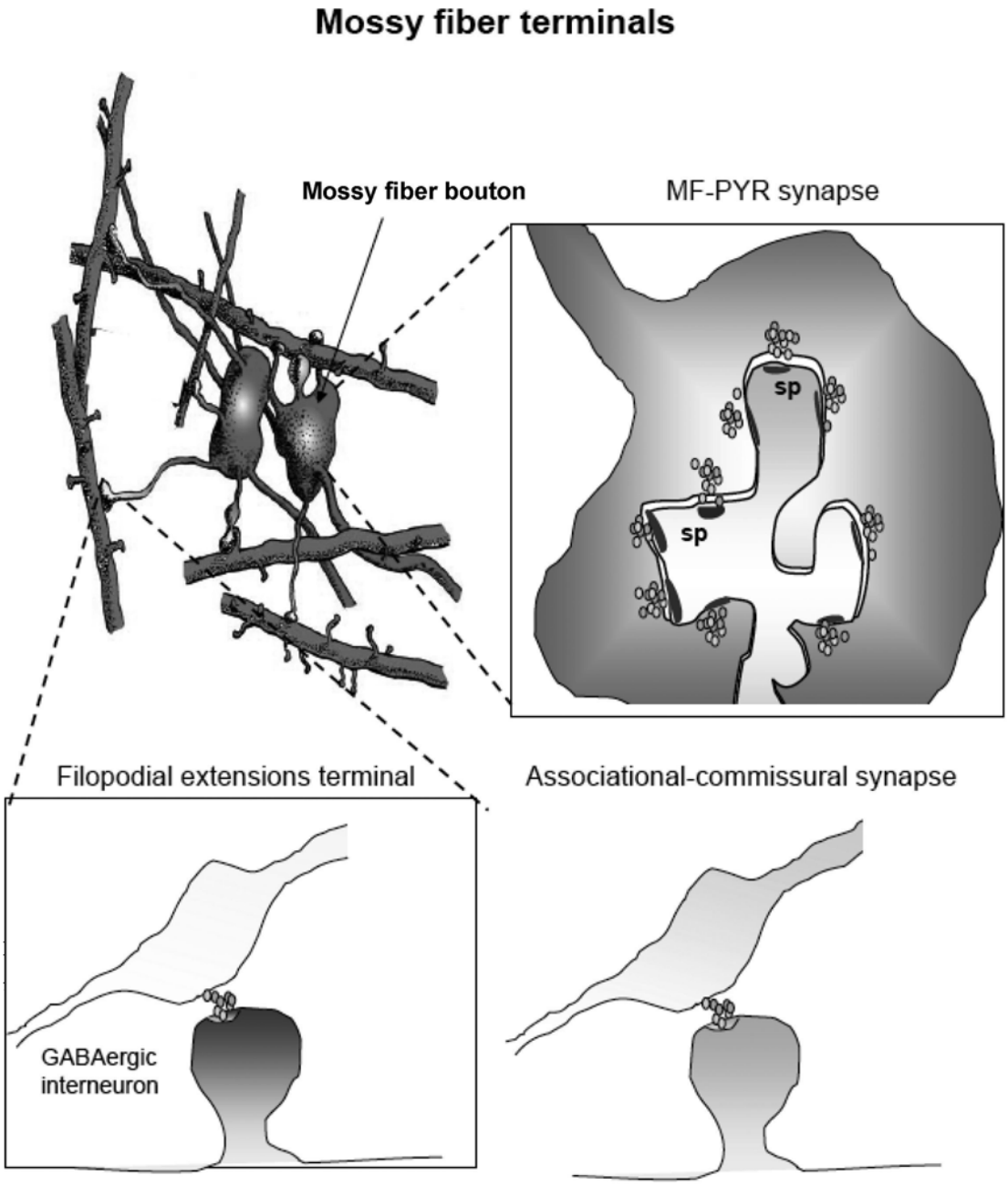

Figure 1.2 Schematic of hippocampal MF. Left upper panel shows the two types of terminals found at MF synapses (yellow: filopodial extensions; red (indicated by arrow): MF bouton). Right upper panel shows the enlarged MF bouton with multiple release sites. Lower panels show the synapse between MF and an interneuron (left), and a typical associational–commissural synapse (right lower panel).

1.2.2 Development of Hippocampal MF Synapses

The development of MF-PYR synapses was extensively studied by Amaral et al (1981) using light and electron microscopy and Golgi stained material. The expansion of the MF axon can be observed as early as day 1. However, MF-PYR synapses only start forming at postnatal day 7. Interestingly, before emergence of thorny excrescences, mossy fibers make immature synapses with the dendritic shafts of PYRs. MF-PYR synapses then start to develop at day 7, with synapses reaching maturation at day 21. This entirely postnatal development of MF-PYR synapses makes it a useful tool for the study of synapsesdevelopment (Amaral & Dent, 1981).

Another striking feature relevant to MF development is the capability for GCs to undergo postnatal or adult neurogenesis (Altman & Das, 1967; Eckenhoff & Rakic, 1988). Under thymidine-^{3}H autoradiography labeling, newly generated cells were observed below the polymorphic cell layer (the layer immediately below the granular layer) with a hundred fold increase in the number of labeled neurons 30 days after tritiated thymidine injection in newborn animals (Altman & Das, 1967). Furthermore after seizure activity, although neuronal loss was observed in other regions of the hippocampus, GCs were found to be relatively preserved (Babb et al., 1984; Obenaus et al., 1993). Though it is not known whether the resistance of GCs toward temporal lobe epilepsy is due to its capability to generate nascent granule cells, neurogenesis of GCs is found to increase after prolonged seizure activity (Parent et al., 1997). In addition, there is evidence to suggest that these newly generated GCs project their axons to their typical postsynaptic targets (Stanfield & Trice, 1988; Seki & Arai, 1993; Toni *et al.*, 2008). Seizure activity not only induces GCs

neurogenesis, it also results in aberrant MF reorganization (Tauck & Nadler, 1985; Cronin & Dudek, 1988; Sutula *et al.*, 1989; Babb *et al.*, 1991; Parent *et al.*, 1997). The phenomenon of aberrant MF reorganization after seizure activity is called "MF sprouting". During sprouting the newly generated MF synapses target other GCs, whose dendrites are in the inner molecular layer (Tauck & Nadler, 1985; Sutula, 2002; Dudek & Shao, 2004). This reorganization is believed to result in more severe seizure activity locally (Molnar & Nadler, 1999; Lynch & Sutula, 2000) and it is also suggested that MF sprouting from existing GCs may participate in promoting seizure pathology (Parent *et al.*, 1999; Henze *et al.*, 2000). However recent findings demonstrated that MF sprouting from newly generated GCs may inhibit seizure activities by synapsing with inhibitory interneurons (Buckmaster & Dudek, 1997; Kotti *et al.*, 1997; Scharfman *et al.*, 2003; Frotscher *et al.*, 2006).

1.3 Overview of iGluRs on Hippocampal MF Transmission

Glutamate is one of the major excitatory transmitter in the brain. Binding of glutamate to the glutamate receptor present in the postsynaptic cell will result in membrane depolarization. In excitatory synapses, receptors for glutamate can be classified into two major groups – iGluR and metabotropic glutamate receptor (mGluR). iGluRs are ion channels that open when the transmitter binds to a recognition receptor site, while mGluRs act indirectly on ion channels by activating typically a G-protein coupled second-messenger system. Both types of receptor activation result in excitation or inhibition depending on the type and properties of receptor and ion channel that the transmitter interact with. Thus, a single transmitter can produce several distinct effects by activating different types of receptors. As I have mentioned in section 1.1, three major types of glutamate-gated ionotropic receptors are found throughout the CNS; the AMPARs, NMDARs, and KARs. In this section, we will focus on the role of these iGluRs on basic synaptic transmission of MF-PYR synapses.

1.3.1 AMPARs

AMPAR mediate most fast excitatory synaptic transmission in the CNS (detailed receptor properties can be found in 1.1) and is activated by the natural agaonist glutamate or by AMPAR agonists. CI-AMPARs are generally believed to dominate expression at MF-PYR synapses (Jonas et al., 1993; Spruston et al., 1995; Toth et al., 2000) while AMPARs found on MF synapses onto stratium lucidium inhibitory interneurons are comprised of either CP-AMPARs or CI-AMPARs (Toth & McBain, 1998; Toth *et al.*, 2000). Interestingly, prominent short-term facilitation was found only in CI-AMPAR

containing MF-PYR synapses, while both short-term facilitation and depression was observed in MF-interneuron synapses indicating that the difference in AMPAR composition can have direct effect in synaptic plasticity among synapses.

1.3.2 NMDA Receptors (NMDARs)

NMDAR has a critical role in regulating synaptic transmission within the CNS. These receptors are heteromeric assemblies of NR1, NR2(A-D) and NR3(A&B) subunits (Moriyoshi *et al.*, 1991; Sugihara *et al.*, 1992; Hollmann & Heinemann, 1994). Functional NMDARs are typically composed of two NR1 subunits and two NR2 subtypes. Receptor properties such as the time course of decay of NMDAR mediated EPSC is highly dependent depended on the NR2 subunits present in the receptor. In recombinant systems, NR2A-containing NMDARs decay 5-6 times faster than that of NR2B or NR2C containing NMDARs (Cull-Candy *et al.*, 2001). Interestingly, during development NR2B subunits were found to be gradually replaced by NR2A during development. This ion channel is also subjected to block by extracellular Mg ions which can only be removed from the channel under depolarizing potentials. NMDARs are highly permeable to Ca^{2+} and their activation always triggers a cascade of Ca-dependent intracellular events that lead to long lasting changes and plasticities in the cell. Compared to most synapses in the CNS, MF-PYR synapses are known to contain a low density of NMDAR expression (Monaghan & Cotman, 1985; Siegel *et al.*, 1994; Watanabe *et al.*, 1998). Consistent with this observation, long term plasticity in MF-PYRs is generally believed to be NMDARs independent independent (Weisskopf *et al.*, 1994; Nicoll &

Malenka, 1995). However, recent findings have suggested that NMDARs may also be involved in a novel form of MF-PYR LTP which will be discussed in section 1.4.2.

1.3.3 Kainate Receptors (KARs)

Kainate receptors likes most glutamate receptors are tetrameric receptors assembled from GluR5-7 and KA1-2 subunits. Of particular relevance for MF physiology, KARs are expressed both pre- and postsynaptically, with the KA2 subunit being critical for proper presynaptic and postsynaptic function of KARs at MF-PYR synapses (Contractor *et al.*, 2003). KARs are not only involved in excitatory synaptic transmission at MF-PYRs (Castillo *et al.*, 1997b; Vignes & Collingridge, 1997), but also act to alter transmitter release (Chittajallu *et al.*, 1996; Kamiya & Ozawa, 2000). Activation of kainate receptors with high dose of ($\geq$200nM) agonists like kainate and glutamate depress MF transmission which is accompanied by a change in paired-pulse ratio and decreased in presynaptic Ca^{2+} influx (Chittajallu *et al.*, 1996; Contractor *et al.*, 2000; Kamiya & Ozawa, 2000). However, KARs were also found to enhance transmission at the MF-PYR synapses when KARs were activated with low doses (~50nM) of KAR agonists (Schmitz *et al.*, 2001; Breustedt & Schmitz, 2004) and GluR6 and GluR5 subunits are responsible for such enhancement (Vignes *et al.*, 1998; Bortolotto *et al.*, 1999; Contractor *et al.*, 2000; Contractor *et al.*, 2001; Breustedt & Schmitz, 2004). The GluR7 subunit was considered to have a relatively unimportant role in MF transmission (Mulle *et al.*, 1998), however, recent findings suggest that heteromeric assemblies of GluR6/GluR7 form presynaptic Ca^{2+} permeable autoreceptor at MF-PYR synapses (Pinheiro *et al.*, 2007), which can facilitate release of glutamate within a narrow time window.

1.4 Expression of Synaptic Plasticity at Hippocampal MF synapses

1.4.1 Short-Term Plasticity

MF-PYR synapses possess a form of short term plasticity that exhibits a high degree of facilitation in response to paired or repetitive stimulation (Salin *et al.*, 1996; Henze *et al.*, 2000; Toth *et al.*, 2000). Closely timed paired pulse stimulation of MF-PYR synapses triggers marked facilitation (PPF). This facilitation is > 2-3 times greater than observed at the associational/commissural synapses onto PYRs or Schaffer collateral synapses in CA1 area (Salin *et al.*, 1996; Dobrunz & Stevens, 1999). This PPF (i.e. within 50ms) is thought to result from the combination of an initial low release probability and the build up of residual Ca^{2+} following the 1^{st} pulse. This combination results in an additive effect which enhances subsequent transmitter release (Zucker, 1989; Regehr *et al.*, 1994). In addition, MF-PYR synapses demonstrate strong facilitation when they are subjected to an increased frequency of stimulation (Salin *et al.*, 1996; Toth *et al.*, 2000; Nicoll & Schmitz, 2005). Frequency facilitation results in part due to the low initial release probability of the synapses. This renders the synapse capable of showing a massive increase in transmitter release under conditions of repetitive stimulation. Salin et al. (1996) did a simple experiment to elegantly elucidate this issue. By lowering the extracellular Ca^{2+}/Mg^{2+} ratio, they were able to decrease the release probability of excitatory synapses in the CA1 region (which have synapse properties similar to that of associational/commissural synapses and are easier for field recording when release probability is low). In this case, they were able to increase the PPF to a level similar to that observed at MF-PYR synapses. However, frequency facilitation is only partially

recovered (Salin et al., 1996), indicating that other mechanisms may also be involved during frequency facilitation. This simple experiment demonstrates that the characteristic frequency facilitation of MF partially results from the initial low release probability of the fibers.

What generates this low initial release probability in MF-PYR synapses? It is generally considered that the tonic activation of Gi/o protein in the presynaptic terminal by adenosine acting on presynaptic A_1 receptors contributes to the low release probability of MF-PYR synapses (Moore *et al.*, 2003; Fedele *et al.*, 2005). A recent study by Klausnitzer et la. (2008) have confirmed this hypothesis by in vivo recording of freely moving animals injected with adenosine A1 receptor antagonist (Klausnitzer & Manahan-Vaughan, 2008).

1.4.2 Presynaptic Long Term Plasticity at MF-PYR Synapses

MF-PYR LTP is generally considered to be NMDAR independent (Weisskopf *et al.*, 1994; Nicoll & Malenka, 1995). Upon high frequency stimulation (HFS), Ca^{2+} influx through N- or P/Q- type Ca^{2+} channels, increases presynaptic Ca^{2+} which activate calcium/calmodulin dependent adenylyl cyclase. This trigger an increase in cAMP levels and activation of PKA to induce a long-lasting enhancement of transmitter release (Weisskopf *et al.*, 1994; Nicoll & Malenka, 1995; Kapur *et al.*, 1998; Tzounopoulos *et al.*, 1998). On the other hand, application of postsynaptic BAPTA prevents MF-PYR LTP (Williams & Johnston, 1989), indicating a role for postsynaptic Ca^{2+} in induction, although this remains controversial (Zalutsky & Nicoll, 1991; Castillo *et al.*, 1994; Nicoll

& Schmitz, 2005) which tend to suggest an entirely presynatpic locus for its induction and expression. MF-PYR LTP involves RIM1α, a presynaptic substrate of PKA that is essential for MF- PYR LTP, but has no effect on basal synaptic transmission, or short term plasticity at MF-PYR synapses (Castillo et al., 2002). RIM1α interacts with Rab3A, another synaptic vesicle protein that is essential for inducing MF-PYR LTP (Castillo *et al.*, 1997a). RIM1α is an effector of Rab3A which acts to scaffold active zone protein and synaptic vesicles and in turn, modulate the release of neurotransmitter (Castillo *et al.*, 1997a; Castillo *et al.*, 2002) While most common postsynaptic LTP induction mechanisms require the influx of Ca^{2+} through NMDARs, the source of Ca^{2+} for MF-LTP is determined by the type of induction protocol being used. LTP induced by brief trains of HFS require Ca^{2+} through voltage gated Ca^{2+} channels i.e. N- and P/Q- type Ca^{2+} channels (Urban & Barrionuevo, 1996; Kapur *et al.*, 1998). For MF-LTP induced by long trains of HFS, the calcium source is mainly from mGluR1 dependent increase in internal Ca^{2+} stores (Yeckel *et al.*, 1999)

MF-PYR LTP also depends on presynaptic KAR. High frequency stimulation of 10 shocks at 100Hz results in MF-PYR long term plasticity which requires GluR5 subunits activation (Bortolotto et al., 1999), however, other studies have suggested that the GluR6 subunit is the critical player in inducing KAR – dependent LTP (Contractor et al., 2001; Schmitz et al., 2003). High K^+ and strong tetani were found to rescue KAR dependent LTP in $GluR6^{-/-}$ mice via MF-PYR synapses, indicating that it is the depolarizing action of KAR, which reduces the threshold for LTP induction (Schmitz et al., 2003). Interestingly, the decrease in LTP induction threshold by the activation of KARs, may

result from the cooperative action of associational commissural (AC) synapses and MF-PYRs. High frequency stimulation of AC synapses converted subthreshold MF LTP stimuli into one capable of inducing LTP (Schmitz et al., 2003).

In contrast to MF-PYR LTP which requires HFS, MF-PYR LTD can be induced with low frequency stimulation (1Hz, 15min) (LFS) in both adult (Kobayashi et al., 1996) and juvenile (Domenici et al., 1998) animals, or in HFS (100Hz, 1s) in juvenile animals (Battistin & Cherubini, 1994; Domenici *et al.*, 1998). Similar to MF-PYR LTP, MF-PYR LTD induced by LFS has a presynaptic locus of expression (Kobayashi *et al.*, 1996; Domenici *et al.*, 1998), however, HFS MF-PYR LTD was found to also require a rise in postsynaptic Ca^{2+} (Domenici et al., 1998). LFS induced MF-PYR LTD is mediated by group II mGluR (Kobayashi et al., 1996; Yokoi et al., 1996) as well as a decrease in cAMP levels (Tzounopoulos et al., 1998). Intracellular tetanization of postsynaptic CA3 PYRs with an intracellular depolarizing pulse of 50 or 100Hz bursts also reduces either LTP or LTD, depending on the initial release probability of the synapse (Berretta et al., 1999).

1.4.3 A Postsynaptic form of Long Term Plasticity at MF-PYRs

Conventional MF-LTP requires a presynaptic rise in calcium, triggering the cAMP formation (Weisskopf *et al.*, 1994; Nicoll & Malenka, 1995; Kapur *et al.*, 1998; Tzounopoulos *et al.*, 1998). However, recent findings have suggested that MF-PYR synapses process a form of LTP that depends on the coactivation of postsynaptic NMDA and mGluR5 receptors as Ca^{2+} sources required for postsynaptically expressed plasticity

(Rebola et al., 2008). This LTP is triggered by either short trains of stimuli (24 stimuli at 25Hz) or by continued bursts (60 pulses at 50Hz) (Kwon & Castillo, 2008a). Interestingly, NMDAR dependent LTP at MF-PYRs is independent of the presynaptic protein RIM1α dependent increase in transmitter release (Castillo et al., 2002; Schoch et al., 2002), and unlike the classical MF-PYR LTP, this plasticity has an entirely postsynaptic expression locus (Kwon & Castillo, 2008a; Rebola *et al.*, 2008). Interestingly, another type of LTD, which is induced by tetanization of MF, also induced a postsynaptic form of LTD that requires a rise of postsynaptic Ca^{2+}, and this LTD was found in P6-P13 animals (Gyori et al., 1996).

Recently, a postsynaptic form of MF LTD induced entirely postsynaptically was demonstrated by Lei et al. (2003). In this study McBain and co-workers found that depolarizing CA3 PYRs of P10-17 animals from -60 to -10mV for 5 minutes can induce a totally postsynaptic form of LTD at developing MF-PYR synapses, which is NMDAR independent but AMPAR dependent, and relies on the activation of L-type voltage gated Ca^{2+} channels (L-VGCCs) (Lei *et al.*, 2003). However, the molecular mechanism involved in this form of LTD was unclear.

1.4.4 Presynaptic regulation of MF-PYR Synapse Plasticity

MFs posses a number of presynaptic G-protein coupled receptors for the regulation of synaptic transmission, which include receptor for glutamate (Manzoni *et al.*, 1995; Yoshino *et al.*, 1996), GABA (Thompson & Gahwiler, 1992), adenosine (Thompson *et al.*, 1992) and dynorphin (Weisskopf *et al.*, 1993). Members of metabotropic glutamate

receptor (mGluR) families play an important role in controlling MF-PYR transmitter release as well as synaptic plasticity. Specific mGluR subtypes are responsible for the inhibitory effect on MF transmission. The group II mGluR agonist (2 S, I'R, 2'R, 3'R)- 2-(2, 3- dicarboxycyclopropyl)glycine (DCG-IV), was found to reversibly inhibit MF-PYR transmission in rats (Yamamoto et al., 1983). Additionally, the inhibitory effect of mGluR2/3 agonist is only specific to MF evoked stimulation, but not to that of CA3 collateral or Schaffer collateral of CA1 and this has become a hallmark feature for identifying synaptic transmission mediated by MF. mGluR2 expresses at the preterminal zone of mossy fibers rather than in the synaptic junction (Yokoi *et al.*, 1996). One of the elegantly studied mechanisms involved in MF-PYR LTD is the negative feedback mechanism that can modulate synaptic transmission during high frequency activity (Scanziani *et al.*, 1997). Scanziani et al. (1997) demonstrated that either increasing the glutamate concentration or blocking glutamate uptake will delay its clearance in the synaptic cleft. The excess glutamate spreads away from the synapse and allows the activation of mGluRs, which are present on the preterminal region of MFs (Yokoi *et al.*, 1996). This mechanism links nicely to the anatomical structure and characteristic properties of MF. As pointed out earlier, MFs possess frequency dependent facilitation which renders them capable of responding to a broad range of frequencies, which coupled to the large bouton structure, facilitates the spillover of transmitter onto neighboring synapses.

mGluRs also interact work with other presynaptic receptors to regulate synaptic function of MFs. KAR activation was found to result in LTD at the layerII/III neurons in the

perirhinal cortex, which requires precise frequency requirement (Park et al., 2006). KAR mediated LTD at MF-PYR synapses results in a persistent depression of transmission at MF-PYR synapses, which can occlude the action of Group II mGluR activation and the LTD of MF-PYR synapses induced by low frequency stimulation (1Hz, 15') (Negrete-Diaz et al., 2007). This suggests that KAR mediated LTD might shares similar mechanism that leads to the same intracellular signaling cascade with that of Group II mGluR dependent LTD. As we have disuccused in 1.3.3, KAR activation by agonists at low dose will facilitate MF synaptic transmission, while activation of group II/III mGluR will have inhitory effect on synaptic transmission mediated by MF. Interestingly, recent finding suggest that presynatpic mGluR activation may surpass the facilitating effect of KAR activation at MF-PYR synapses, suggesting the dominant role of mGluRs in moderating MF-PYR synapses during negative feedback mechanism results from moderate synapse activity (Kwon & Castillo, 2008b).

Since MF also synapses with interneurons, repetitive firing also results in activation of presynaptic $GABA_B$ receptors through GABA released from neighbouring interneurons. This kind of heterosynaptic activation increases the threshold for MF-LTP induction (Vogt & Nicoll, 1999). Togther with the mGluR autoreceptor, excitatory synaptic transmission at MF-PYR synapses is further controlled by these inhibitory signals, which can be an important mechanism for information storage and segregation of the vast amount of inputs from enthorhinal cortex (Vogt & Nicoll, 1999).

1.4.5 Long Term Plasticity a MF-Interneuron Synapses

High frequency stimulation of the dentate gyrus and stratum lucidum in the presence of NMDAR antagonists results in LTP at MF-PYRs (Weisskopf *et al.*, 1994; Xiang *et al.*, 1994; Langdon *et al.*, 1995) while the same stimulation protocol results in LTD, at MF-interneuron synapses (Maccaferri et al., 1998). This phenomenon results from the target specific expression of plasticity at MF synapses. In fact, while MF-PYRs are generally considered to contain Ca^{2+}- impermeable channels (CI-AMPARs) (Jonas et al., 1993; Toth et al., 2000), AMPAR content in MF-interneuron synapses can be classified into calcium-permeable channels (CP-AMPAR) and CI-AMPAR synapses (Toth & McBain, 1998; Toth *et al.*, 2000). CP-AMPAR containing MF-interneurons process long term plasticity which is NMDAR independent, expressed presynaptically, utilizing Ca^{2+} source from CP-AMPARs (McMahon & Kauer, 1997; Toth *et al.*, 2000; Lei & McBain, 2002, 2004) and is regulated by mGluR7 to result in bi-directional plasticity (Pelkey et al., 2005), while LTD at CI-AMPAR containing MF-interneurons dependence on NMDAR activiation and expressed postsynaptically (Lei & McBain, 2002, 2004). The Ca^{2+} source for this type of plasticity is contributed by the distribution of NR2B containing NMDARs, which are present in lower numbers in CI-AMPAR containing synapses (Lei & McBain, 2002), results in faster channel kinetics and thus more Ca^{2+} efficient influx for plasticity induction.

CI-AMPARs are generally believed to dominate expression at MF-PYR synapses (Jonas et al., 1993; Spruston et al., 1995; Toth et al., 2000) while AMPARs found on MF synapses onto stratum lucidium inhibitory interneurons are comprised of either CP-

AMPARs or CI-AMPARs (Toth & McBain, 1998; Toth *et al.*, 2000). Interestingly, prominent short-term facilitation was found only in CI-AMPAR containing MF-PYR synapses, while both short-term facilitation and depression was observed in MF-interneuron synapses. However, facilitation ratios in MF-interneurons are smaller than that obtained in MF-PYR synapses (Toth et al., 2000).

1.5 Synapse Development Utilizing Network Activity in the Hippocampus

1.5.1 General Overview for Synapse Development

During synapse development, the ability of axons/synapses to reach their target and establish appropriate synaptic connections involves both chemical signaling and electrical activity (Goodman & Shatz, 1993). Before the appearance of morphologically specialized and functional synapses, developing axons searching for their targets are generally considered to be activity independent and require a chemical form of guidance from nearby tissue (Sperry, 1963; Walter *et al.*, 1987; Dodd & Jessell, 1988; Fraser & Perkel, 1990). Those molecular cues include a number of extracellular matrix glycoproteins, with laminin being the most effective and precise molecule in promoting axon extension in developing central and peripheral axons (Rogers *et al.*, 1983; Bronner-Fraser, 1986; Dodd & Jessell, 1988; Mackie *et al.*, 1988). Diffusible chemotropic factors released by cells of the target region are also important for axon attraction and repulsion (Letourneau, 1978; Gundersen & Barrett, 1979, 1980; Lumsden & Davies, 1983; Tessier-Lavigne *et al.*, 1988). Indeed the response of growth cones was found to increase with the chemical gradient of the molecular cues (Baier & Bonhoeffer, 1992) and their routing is ultimately determined by the balance between attractive and repelling forces created by the concentration and types of cue present in the environment (Gierer, 1983).

Even though the path finding processes of growth cones are generally believed to be activity independent, several studies have shown that electrical activity is also important for this process (Wiesel & Hubel, 1974; Cohan, 1990; Fields *et al.*, 1990; Chapman &

Stryker, 1992; Ming *et al.*, 2001). Electrical activity alters the axonal navigation process by the release of transmitter (Haydon *et al.*, 1984; Xie & Poo, 1986), or by converting a repulsive cue into an attractive one (Ming et al., 2001). For example, neural muscle contact results in the release of neurotransmitter acetylcholine at growth cones, which then triggers an inward current (Xie & Poo, 1986). All these experiments show that electrical activity can actually participate in the process of axon guidance, however, guidance from molecular cues still have a dominant role in the navigation of early growth cone development (Garyantes & Regehr, 1992). Even though the requirement for electrical activity may not be a crucial factor in growth cone path finding process, it is important for the precise connections between individual neurons and their postsynaptic targets for the completion of the circuitry. After the formation of functional synapses, refinement and wiring are required in order to form a functional circuit. Using the visual system as an example, in order to resolve a visual image, a fine topographic map has to be formed after the retinal ganglion cells send their axons to the optic tectum or visual thalamus. This process requires electrical activity as was indicated by the inability of fine mapping formation after the injection of TTX (Riccio & Matthews, 1985; Schmidt, 1985b, a; Chapman & Stryker, 1993), however, column formation resumed once TTX application stopped (Meyer, 1982). All these experiments demonstrate the importance of electrical activity in synapse refinement.

1.5.2 Synchronous Bursting Activity in Early Hippocampal Network Development

Hippocampal CA3 PYRs are able to generate repetitive bursts of APs such as giant depolarizing potentials (GDPs), and synchronous AP burst firing (BF). Giant

depolarizing potentials are a developmental phenomenon consisting of recurrent membrane depolarization with fast APs, separated by intervals of relative inactivity (Ben-Ari et al., 1989). GDPs result from the depolarizing action of GABA early in development (Cherubini *et al.*, 1991; Bolea *et al.*, 1999), which is due to the developmental expression of 2 types of Cl^- co-transporter – the NKCC1 and KCC2 (Rivera *et al.*, 1999; Yamada *et al.*, 2004; Sipila *et al.*, 2005). NKCC1 is highly expressed in immature CA3 PYRs, and serve to increase the intracellular $C1^-$ concentration (Staley et al., 1996), so that activation of $GABA_A$ receptors results in an outward flux of Cl^- triggering a depolarization. Since intracellular Cl^- concentration at immature CA3 PYRs is high (due to the action of NKCC1), activation of $GABA_A$ receptors depolarizes the membrane through an outward flux of Cl^-. In fact, generation of GDPs also involve the action of AMPARs, as the release of GABA is triggered by glutamate acting on AMPAR from recurrent collaterals (Bolea *et al.*, 1999). However, as the expression of KCC2 increases at the end of postnatal 2 weeks (Rivera et al., 1999), intracellular $C1^-$ concentrations become lower, resulting in a net inward flux of Cl^- upon $GABA_A$ receptor activation. At that time, the inhibitory hyperpolarizing action of $GABA_A$ receptors results in a cessation of GDP activity.

In contrast to GDPs, CA3 PYRs demonstrate AP burst firing (BF) that can be observed throughout development; becoming more intense during the second and third postnatal weeks (Swann *et al.*, 1993; Smith *et al.*, 1995). Typical spontaneous bursting events consist of rapid sequences of action potentials (APs) riding on a slow 5-15mV depolarizations that last for 20-100ms (Kandel *et al.*, 1960; Wong & Prince, 1978).

Furthermore, bursting in one neuron can initiate synchronized population bursts in the hippocampal network (Miles & Wong, 1983). Importantly, generation of synchronous BF can result from both the intrinsic properties of individual CA3 PYRs or by synaptic input between the recurrent collaterals, as well as inhibition of GABAergic inputs that may help magnifying the existing recurrent inputs (Traub & Wong, 1982; Miles & Wong, 1983; Prince & Connors, 1986; Yaari *et al.*, 1986). Interestingly, not all PYRs generate bursting activity (Bilkey & Schwartzkroin, 1990; Hemond *et al.*, 2008), cells in CA3a and CA3b subfields burst more frequently than those of CA3c. In addition cells closer to stratum pyramidale (compared to those closes to stratum oriens) typically are more prone to burst firing in response to intracellular injection of depolarizing current pulses (Bilkey & Schwartzkroin, 1990).

1.5.3 Induction of Long Term Plasticity by Synchronous Bursting Behavior

Previous studies have reported that PYR network bursts can induce long-lasting plastic changes within the CA3 recurrent network. This plasticity is dependent on NMDAR activation (Ben-Ari & Gho, 1988; Schneiderman *et al.*, 1994; Bains *et al.*, 1999). Induction of synchronized bursts in vitro can be achieved by exposing hippocampal slices to either $GABA_A$ antagonists (Schwartzkroin & Prince, 1977; Wong & Traub, 1983; Schneiderman *et al.*, 1994; Stoop *et al.*, 2003) or by elevation of extracellular potassium (Traynelis & Dingledine, 1988; McBain & Dingledine, 1993; Aradi & Maccaferri, 2004). Application of elevated $[K^+]_o$ for 15-30' results in a persistent potentiation of EPSPs at CA3 PYRs (Bains et al., 1999). Additonally, application of a $GABA_A$ antagonist induced synchronized discharges resulting in an NMDAR- and mGluR5- dependent form of

plasticity at collateral fibers in mature animals, while no significant change was observed at MF-PYR synapses (Stoop et al., 2003). However, network bursting induced by stimulating the axons of perforant path, together with disinhibition induces persistent depression at perforant path EPSPs in juvenile animals (Smith & Swann, 1999), indicate that immature synapses may undergo different synaptic modification, compare to mature synapses.

1.6 Concluding Remarks

MF synapses made by dentate gyrus granule cell axons convey the major extrinsic input from neocortex to hippocampal CA3 PYRs. The characteristic anatomical structure and properties endow them with unique mechanism of synaptic plasticity compared to other synapses present in the CNS. Additionally, the postnatal maturation of this synapse provides an attractive model to probe for receptor changes during synapse development and plasticity in a defined central pathway. The GluR2 subunit dictates several AMPAR biophysical properties and interacts with various molecules implicated in receptor trafficking. Its c-terminal tail interacts with various trafficking proteins like GRIP and PICK1, leading to changes in synaptic plasticity and Ca^{2+} permeability as a result of changes in receptor subunit composition. Thus, the presence or absence of the GluR2 subunit can greatly influence AMPARs and, hence, synaptic function. Classically long-term plasticity at MF-PYR synapses is considered to involve alterations in presynaptic release via cAMP/PKA-dependent signaling cascades, and is further regulated by presynaptic G-protien coupled receptors like mGluR and $GABA_BR$. However, as demonstrated by Lei et al. (2003) and Kwon et al. (2008), MF-PYR synapses also possess some forms of long term plasticities that involve a totally postsynaptic mechanism. While the postsynaptically expressed form of LTP is NMDAR dependent, the expression of DiLTD is AMPAR dependent. However, molecular mechanism involved in DiLTD is poorly understood and it is of great interest to address the question of how CP- and CIs AMPAR participate in this form of plasticity.

1.7 Specific Objectives of the Thesis

The investigation documented in this thesis will focus on how CP-AMPARs contribute to the development of MF-PYR synapses and whether the late development of MF-PYR synapses can be fulfilled by naturally occurring activity. Major objectives for my Ph.D. dissertation are:

1. The existing literature suggests that excitatory synapses undergo developmental alterations in both the molecular and biophysical characteristics. These changes often involve alterations in postsynaptic ionotropic glutamate receptor function due to changes in AMPA/NMDA subunit composition. While GluR2- containing CI-AMPARs prevail at synapses between mature principal neurons, accumulating evidence indicates that GluR2-lacking CP-AMPARs can contribute at many excitatory synapses early in development. In the first study of this thesis, the focus of research will be on whether CP-AMPARs contribute to the development of MF-PYR synaptic transmission. Additionally, we have previously identified an entirely postsynaptic form of plasticity – DiLTD. DiLTD is developmentally regulated, AMPAR dependent and requires the activation of L-type voltage gated Ca^{2+} channels (L-VGCCs). We will investigate the role of AMPAR in this developmentally regulated form of long term plasticity.

2. Synaptic network formation and refinement are highly activity-dependent which utilize spontaneous action potential activity for the establishment and maturation of synaptic connections. PYRs exhibit intense BF early in development,

concomitant with the period of MF development, as well as the period of depolarization induced LTD (DiLTD) competance. Whether developing MF-PYR synapses utilize the intense BF activity of PYRs to promote MF synapse maturation remains unknown. Since DiLTD is driven by the activation of L-VGCCs, the aim of this investigation will be to determine whether these physiologically relevant phasic AP patterns of PYR neuron activity activate L-VGCCs to trigger DiLTD. Phasic AP patterns will be induced by injecting depolarizing current pulses, as well as using elevation of $[K^+]_o$.

Chapter 2

Developmental expression of Ca^{2+}-permeable AMPA receptors underlies depolarization-induced long-term depression at mossy fiber CA3 pyramid synapses.

2.1 Introduction

The GluR2 subunit dictates several AMPAR biophysical properties and interacts with various molecules implicated in receptor trafficking (Dingledine *et al.*, 1999; Collingridge *et al.*, 2004; Isaac *et al.*, 2007). Typically GluR2 mRNA undergoes efficient editing at the "Q/R site" (Hollmann *et al.*, 1991; Sommer *et al.*, 1991; Verdoorn *et al.*, 1991; Burnashev *et al.*, 1992a; Seeburg *et al.*, 1998) and incorporation of these edited subunits into AMPARs results in low-conductance, CI-AMPARs with relatively linear current voltage (I–V) relationships. In contrast, AMPARs lacking edited GluR2 have higher conductance, are readily CP-AMPARs, and exhibit inwardly rectifying I–V relationships caused by voltage-dependent channel block by intracellular polyamines (Bowie & Mayer, 1995; Donevan & Rogawski, 1995; Kamboj *et al.*, 1995; Koh *et al.*, 1995). Thus, the presence or absence of GluR2 greatly influences AMPAR and, hence, synaptic function.

The ubiquitous expression and efficient editing of GluR2 within principal neurons ensures that CI-AMPARs dominate transmission between excitatory neurons throughout the nervous system. However, recent findings indicate GluR2-lacking, CP-AMPARs are assembled in principal neurons and become synaptically incorporated under certain conditions (Aizenman *et al.*, 2002; Kumar *et al.*, 2002; Eybalin *et al.*, 2004; Ju *et al.*, 2004; Terashima *et al.*, 2004; Bagal *et al.*, 2005; Harms *et al.*, 2005; Ogoshi *et al.*, 2005; Shin *et al.*, 2005; Thiagarajan *et al.*, 2005; Clem & Barth, 2006; Plant *et al.*, 2006; Sutton *et al.*, 2006). One compelling line of evidence suggests that CP-AMPARs are transiently

expressed by principal neurons early in development. For example, synaptic CP-AMPARs occur in layer 5 pyramids until postnatal day 16 after which CI-AMPARs dominate transmission (Kumar et al., 2002). Similar developmental switches happen at inner hair cell synapses (Eybalin et al., 2004), Xenopus retinotectal synapses (Aizenman et al., 2002), and chicken forebrain synapses ((Migues et al., 2007). Moreover, developmental increases in the ratio of GluR2 to other AMPAR subunits occur throughout the CNS (Pellegrini-Giampietro et al., 1992b; Pickard et al., 2000; Zhu et al., 2000). Such transient CP-AMPAR expression could provide a potentially important route for Ca^2 entry during synapse maturation and impart distinct short/long-term plastic properties to developing networks (Rozov & Burnashev, 1999; Liu & Cull-Candy, 2000).

In the hippocampus, MF–PYR connections mature entirely postnatally providing an attractive model to probe for AMPAR changes during synapse development in a defined central pathway (Amaral & Dent, 1981; Henze *et al.*, 2000). Moreover, MF–PYR synapses constitutively insert overexpressed GluR1 homomers in contrast to synapses between PYRs in which such recombinant CP-AMPARs are excluded unless driven by CaMKII (calcium/calmodulin-dependent protein kinase II) (Kakegawa et al., 2004), suggesting that MF–PYR synapses are inherently permissive sites for CP-AMPARs. Hence, in the current study we investigated whether native CP-AMPARs contribute to basal transmission and synaptic plasticity at developing MF–PYR synapses.

2.2 Materials and Methods

2.2.1 Hippocampal Slice Preparation

Slices were prepared as previously described (Gardner et al., 2005; Pelkey et al., 2005; Topolnik et al., 2005) using P10-30 Sprague-Dawley rats or C57BL/6 mice as indicated throughout the manuscript, except for experiments involving transgenic animals which were created on a hybrid genetic background of 129/Svj and C57BL/6 strains (Gardner et al., 2005). Briefly, animals were anesthetized with isoflurane and decapitated allowing for removal of the brain into ice-cold saline solution containing (in mM): 130 NaCl, 24 $NaHCO_3$, 3.5 KCl, 1.25 NaH_2PO_4, 0.5 $CaCl_2$, 5.0 $MgCl_2$ (or $MgSO_4$), and 10 glucose, saturated with 95% O_2 and 5% CO_2 (pH 7.4). In some cases NaCl was substituted with sucrose (250 mM). After decapitation, skull was cut open with scissors while tissue and meningeal connections were removed with the help of forceps in a petri dish filled with ice-cold saline; the whole brain was then removed and transfered to another ice-cold saline filled petri dish. A piece of filter paper was placed inside the petri dish to avoid sliding of brain tissue while dissecting. Keep bubbling the saline solution in the petri dish with carbogen. Cerebellum was removed first before making a saggital cutting through the corpus callosum to separate the two hemispheres. Move one hemisphere aside, while placing the remaining hemisphere with its sagittal plane down and the temporal surface up. Getting ready for the buffer tray of the slicer by putting thin cyanoacrylate glue (K&R International diamond Bar, CA) of about 0.5 cm in diameter, then cut away around 2/5 dorsal part of the brain and right after this, flipped the scalpel quickly so the cut surface of the hemisphere lay on the scalpel. Use a spatulum to push the hemisphere slightly onto

the glued surface of the buffer tray. The hemisphere was placed into ice-cold saline inside the buffer tray, and was ready for slicing immediately. From decapitation to the time when the brain hemisphere was placed on the buffer tray for slicing, it should not take more than 5-8 minutes to gurantee the healthiness of the CA3 neurons. Individual hemispheres were sliced with a VT-1000S vibratome (Leica Microsystems, Bannockburn, IL) and sectioned to yield transverse hippocampal slices (300 μm) which were incubated in the above solution at 35°C for recovery until use (minimum 1 hour recovery). All animal procedures conformed to the National Institutes of Health and Université de Montréal animal welfare guidelines.

2.2.2 Whole-Cell Recordings

Individual slices were transferred to a recording chamber and perfused (2-3 ml/min) with extracellular solution (in mM): 130 NaCl, 24 $NaHCO_3$, 3.5 KCl, 1.25 NaH_2PO_4, 2.5 $CaCl_2$, 1.5 $MgCl_2$ (or $MgSO_4$), 10 glucose, 0.0025 bicuculline methobromide, and 0.05-0.100 DL-AP5, saturated with 95% O_2 and 5% CO_2 (pH 7.4, 32-35°C). Whole-cell patch-clamp recordings using a multiclamp 700A or Axopatch 200B amplifiers (Axon Instruments, Foster City, CA) in voltage-clamp mode (V_h=-60 mV) were made from individual CA3 pyramidal neurons, visually identified with infrared video microscopy and differential interference contrast optics. For Ca^{2+} imaging recordings electrodes (4-5 MΩ) pulled from borosilicate glass (World Precision Instruments) were filled with ICS composed of (in mM): 130 $CsMeSO_3$, 5 CsCl, 2 $MgCl_2$, 5 diNa-phosphocreatine, 10 HEPES, 2 ATP_2Na, 0.4 GTPNa, 0.1 spermine, 1 QX314 and 0.05 Oregon green-488-BAPTA-I- hexapotassium salt (OGB1, Molecular Probes, Eugene, OR, USA), pH 7.2–

7.3, 275-285 mOsm. For all other recordings electrodes were filled with ICS of the following composition (in mM): 100 Cs-gluconate, 5 CsCl; 0.6 EGTA, 5 $MgCl_2$, 8 NaCl, 2 Na_2ATP, 0.3 NaGTP, 40 HEPES, 1 QX-314 and 0.1 spermine (pH 7.2-7.3, 290-300 mOsm). In experiments where reagents were delivered postsynaptically through the recording pipette I waited a minimum of 15 minutes after establishing the whole-cell configuration before any attempt was made to induce plasticity to ensure adequate diffusion of reagents into proximal dendritic compartments. The sequences and generation of the EVKI and SKGA peptides have previously been described (Gardner et al., 2005). These peptides (200 μM), were applied together with a peptidase inhibitor cocktail containing leupeptin, bestatin, and pepstatin (all at 0.1 mM) to prevent degradation. Uncompensated series resistance (8-15 MΩ) was rigorously monitored by the delivery of small voltage steps at regular intervals and recordings were discontinued following changes of >15%. Synaptic responses were typically evoked at 0.33Hz by low-intensity microstimulation (100 μsec duration; 20-40 μA intensity) via a constant-current isolation unit (A360, World Precision Instruments, Sarasota, FL) connected to a patch electrode filled with oxygenated extracellular solution. For MF-PYR synaptic recordings the stimulating electrode was placed in either the dentate gyrus or stratum lucidum. Except in Ca^{2+} imaging recordings, MF-origin of EPSCs was always confirmed by perfusion of slices with the group II mGluR agonist DCGIV (1 μM) (Kamiya et al., 1996). For PYR collateral fiber stimulation the stimulating electrode was placed in CA3 stratum radiatum and evoked events did not exhibit DCGIV sensitivity. MF-PYR DiLTD was induced by depolarizing the postsynaptic CA3 PYR from -60mV to -10mV for 5 minutes

in the absence of stimulation (Lei et al., 2003). Data for I-V curves was obtained by varying the postsynaptic membrane potential between -60 and +40 mV in steps of 20 mV.

2.2.3 Data Analysis

For each recording EPSC amplitudes from individual sweeps were measured during a 1-2 ms window around the peak of the waveform. Then for incorporation into group data the EPSC amplitudes for a given recording were binned in 1 minute running averages and normalized to the mean amplitude obtained during the base-line period (first 3-10 min). Data are presented as means ± SEMs, with paired or unpaired t-tests used to assess statistical significance as appropriate. For some recordings paired-pulse ratios (PPRs) were obtained by calculating mean P2/mean P1, where P1 represents the amplitude of the first evoked current and P2 the amplitude of the second for 20 consecutive individual traces. For I-V relations a minimum of 5 events were averaged for each holding potential. To determine RIs, the negative portion of individual I-V relations (between V_h=-60 and 0 mV) was fit by a linear regression and then RI was calculated as the ratio of the actual current amplitude observed at +40 mV to the predicted linear value at +40mV. Alternatively, in experiments where the RI was monitored before and after DiLTD, RI was determined as the absolute value of the ratio of the mean current amplitude at +40mV to the mean current amplitude at -60 mV (RIEPSC+40/EPSC-60).

2.2.4 Ca^{2+}-imaging of Thorny Excrescences

After obtaining the whole cell configuration, 20-30 min were allowed for intracellular diffusion of the fluorophore. Imaging was performed using a two-photon laser scanning

microscope LSM 510 (Carl Zeiss, Kirkland, QC) based on a mode-locked Ti:Sapphire laser operating at 800 nm, 76-MHz pulse repeat, < 200 fsec pulse width and pumped by a solid state source (Mira 900 and 5W Verdi argon ion laser, Coherent, Santa Clara, CA). A long-range water-immersion objective (40×, NA 0.8) was used. Fluorescence was detected through a long-pass filter (cut-off 680 nm) in non-descanned detection mode and images were acquired using the LSM 510 software (Carl Zeiss, Kirkland, QC). Ca^{2+} transients (average of 4 responses) evoked by local electrical stimulation were measured at 20-40 μm from the soma by scanning a line through the thorny excrescence. Changes in fluorescence were calculated relative to the baseline and expressed as $\%\Delta F/F = [(F - F_{rest})/F_{rest}] \times 100$. Summary data are expressed as mean ± SE. Statistical significance between groups was determined using a two-tailed Student's t -tests.

2.2.5 Immunogold Electron Microscopy

Immunogold studies were done as described previously (Petralia *et al.*, 1999; Petralia & Wenthold, 1999; Rouach *et al.*, 2005). Briefly, mice were perfused with 4% paraformaldehyde + 0.5% glutaraldehyde and sections were frozen in liquid propane in a Leica CPC and freeze-substituted into Lowicryl HM-20 in a Leica AFS. Ultrathin sections were incubated in 0.1% sodium borohydride plus 50 mM glycine in Trisbuffered saline plus 0.1% Triton X-100 (TBST), then in 10% normal goat serum (NGS) in TBST, then in primary antibody in 1% NGS/TBST, followed by immunogold in 1% NGS/TBST/0.5% polyethylene glycol (20K MW), and then stained with uranyl acetate and lead citrate. Figures were processed with Adobe Photoshop with minimal use of levels, brightness and contrast employed uniformly over the images. Double immunogold

labeling used a rabbit polyclonal antibody to GluR1 (Petralia & Wenthold, 1992) with 5 nm immunogold, and a mouse monoclonal antibody to GluR2 (Steinberg et al., 2006) with 15 nm immunogold. Micrographs were taken in the CA3 stratum lucidum at 20,000x for identification of mossy terminal/spine associations and at 40,000x for quantitative analysis. Mossy fiber terminals were identified as large, irregular structures with many round synaptic vesicles contacting complex spines (thorny excrescences) originating from CA3 PYR apical dendrites. Identification and characterization of these structures have been described in great detail (Petralia & Wenthold, 1992; Darstein *et al.*, 2003). Gold particles in both the synaptic cleft and postsynaptic density were considered membrane associated and synaptic. At extrasynaptic sites of spine profile membranes, only gold particles within 20 nm of the membrane were considered membrane associated [based on the resolution of the immunogold method (Rouach et al., 2005) and the total surface labeling by combining the synaptic and extrasynaptic counts on each spine profile was then examined. Then, for each spine profile, synapses in which 5 nm gold labeling for GluR1 was >100 nm from any 15 nm gold particle ("5 nm only") to those in which 5 and 15 nm gold particles were <100 nm apart ("5 + 15 nm") was compared. The former group was intended to represent synaptic AMPA receptors that were more likely to lack GluR2 than the latter group; 100 nm was selected arbitrarily for the sake of comparison between the wild-type and mutant mice. Immunogold labeling is expected only to represent some fraction of total receptor labeling (Petralia et al., 1999)

2.3 Results

2.3.1 Transient Expression of CP-AMPARs at Developing MF–PYR Synapses

AMPARs lacking edited GluR2 subunits exhibit pronounced inward rectificaiton caused by voltage-dependent block of the channel pore by intracellular polyamines, providing a convenient electrophysiological signature to assess the contribution of CP-AMPARs to synaptic transmission (Bowie & Mayer, 1995; Donevan & Rogawski, 1995; Kamboj *et al.*, 1995; Koh *et al.*, 1995). Thus, to initially probe for the presence of CP-AMPARs at developing MF–PYR synapses, I-V relationships of pharmacologically isolated (50–100 μM DL-APV) AMPAR-mediated MF–PYR EPSCs in slices from young (P10–P17) mice was examined. At this stage of development, using an intracellular recording solution (ICS) supplemented with the polyamine spermine (100 μM), significant rectification in MF–PYR EPSC I–V relationships (Fig. 2.1A, top panel) was consistently observed. The degree of rectification for each recording was quantified by calculating the ratio of the actual EPSC value observed at a holding potential (V_h) of +40 mV to that predicted by a linear fit of the I–V relationship at holding potentials between –60 and 0 mV (see Materials and Methods). For MF–PYR synapses in slices obtained from P10–P17 mice, this RI ranged from 0.12 to 0.69 (mean ± SEM, 0.45 ± 0.05; n = 13) (Fig. 2.1C&D) Importantly, synaptic events were inhibited by >90% during treatment with the AMPAR-specific antagonist GYKI-53655 [1-(4-aminophenyl)-3-methylcarbamyl-4-methyl-7,8-methylenedioxy-3,4-dihydro-5H-2,3-benzodiazepine] (40 μM) (Fig. 2.1A, top panel, inset) eliminating the possibility that rectification resulted from KAR contamination of EPSCs.

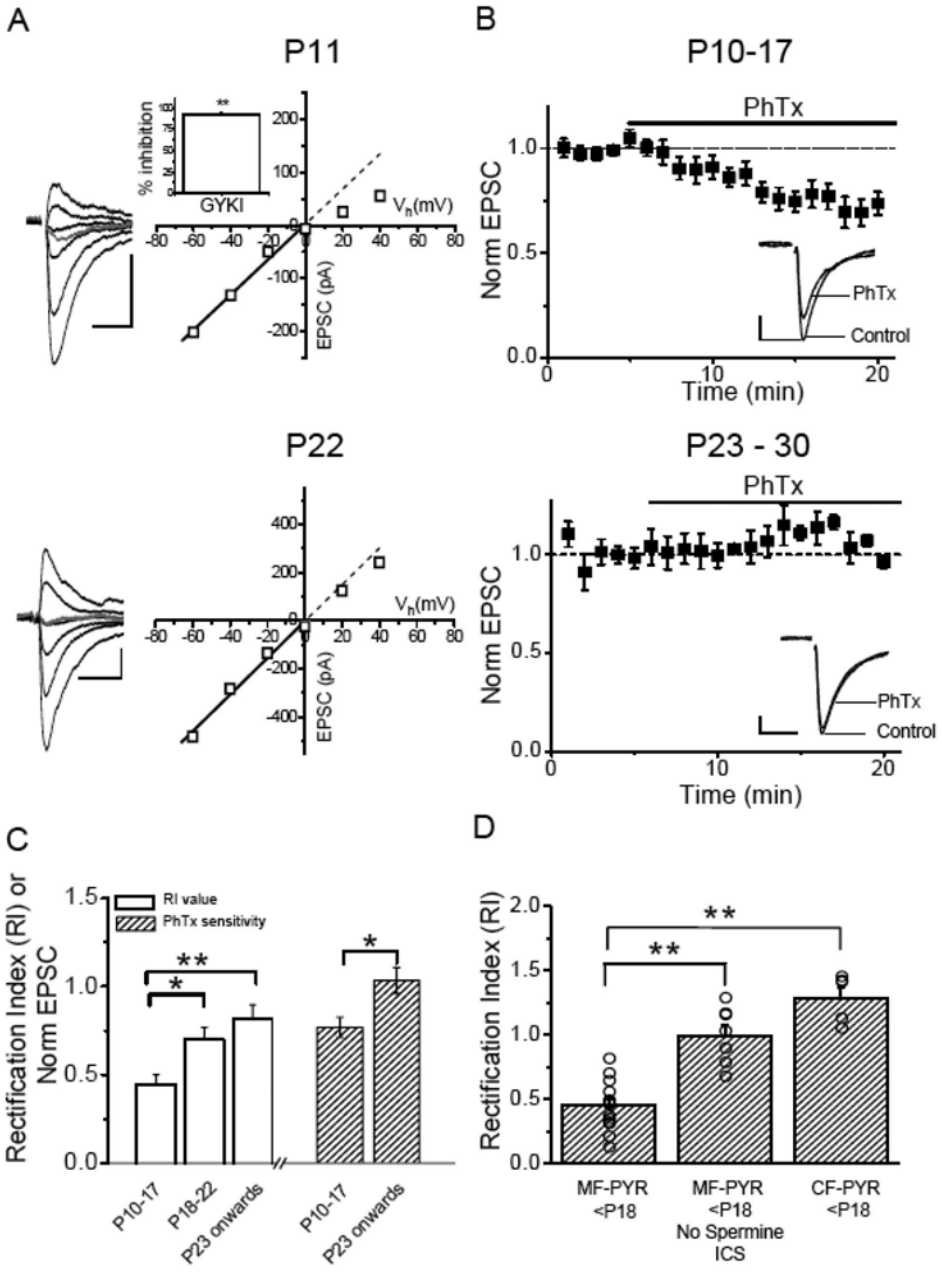

Figure 2.1 Developmental expression of CP-AMPARs at MF–PYR synapses. A, Representative MF–PYR evoked EPSC I–V relationship (V_{hold} from –60 to +40 mV in steps of 20 mV) obtained from a P11 mouse (top panel) and a P22 mouse (bottom panel). Traces are the average of 5–10 events at each holding potential (black). The EPSC at –60 mV after 5 min of DCGIV application to confirm MF origin is indicated in gray. The right panels show plots of the I–V relationship: the solid lines represent the linear fit to data points between the –60 and 0 mV holding potentials. The dotted line extends this fit to highlight the deviation of the I–V relationship at P11 from linearity. **B**, Normalized group data show dot plots for the effect of PhTx (2 μM) on evoked MF–PYR EPSCs in slices from mice aged P10–P17 (top panel; n = 16) and P23–P30 (bottom panel; n = 4).

Plotted are the 1 min running average EPSC amplitudes normalized to the average response obtained from the first 5 min of recording before PhTx application. The inset traces are from representative recordings showing average EPSCs (20 events) before (control) and after PhTx treatment (PhTx). **C**, Summary histogram illustrating the average RI values for, and effects of PhTx on, MF–PYR transmission for the indicated age ranges. PhTx data are expressed as the average EPSC amplitude at the end of PhTx treatment normalized to the average EPSC amplitude obtained immediately preceding PhTx application and are from the recordings in **B**. RI values were calculated as the ratio of the actual current amplitude at +40 mV to the predicted linear value at +40 mV based on the linear fits of I–V relationships illustrated in **A** (n = 13 for P10–P17; n = 10 for P18–P22; and n = 10 for P23). **D**, Bar graph summary comparing the RIs obtained in recordings from P10–P17 mice for MF–PYR synapses (n = 13; replotted from **C**), collateral fiber–PYR synapses (n = 5), and for MF–PYR synapses when spermine was omitted from the ICS (n = 7). Calibration: 100 pA, 10 ms (throughout the figure). Error bars indicate SEM. Here and throughout, *$p < 0.05$ and **$p < 0.01$.

It is unlikely that rectification resulted from inadequate voltage clamp of MF–PYR synapses clamp of MF–PYR synapses as AMPAR-mediated EPSCs at more distally located collateral fiber–PYR synapses displayed near-linear I–V relationships, yielding significantly greater RIs (1.29 ± 0.08; n = 5) in slices of comparable age (2.1D). Moreover, linear I–V relationships with RI values close to unity were obtained in control MF–PYR recordings from young mice using ICS not supplemented with spermine (RI, 0.99 ± 0.08; n = 7) (Fig. 2.1D), consistent with a specific role for polyamines in mediating the rectification. The spermine-dependent rectification of EPSCs suggests that CP-AMPARs participate in transmission at developing MF–PYR synapses. Such a contribution of CP-AMPARs to transmission at nascent MF–PYR contacts was subsequently confirmed when partial inhibition of MF–PYR EPSCs was observed by the CP-AMPAR specific antagonist philanthotoxin-433 (PhTx) (2 μM): with 15 min of PhTx perfusion, EPSCs were significantly depressed to 73 ± 4.9% of control (n = 16; p = 0.004) (Fig. 2.1B, top panel; C). Considered together the range of RI values observed and the partial PhTx sensitivity of MF–PYR EPSCs in slices from P10–P17 mice demonstrates that transmission is mediated by a mixed population of both CP- and CI-AMPARs early in development.

Previous investigations did not observe significant rectification (Jonas et al., 1993) or PhTx sensitivity (Toth et al., 2000) of MF–PYR synaptic events in acute rat hippocampal slices. Importantly, this discrepancy with the current findings is not attributable to species differences (Bellone & Luscher, 2005, 2006) because rectification of MF–PYR EPSCs in acute slices from young (P15–P17) rats (RI, 0.53 ± 0.04; n = 8) was also observed.

Although a lack of spermine supplementation may have contributed to the previous failure to observe rectification (Jonas et al., 1993), it is also possible that the contribution of CP-AMPARs at MF–PYR synapses decreases with development as the age range used in the previous studies (P15–P25) was skewed toward animals older than those used in our recordings described above. Indeed, when I examined MF–PYR transmission in slices from older mice (>P17), I–V relationships became progressively more linear with increasing age; yielding significantly larger RI values (Fig. 2.1A bottom panel & Fig. 2.1C). Similarly, slices from older rats (>P23) yielded significantly greater MF–PYR RIs (0.80 ± 0.06; n = 7; p = 0.006 vs recordings from P15–P17 rat slices). Furthermore, I did not observe any PhTx sensitivity of MF–PYR synaptic events in slices from older mice (Fig. 2.1B bottom panel). Thus, the contribution of native CP-AMPARs to MF–PYR transmission is transient, being limited to early developmental time points with subsequent replacement by CI-AMPARs as reported for various other synapses between principal neurons (Aizenman *et al.*, 2002; Kumar *et al.*, 2002; Eybalin *et al.*, 2004).

As an independent test for the participation of CP-AMPARs at developing MF–PYR synapses, we attempted to observe postsynaptic CP-AMPAR-mediated Ca^{2+} transients (CaTs) at MF–PYR contacts in acute hippocampal slices obtained from young (P10–P16) rats (Fig. 2.2). We collaborated with Dr. Jean Claude Lacaille's laboratory and all the calcium transient experiments presented in this section were carried out by Dr. Lisa Topolnik. PYRs were filled with the fluorescent Ca^{2+} indicator oregon green BAPTA-1 (OGB-1) through a whole-cell recording electrode and imaged using two-photon laser-scanning

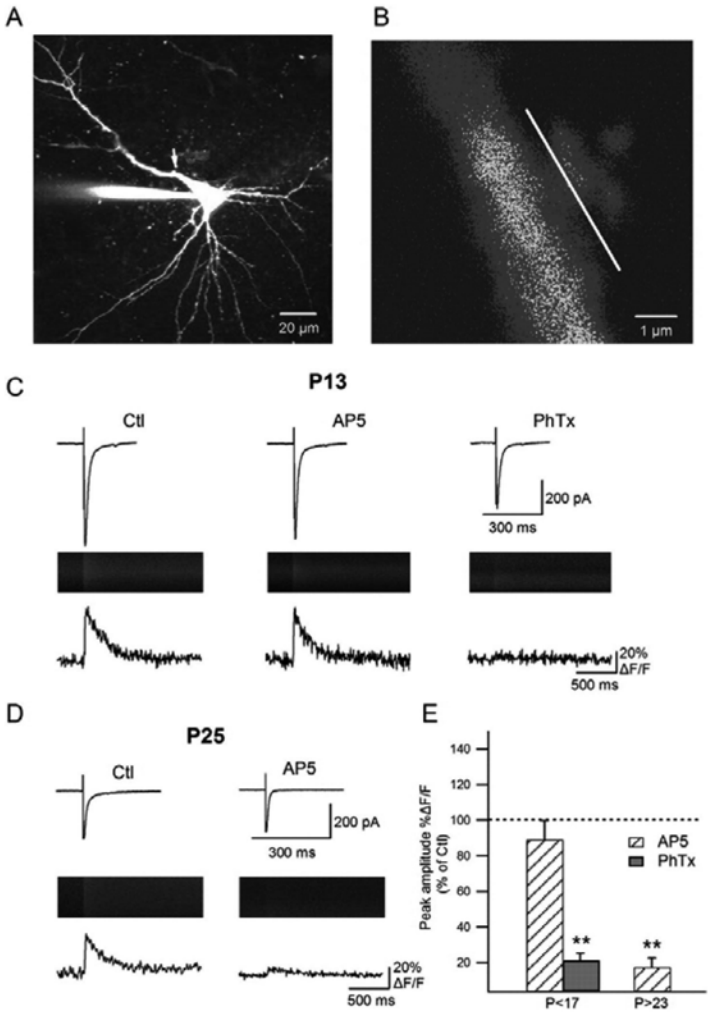

Figure 2.2 CP-AMPARs mediate CaTs at developing MF–PYR synapses. A, A multiphoton image (z-stack) of 60 optical sections taken at 1 µm intervals of an Oregon Green-filled PYR in which MF stimulation evoked CaTs were monitored. **B**, A pseudocolor image showing basal fluorescence in a thorny excrescence located along the proximal dendrite of the PYR in **A** (arrow). The position of the line scan used to monitor stimulus evoked Ca^{2+} signals is indicated parallel to the parent dendrite. **C**, A representative recording from a P13 rat showing the effects of D-AP5 (50 µM) and PhTx (2 µM) on stimulus evoked CaTs recorded in a thorny excrescence (middle images and bottom traces show raw line scan images and associated CaTs, respectively; average of 4 consecutive events under each condition) and simultaneously monitored EPSCs (top traces; average of 4 consecutive events under each condition). **D**, Representative recording from a P25 rat showing the effects of AP5 on stimulus evoked CaTs and simultaneously monitored EPSCs. **E**, Summary histogram for group data examining the effects of AP5 and PhTx on stimulus-evoked CaTs in thorny excrescences from rats aged P10–P16 (n = 5) and of AP5 on CaTs in rats older than P23 (n = 4). Data are expressed as percentage of control responses that were obtained before any drug treatment. Error bars indicate SEM. **$p < 0.01$, paired t test.

microscopy (Fig. 2.2A). After an initial dye loading period (20–30 min), MF–PYR postsynaptic elements were identified as large, complex, spine-like protrusions (thorny excrescences) along the proximal apical dendrite (Fig. 2.2B) (Chicurel & Harris, 1992; Reid *et al.*, 2001; Reid *et al.*, 2004). Subsequently, postsynaptic CaTs evoked by local microstimulation within stratum lucidum were monitored within these developing thorny excrescences in line-scanning mode (Fig. 2.2B–D). To maximize the likelihood of observing postsynaptic CaTs, recordings were started with both AMPAR- and NMDAR-mediated transmission intact. Strikingly, in slices from young rats (<P17), MF–PYR CaTs were not significantly affected by NMDAR inhibition but were strongly depressed by subsequent inhibition of CP-AMPARs: CaTs were 89 ± 11% of control after 10 min of D-APV (50 μM) perfusion and further decreased to 21 ± 4% of control after 15 min of PhTx (2 μM) applied with constant synaptic stimulation (0.5Hz) to facilitate use-dependent block of CP-AMPARs (Fig. 2.2C&E). Similarly, simultaneously monitored EPSCs from these recordings were not significantly affected by D-APV (85 ± 7% of control; $p = 0.9$) but exhibited partial sensitivity to PhTx (70 ± 7% of control; $p = 0.04$) (Fig. 2.2C). Although these compound EPSCs represent not only activity at the imaged synapses but also activity at other synapses not under observation, the findings are consistent with those reported above for young mice (compare Fig. 2.1B). In slices from older animals (>P23), MF–PYR CaTs were almost entirely inhibited by D-APV (17 ± 5% of control), indicating that NMDARs are the primary mediators of postsynaptic Ca^{2+} influx at more mature MF–PYR synapses with little or no contribution of CP-AMPARs (Fig. 2.2D&E). Together, the results from our imaging experiments confirm that CP-

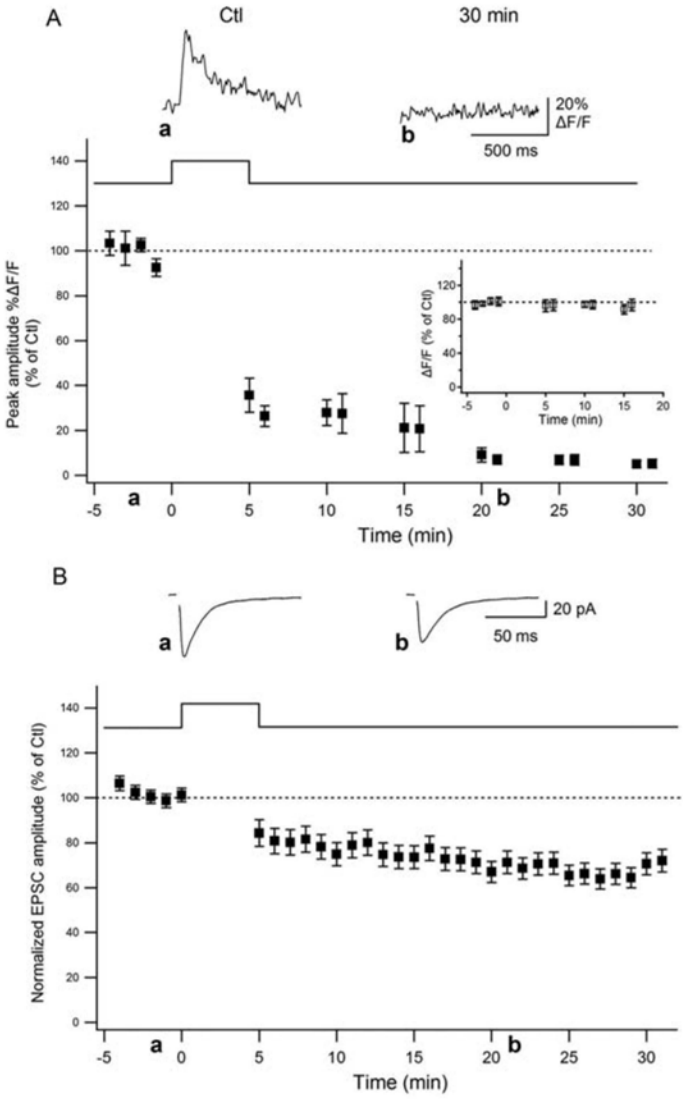

Figure 2.3 DiLTD results in a loss of postsynaptic MF–PYR CaTs. A, Group data time course plot for experiments in which stimulus evoked CaTs were continuously monitored before and after the DiLTD induction protocol (time, 0 min) was applied (n = 5). CaTs (average of 4 events) were monitored at regular intervals during the recordings and expressed as percentage of control CaTs obtained during the baseline recording period. The traces above are CaTs obtained at the times indicated from a representative recording that was subject to the DiLTD induction protocol. The inset time course plot summarizes control recordings in which stimulation was interrupted but PYRs were not subject to depolarization (n = 3). **B**, Group data time course plot showing DiLTD of EPSCs that were recorded during CaT monitoring. EPSC amplitudes for each recording were binned to yield 1 min running averages and are expressed as percentage of control responses obtained during the baseline (preinduction) period. The traces above are EPSCs obtained at the times indicated from the same representative recording that yielded the example CaTs in **A**. Error bars indicate SEM.

AMPARs transiently participate in transmission greatly contributing to postsynaptic Ca^{2+} dynamics at developing MF–PYR synapses.

2.3.2 CP-AMPARs are Preferentially Downregulated during MF–PYR DiLTD

In cerebellar stellate cells and dopaminergic neurons of the ventral tegmental area (VTA), CP-AMPARs impart a distinct form of long-term plasticity in which CP-AMPAR-mediated transmission is persistently lost and synapses become dominated by CI-AMPARs (Liu & Cull-Candy, 2000; Bellone & Luscher, 2005; Gardner *et al.*, 2005) In both cases, plasticity is triggered by a rise in postsynaptic Ca^{2+} mediated by influx through the CP-AMPARs themselves or group I mGluR activation during high-frequency stimulation. Recently, our laboratory described a novel postsynaptic form of LTD at MF–PYR synapses that is activity independent, being induced simply by transient postsynaptic depolarization (Lei et al., 2003). This DiLTD is expressed as a persistent depression of AMPAR function and, like the plasticities described above, is triggered by a rise in postsynaptic Ca^{2+}, although in this case via influx through L-type voltage-gated Ca^{2+} channels (VGCCs). Importantly, this DiLTD exhibits a developmental profile similar to that observed for the expression of CP-AMPARs at MF–PYR synapses: DiLTD is robust at nascent MF–PYR synapses during the second postnatal week, gradually declines during the third postnatal week, and is absent beyond P35 (Lei et al., 2003) Thus, given the overlapping developmental windows for CP-AMPAR expression and DiLTD competence as well as the role of postsynaptic Ca^{2+} in triggering DiLTD, a potential role for modulation of CP-AMPARs in DiLTD was investigated.

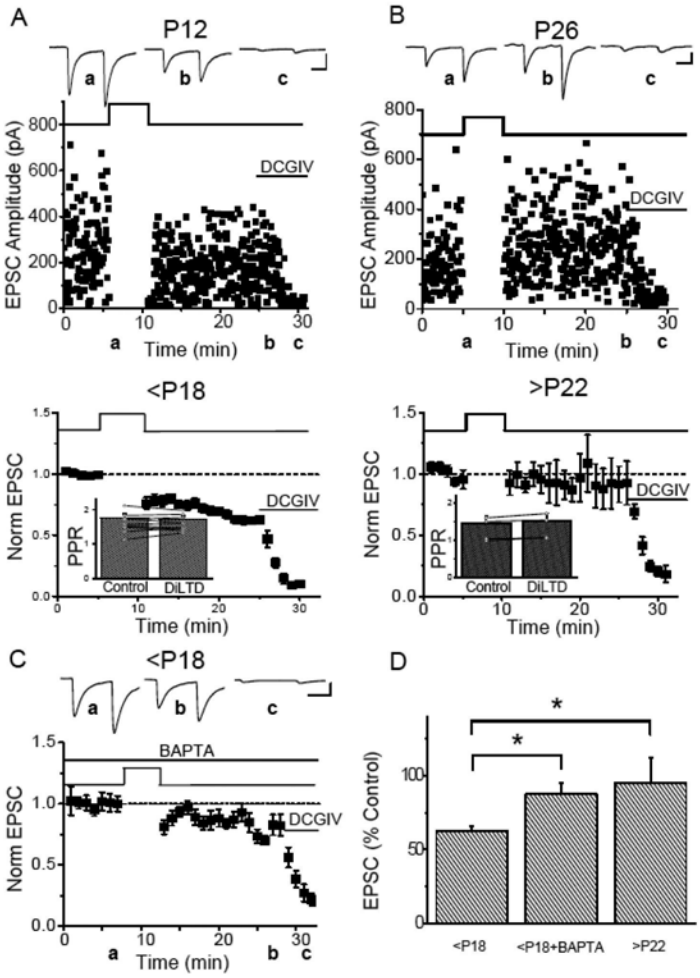

Figure 2.4 Developmental expression of DiLTD at mouse MF–PYR synapses. A, EPSC amplitude time course plot from a representative recording (top panel) and normalized group data (bottom panel; binned in 1 min intervals and normalized to the first 5 min of recordings) illustrating DiLTD in slices from mice younger than P18 (n = 26). The traces above (and throughout the figure) are the average of 20 consecutive EPSC pairs obtained at the times indicated [calbration: 100 pA, 20 ms (throughout the figure)]. Stimulation is paused during induction when the holding potential is moved from –60 to –10 mV for 5 min as indicated. Sensitivity of synaptic events to DCGIV (1 μM) at the end of recordings confirms that inputs are mossy fiber in origin. The inset bar graph in the bottom panel summarizes the PPRs obtained before and after DiLTD induction for a subset of the recordings. **B**, Similar to **A**, but for recordings performed in slices from mice older than P22 (n = 4). **C**, Normalized group data for recordings in which the DiLTD induction protocol was attempted in slices from mice younger than P18 with BAPTA (20 mM)-supplemented ICS (n = 5). **D**, Bar graph summary comparing DiLTD for interleaved recordings performed under the conditions indicated. Data are from the recordings making up the group plots in **A–C** and represent EPSC amplitudes measured at 15 min after induction expressed as percentage of control responses obtained immediately preceding induction (*$p < 0.05$). Error bars indicate SEM.

If MF–PYR DiLTD proceeds as a loss of synaptic CP-AMPARs, similar to CP-AMPAR-associated LTD in the cerebellum and VTA (Liu & Cull-Candy, 2000; Bellone & Luscher, 2005; Gardner *et al.*, 2005), then stimulus evoked synaptic Ca^{2+} influx should be reduced, resulting in a persistent depression of MF–PYR CaTs. Therefore, effects of DiLTD induction on MF–PYR CaTs in slices from P10–P16 rats (Fig. 3) were initially investigated. Synaptic events were evoked at 0.33 Hz and associated CaTs within thorny excrescences were monitored at 1–5 min intervals to minimize potential photodamage. After a stable baseline recording period, presynaptic stimulation was interrupted and the postsynaptic cell was transiently depolarized from a holding potential of –60 to –10 mV for 5 min (Lei et al., 2003) (see Materials and Methods). Subsequently, the postsynaptic membrane potential was returned to –60 mV, presynaptic stimulation was resumed, and the resulting MF–PYR CaTs were recorded for comparison to baseline responses. Using this protocol, stable CaTs during the baseline recording period were obtained; however, immediately after DiLTD induction, a persistent depression of MF–PYR CaTs was evident: CaTs were 36 ± 7.6% of baseline responses immediately after DiLTD induction and ultimately depressed to 6.5 ± 3.4% of baseline responses within 25 min after induction (n = 5) (Fig. 2.3A). This LTD of MF–PYR CaTs was paralleled by a persistent inhibition of simultaneously recorded EPSCs (to 73 ± 8.8% of control at 25 min after induction; p = 0.03) (Fig. 2.3B). Importantly, in interleaved control recordings, stimulus interruption without concomitant PYR depolarization did not significantly affect MF–PYR CaTs, indicating that CaT LTD did not result from nonspecific rundown of MF–PYR CaTs or photodamage (Fig. 2.3A, inset). Because MF–PYR CaTs measured in thorny excrescences of slices from P10–P16 rats are mediated primarily by CP-AMPARs

(Fig. 2), these findings indicate that CP-AMPARs are persistently depressed during DiLTD.

The dramatic depression of MF–PYR CaTs associated with DiLTD is consistent with a long-term inhibition of CP-AMPAR-mediated transmission at MF–PYR synapses allowing transmission to become dominated by CI-AMPARs. If this is the case, then I should be able to detect a DiLTD-induced change in the rectification properties of MF–PYR EPSCs as reported for LTD in cerebellar stellate cells and VTA dopaminergic neurons (Liu & Cull-Candy, 2000; Bellone & Luscher, 2005; Gardner *et al.*, 2005). Thus, to complement our imaging studies, DiLTD-induced changes in RIs of MF–PYR EPSCs were investigated. For these experiments, slices from young mice were studied because transgenic animals would be examined in later experiments (see below). Moreover, this return to mouse slices allowed us to confirm that the phenomenon of DiLTD, like the expression of CP-AMPARs at MF–PYR synapses, is not species specific. Thus, mice express DiLTD with properties similar to those observed in rat (Lei et al., 2003) was confimred. In slices obtained from mice aged P10–P17, transient PYR depolarization from –60 to –10 mV for 5 min produced a depression of MF–PYR EPSCs assayed at –60 mV that persisted for the duration of recordings: 15 min after induction, EPSCs were 63 ± 3.4% of control responses obtained before the depolarization protocol (Fig. 2.4A&D). In contrast, transient depolarization did not affect MF–PYR transmission in slices from animals older than P22: EPSCs were 95 ± 17% of control at 15 min after induction (Fig. 2.4B&D). As in the rat, DiLTD observed in slices from young mice (P10–P17) did not require synaptic activity during induction and proceeded independent of changes in

paired-pulse ratio consistent with postsynaptic induction and expression loci (Fig. 4A, inset, bottom panel). Furthermore, loading PYRs with BAPTA significantly inhibited DiLTD in slices from young mice revealing a central role for Ca^{2+} in mouse DiLTD similar to that previously observed in rats (Fig. 2.4C&D).

Having confirmed the presence of DiLTD in slices from young mice, next, we studied whether rectification of AMPAR-mediated MF–PYR EPSCs is altered by DiLTD by comparing RIs before and after induction (Fig. 2.5). To avoid potentially confounding influences of the prolonged depolarization periods required to obtain full I–V relationships, an abbreviated RI measure using the absolute value of the ratio of EPSC amplitudes obtained at holding potentials of +40 mV and –60 mV ($RI_{EPSC40/EPSC-60}$) (see Materials and Methods) was adopted. Importantly, the brief monitoring of EPSCs at +40 mV (average of 5–10 events obtained at 0.33 Hz, thus 15–30 s) during the baseline period did not significantly affect MF–PYR transmission (data not shown), consistent with a minimal 1–3 min depolarization requirement to observe any depression (Lei et al., 2003). In 9 of 10 recordings, I observed that DiLTD produced a greater depression of EPSCs monitored at –60 mV compared with those obtained at +40 mV (Fig. 2.5A). Accordingly, DiLTD was associated with a significant increase in MF–PYR $RI_{EPSC40/EPSC-60}$ values to 157 ± 16% of control at 10 min after induction (Fig. 2.5B). This RI increase indicates that the contribution of inwardly rectifying CP-AMPARs to MF–PYR EPSCs is depressed after DiLTD induction, leaving transmission to be primarily supported by CI-AMPARs. While monitoring $RI_{EPSC40/EPSC-60}$, DiLTD associated increase in the PPR for EPSCs monitored at +40 mV was observed, in contrast to events recorded at –60 mV at

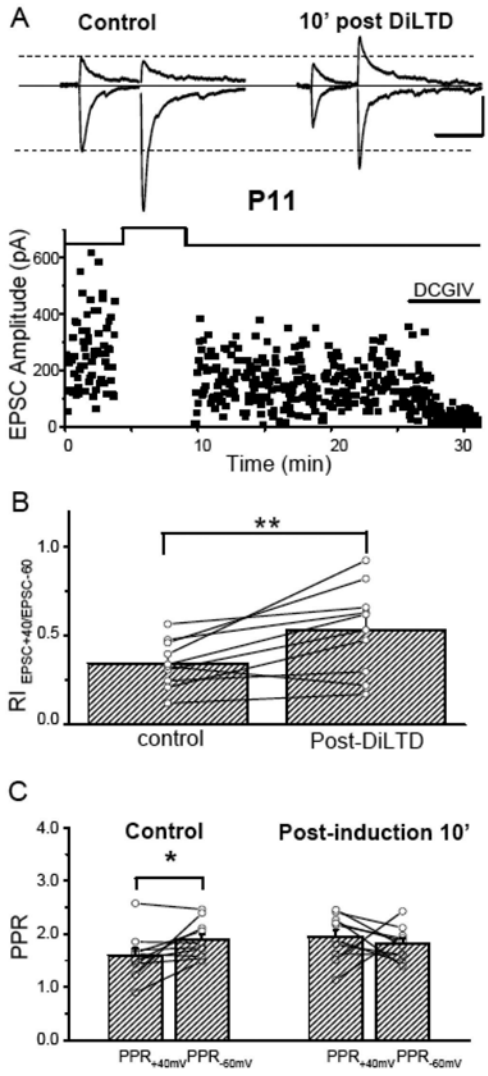

Figure 2.5 DiLTD reduces rectification of MF–PYR synapses. A, Representative recording in which $RI_{EPSC+40/EPSC-60}$ was monitored before and after DiLTD induction in a slice from a P11 mouse (calibration: 100 pA, 50 ms). The traces above show averaged EPSC pairs evoked at V_h of +40 and –60 mV before DiLTD induction (Control) and 10 min after DiLTD induction (10' post DiLTD). The bottom panel shows the time course plot of all MF–PYR EPSC amplitudes for this recording before and after DiLTD induction. **B**, Group data for 10 recordings similar to that illustrated in **A** performed in slices from mice aged P10–P17 reveals a significant increase in $RI_{EPSC+40/EPSC-60}$ after DiLTD induction (**$p < 0.01$). Each individual recording is represented by an open circle with the group mean plotted as a bar. **C**, PPRs measured at holding potentials of +40 and –60 mV before and after DiLTD induction for a subset of the recordings in which $RI_{EPSC+40/EPSC-60}$ was monitored ($n = 8$; *$p < 0.05$). Individual recordings are represented by open circles with group means plotted as bars. Before DiLTD induction the PPR at +40 mV is significantly less than that observed at –60 mV in the same recordings, but after DiLTD the PPRs at +40 and –60 mV are not significantly different.

which no DiLTD-induced change in PPR was detected (Figs. 2.4A, 2.5A, traces). This seemingly contradictory observation likely reflects the inability of spermine blocked CP-AMPARs to contribute to transmission at +40 mV despite the increased release of transmitter on the second pulse of two closely timed stimuli. Indeed the PPR of naive MF–PYR EPSCs measured at +40 mV was significantly less than that obtained at –60 mV with spermine in the recording pipette (1.6 ± 0.12 vs 1.9 ± 0.11 at V_h of +40 and –60, respectively; n = 10; p = 0.04) (Fig. 2.5C); however, no difference in PPRs at the two holding potentials was evident under spermine-free recording conditions (1.8 ± 0.16 vs 1.7 ± 0.16 at V_h of +40 and –60, respectively; n = 7; p = 0.6). At naive MF–PYR synapses, use-dependent relief from polyamine block of CP-AMPARs (Rozov *et al.*, 1998; Rozov & Burnashev, 1999; Toth *et al.*, 2000) might be expected to contribute to an increased PPR at +40 mV compared with that at –60 mV (i.e., the larger the degree of initial block the greater opportunity for use-dependent unblock). However, use-dependent unblock does not occur at positive holding potentials between 0 and +60 mV (Rozov *et al.*, 1998; Rozov & Burnashev, 1999). After DiLTD induction, the increased PPR at +40 mV approximates the PPR observed at –60 mV (Fig. 2.5C) consistent with a switch to transmission being dominated by spermine-insensitive CI-AMPARs. Thus, together, our imaging and electrophysiological data provide compelling evidence for the preferential inhibition of CP-AMPARs during DiLTD at developing MF–PYR synapses, explaining the limited developmental window for this form of synaptic plasticity.

2.3.3 A Role for PICK1 in Regulating the GluR2 Content of MF–PYR Synapses

A number of investigations have described a role for the PDZ domain-containing protein PICK1 in regulating the CP-AMPAR content of various central synapses (Terashima *et al.*, 2004; Gardner *et al.*, 2005; Liu & Cull-Candy, 2005; Bellone & Luscher, 2006). Since PICK1 is a PKC interacting protein (Staudinger et al., 1995), before studying the participation of PICK1 participates in controlling the levels of CP-AMPARs at developing MF–PYR synapses, whether DiLTD required PKC activity was studied by inducing DiLTD in the presence of PKC inhibitor – chelerythrine (5 μM). In the presence of chelerythrine, DiLTD was inhibited with EPSCs maintained at 89 ± 8.5% of control responses (n = 4) (Fig. 2.6C), indicated that DiLTD induction is a PKC dependent process.

In cerebellar stellate cells, LTD associated with a loss of CP-AMPAR-mediated transmission is prevented by disruption of PICK1–GluR2 interactions (Gardner *et al.*, 2005; Liu & Cull-Candy, 2005). Because our findings thus far indicate that DiLTD similarly leads to a loss of synaptic CP-AMPARs and depended on PKC activity, the potential roles for PICK1 in DiLTD using a combination of peptide interference and genetic deletion strategies was investigated. Initially, small interfering peptide EVKI was postsynaptically applied, which selectively disrupts GluR2–PICK1 interactions, through the recording pipette and attempted to induce DiLTD (Daw *et al.*, 2000; Xia *et al.*, 2000; Kim *et al.*, 2001; Gardner *et al.*, 2005; Liu & Cull-Candy, 2005). Because of the variability in time required to find an appropriate MF input after establishing whole-cell

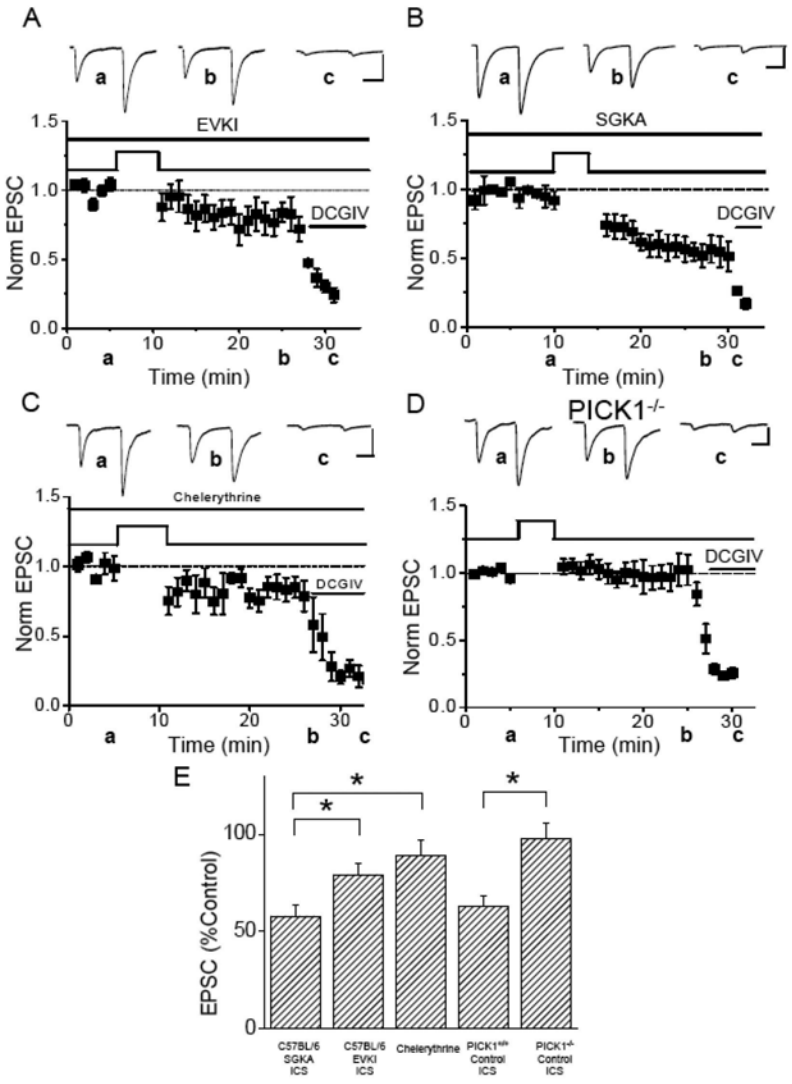

Figure 2.6 Disruption of PICK1 inhibits DiLTD. A, **B**, Group data EPSC amplitude time course plots for recordings in which DiLTD induction was attempted in slices from P10–P17 C57BL/6 mice using EVKI-supplemented ICS (**A**; n = 5) or SGKA-supplemented ICS (**B**; n = 5). The traces above are from representative recordings obtained at the times indicated. **C**, Group data EPSC amplitude time course plot for recordings in which DiLTD induction was attempted in slices from P10–P17 PICK1$^{-/-}$ mice (n = 11 and 10, 10 and 15 min after induction, respectively). The traces above were obtained during a representative recording at the times indicated. For **A–C**, EPSC amplitudes were binned as 1 min running averages and normalized to the average EPSC amplitude obtained during the baseline (preinduction) recording period. **D**, Summary histogram for data presented in **A–C** and for recordings performed in P10–P17 PICK1$^{+/+}$ littermate control mice (n = 4). Data represent the EPSC amplitudes at 15 min after induction expressed as a percentage of control responses obtained immediately preceding induction (*$p < 0.05$). The traces throughout are the average of 20 consecutive events. Calibration: 100 pA, 20 ms. Error bars indicate SEM.

configuration, and the close proximity of MF–PYR synapses to the somatic recording location (facilitating rapid dialysis), no effort was made to examine potential peptide influence on transmission during the baseline period. In these recordings, ICS supplemented with the peptide EVKI significantly inhibited DiLTD: 15 min after induction, EPSCs remained at 80 ± 5.7% of control responses (n = 5) (Fig. 2.6A&E). This inhibition of DiLTD did not result from nonspecific effects of peptide infusion because typical DiLTD was observed in recordings performed with a control peptide SGKA that does not affect PDZ domain-mediated interactions (60 ± 5.3% of control; n = 5) (Fig. 2.6B&E). Next, I examined DiLTD in slices from young (P10–P17) PICK1 knock-out ($PICK1^{-/-}$) mice (Gardner et al., 2005; Steinberg et al., 2006). Consistent with the data from our peptide interference experiments, recordings in slices from $PICK1^{-/-}$ mice revealed a severe deficit in DiLTD: at 15 min after induction, EPSCs were 97 ± 8.6% of control responses (n = 10) (Fig. 2.6D&E). In contrast, slices from age-matched wild-type ($PICK1^{+/+}$) littermates exhibited robust DiLTD with EPSCs depressing to 63 ± 5.3% of control (n = 4) (Fig. 2.6E) comparable with that observed in young C57BL/6 mice used throughout the study to this point (compare Fig. 2.4D).

The blockade of DiLTD by disrupting PICK1 function could be interpreted as evidence for an acute active role of PICK1 in the loss of synaptic CP-AMPARs during DiLTD induction. Alternatively, PICK1 disruption could occlude DiLTD by causing the removal of CP-AMPARs from MF–PYR synapses before induction. Indeed, previous studies have reported alterations in basal synaptic GluR2 content after manipulations of PICK1 function by peptide perfusion or overexpression (Terashima *et al.*, 2004; Gardner *et al.*,

2005). To determine whether EVKI perfusion and PICK1 knock-out alter the basal contribution of CP-AMPARs to MF–PYR synapses, the rectification properties of MF–PYR EPSCs after peptide treatment and in PICK1$^{-/-}$ mice was examined. Surprisingly, in slices from young C57BL/6 mice, recordings with EVKI-supplemented ICS yielded MF–PYR EPSCs with near-linear I–V relationships resulting in RI values (0.90 ± 0.10; n = 5) significantly greater than those obtained with SGKA-supplemented ICS (0.53 ± 0.08; n = 5) (Fig. 2.7A&C). Similarly, in slices from young PICK1$^{-/-}$ mice, MF–PYR synapses exhibited RIs significantly greater than those obtained in slices from littermate control PICK1$^{+/+}$ mice (PICK1$^{-/-}$: 0.84 ± 0.08, n = 11; PICK1$^{+/+}$: 0.54 ± 0.06, n = 5) (Fig. 2.7B&C). Furthermore, MF–PYR EPSCs from PICK1$^{-/-}$ mice were not significantly affected by

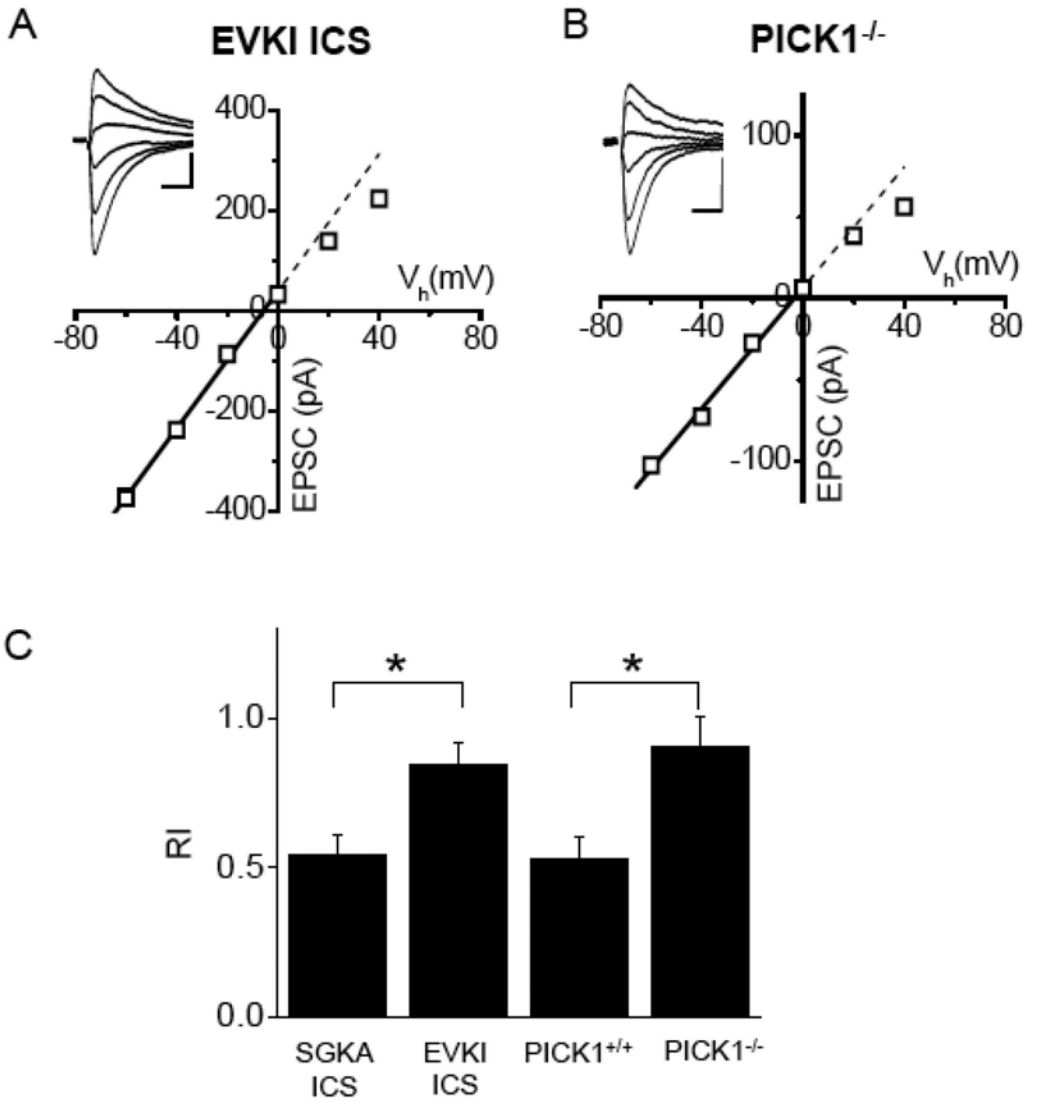

Figure 2.7 Loss of CP-AMPARs at developing MF–PYR synapses after PICK1 disruption. A, MF–PYR EPSC I–V relationship (V_{hold} from –60 to +40 mV in steps of 20 mV) obtained during a representative recording in a slice from a P14 C57BL/6 mouse using EVKI-containing ICS. The line is the linear fit to data points for holding potentials between –60 and 0 mV. The traces are the average of 5–10 events at each holding potential (calibration: 100 pA, 10 ms). **B**, Representative MF–PYR EPSC I–V relationship obtained in a slice from a P14 $PICK1^{-/-}$ mouse (calibration: 50 pA, 10 ms). **C**, Group data summary bar chart for RI values obtained in slices from C57BL/6 mice aged P10–P17 using ICS supplemented with EVKI (n = 5) or SGKA (n = 5). Also shown is the group data summary bar chart of RI values obtained in P10–P17 $PICK1^{-/-}$ (n = 11) and $PICK1^{+/+}$ (n = 5) mice. Error bars indicate SEM. *$p < 0.05$ throughout the figure.

PhTx treatment (EPSCs were 92 ± 8.7% of control after 15 min of treatment). Together, these data indicate that loss of PICK1 function acutely by peptide interference, or chronically by genetic ablation, reduces the contribution of CP-AMPARs to developing MF–PYR synapses. Thus, rather than revealing an acute active role for PICK1 in DiLTD, the lack of DiLTD observed in PICK1$^{-/-}$ mice or after EVKI treatment likely reflects a deficit in the contribution of CP-AMPARs at developing MF–PYR synapses, indicating a critical role for PICK1 in regulating the GluR2 content of developing MF–PYR synapses.

Finally, as an independent assay to probe whether PICK1 regulates the subunit composition of MF–PYR synapses, immunogold electron microscopy (EM) in PYR thorny excrescences of PICK1$^{+/+}$ and PICK1$^{-/-}$ mice was performed. This set of experiment was performed by Dr.Ronald S. Petralia. Tissue from three different P14 animals for each genotype was double labeled using a polyclonal GluR1-specific antibody and a monoclonal GluR2-specific antibody, and then anti-GluR1 and anti-GluR2 signals were revealed with 5 and 15 nm gold particles, respectively. Consistent with our electrophysiological data, PYR spine profile membranes of PICK1$^{-/-}$ mice showed a modest reduction in GluR1 signal and a modest increase in GluR2 signal compared with PICK1$^{+/+}$ littermate controls yielding a significantly larger GluR2/GluR1 signal ratio in PICK1$^{-/-}$ mice: 0.62 ± 0.1 and 1.0 ± 0.2 for PICK1$^{+/+}$ and PICK1$^{-/-}$, respectively ($p = 0.04$) (Fig. 2.8). Moreover, an increase in the number of synaptic profiles doubly labeled for GluR1 and GluR2 in the absence of PICK1 was observed. The ratios of synapses labeled with 5 nm gold particles only, to those labeled with 5 and 15 nm gold particles were 0.98

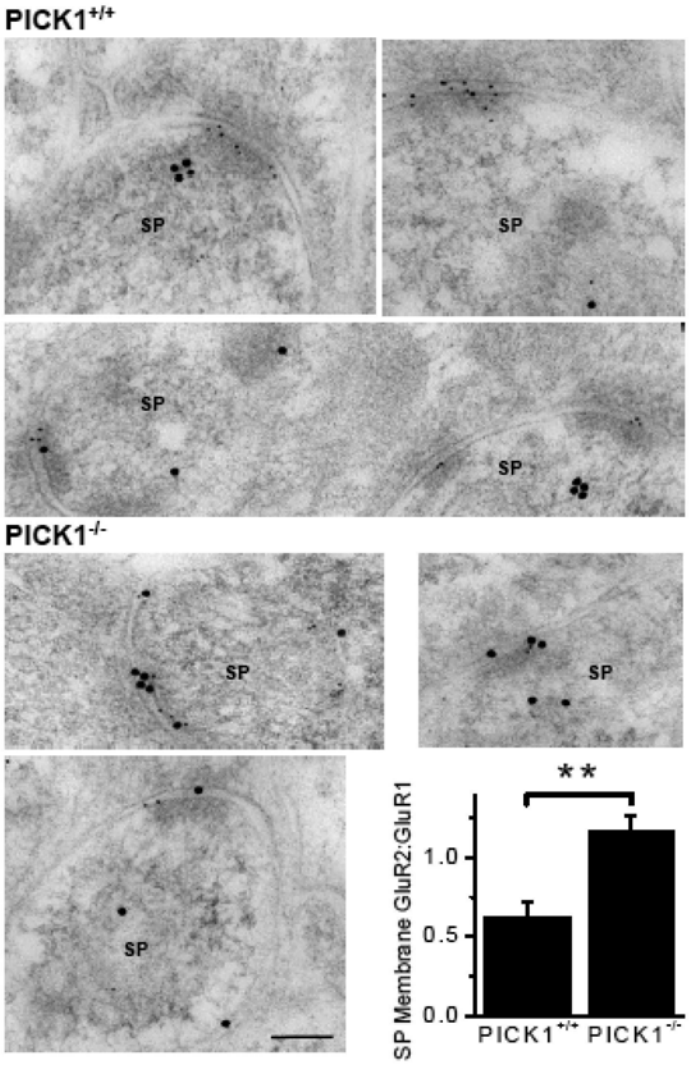

Figure 2.8 Loss of CP-AMPARs at developing MF–PYR synapses in PICK1$^{-/-}$ mice. Representative photomicrographs of immunogold labeling in PYR spine profiles (SPs) for GluR1 (5 nm gold particle) and GluR2 (15 nm gold particles) in PICK1$^{+/+}$ mice (top panel; three micrographs showing 4 SPs) and PICK1$^{-/-}$ mice (bottom left panel; 3 micrographs each with 1 SP). The bottom right panel is a cumulative probability histogram (bin width, 0.1) of GluR2/GluR1 signal ratios in SP membranes of PICK1$^{+/+}$ mice (n = 87 SPs from 3 animals) and PICK1$^{-/-}$ mice (n = 66 SPs from 3 animals). Scale bar (bottom left photomicrograph), 100 nm. *$p < 0.05$ throughout the figure.

and 0.64 for PICK1$^{+/+}$ and PICK1$^{-/-}$ MF–PYR synapses, respectively (Fig. 2.8, micrographs) (see Materials and Methods). Thus, considered together, our immuno-EM and electrophysiological data indicate a critical role for PICK1 in the developmental expression of CP-AMPARs at MF–PYR synapses.

Chapter 3

Burst firing induces postsynaptic LTD at developing mossy fiber-CA3 pyramid synapses

3.1 Introduction

Spontaneous network activity is important for neuronal network formation and refinement (Katz & Shatz, 1996). APs emerge even before the appearance of morphologically specialized and functional synapses (Wiesel & Hubel, 1974; Chapman & Stryker, 1992; Ming et al., 2001) and the formation of appropriate synaptic connections may rely on AP generation (Stryker & Harris, 1986; Chapman & Stryker, 1993; Goodman & Shatz, 1993). The role of spontaneous APs in synapse development has been widely studied in diverse systems (Xie & Poo, 1986; Shatz & Stryker, 1988; Penn et al., 1998; Sanes & Lichtman, 1999; McLaughlin et al., 2003; Chandrasekaran et al., 2005; Wang & Manis, 2005, 2008). In the hippocampus, synchronized bursts of pyramidal cell APs driven by GDPs provided by GABAergic depolarization (Ben-Ari et la., 1989) are implicated in the early recruitment of new excitatory synapses (Hanse et al., 1997; Leinekugel, 2003). Although GDPs disappear around the end of the second postnatal week as GABA becomes hyperpolarizing (Ben-Ari et al., 1989), CA3 PYRs preserve synchronized AP BF which can be detected both in vivo and in vitro (Traub & Wong, 1982; Miles & Wong, 1983; Buzsaki, 1986). Typical spontaneous bursting events consist of rapid sequences of APs riding on slow depolarizations that last for ~100ms (Kandel et al., 1960; Wong & Prince, 1978) and bursting in one neuron can initiate synchronized population bursts throughout the hippocampus (Miles & Wong, 1983). Synchronized bursting results from a combination of both the intrinsic excitability of individual CA3 PYRs and synaptic interactions within the CA3 PYR recurrent collateral network (Schwartzkroin & Prince, 1977; Traub & Wong, 1982; Miles & Wong, 1983; Wong & Traub, 1983; Prince & Connors, 1986; Yaari et al., 1986; Bains et al., 1999).

Importantly, these synchronous bursts are developmentally regulated becoming more intense during the second and third postnatal weeks (Swann et al., 1993; Smith et al., 1995) and are capable of driving synaptic plasticity within the CA3 network (Ben-Ari & Gho, 1988; Merlin & Wong, 1993; Moore et al., 1993; Smith & Swann, 1999). Of particular relevance to the current study, previous investigations revealed that PYR network bursts promote NMDAR-dependent long-term potentiation (LTP) of mature collateral synapses in the adult hippocampus (Bains et al., 1999; Stoop et al., 2003) but did not alter the efficacy of transmission at MF-PYR connections (Bains et al., 1999). The lack of BF induced plasticity at mature MF-PYR synapses likely reflects the fact that adult MF-PYR inputs predominantly express NMDAR-independent presynaptic plasticity that does not rely on postsynaptic depolarization (Weisskopf et al., 1994; Nicoll & Malenka, 1995; Tzounopoulos et al., 1998). However, a potential role for BF at developing MF-PYR synapses, which may express distinct forms of synaptic plasticity (Lei et al., 2003; Kasyanov et al., 2004), has not previously been investigated.

Recently, we demonstrated that transient tonic depolarization of postsynaptic PYRs induces a persistent postsynaptic form of LTD at immature MF-PYR synapses (Lei et la., 2003; Ho et al., 2007). DiLTD induction relies on the activation of L-VGCCs and is expressed by a reduction in AMPAR function through the loss of GluR2-lacking AMPARs at immature MF-PYR synapses, converting them to GluR2-containing AMPAR dominated synapses that prevail at mature MF-PYR synapses (Lei et al., 2003; Ho et al., 2007). The physiological trigger for this developmental form of plasticity is presently unknown. However, BF of developing PYRs could potentially activate L-

VGCCs, which may themselves further support the generation of intrinsic bursts in developing PYRs (Wong & Prince, 1978; Aicardi & Schwartzkroin, 1990). This complex interplay between BF generation and L-VGCC activation could serve as the critical trigger for DiLTD. Indeed L-VGCC expression on CA3 PYR proximal dendrites is upregulated between P8-21 coincident with the period of DiLTD competence and BF emergence. (Westenbroek et al., 1990; Glazewski et al., 1993; Hell et al., 1993; Elliott et al., 1995). Thus, L-VGCC activation triggered during network bursting provides an attractive physiological model for DiLTD induction, and hence MF-PYR synapse maturation. In the present investigation we have examined whether phasic L-VGCC activation driven by PYR BF can trigger DiLTD.

3.2 Materials and Methods

3.2.1 Hippocampal Slice Preparation

Slices were prepared as described previously (Pelkey *et al.*, 2005; Ho *et al.*, 2007) using P10-15 C57BL/6 mice, except for experiments involving transgenic animals which were created on a hybrid genetic background of 129 and C57BL/6 strains (Gardner et al., 2005). Briefly, animals were deeply anesthetized with isoflurane and decapitated allowing for removal of the brain into ice-cold saline solution containing (in mM): 130 NaCl, 24 $NaHCO_3$, 3.5 KCl, 1.25 NaH_2PO_4, 0.5 $CaCl_2$, 5.0 $MgCl_2$ (or $MgSO_4$), and 10 glucose, saturated with 95% O_2 and 5% CO_2 (pH 7.4). Dissection procedure was same as that mentioned in 2.2.1. After dissection of the brain, individual hemispheres were transferred to the stage of a VT-1000S vibratome (Leica Microsystems, Bannockburn, IL) and sectioned to yield transverse hippocampal slices (300 μm) which were incubated in the above solution at 35°C for 30 min after slicing and then stored at room temperature until use. All animal procedures were approved and conformed to the National Institutes of Health animal welfare guidelines.

3.2.2 Whole-Cell Recordings

Individual slices were transferred to a recording chamber and perfused (2-3 ml/min) with extracellular solution (in mM): 130 NaCl, 24 $NaHCO_3$, 3.5 KCl, 1.25 NaH_2PO_4, 2.5 $CaCl_2$, 1.5 $MgCl_2$ (or $MgSO_4$), 10 glucose, 0.0025 bicuculline methobromide, and 0.100 DL-AP5, saturated with 95% O_2 and 5% CO_2 (pH 7.4, 32-35°C). Whole-cell patch-clamp recordings using a multiclamp 700A amplifier (Axon Instruments, Foster City, CA) switched between voltage-clamp mode (V_h=-60 mV) and current clamp mode were made

from individual CA3 PYRs, visually identified with infrared video microscopy and differential interference contrast optics. In current clamp mode, cells were held at a control potential -60 mV by current injection with the bridge balanced. Whole-cell recordings were obtained using glass electrodes (3-4 MΩ) pulled from borosilicate glass (World Precision Instruments). All recording electrodes were filled with intracellular solution (ICS) of the following composition (in mM): 135 K-gluconate, 10 HEPES, 0.2 EGTA, 20 KCl, 2 Mg_2ATP, and 0.3 NaGTP, pH 7.2–7.3 and 290–300 mOsm. In some experiments, to prevent the firing of Na-dependent APs, QX-314 (1 mM) was included in the ICS. Uncompensated series resistance (8-15 MΩ) was rigorously monitored during voltage clamp by the delivery of small voltage steps at regular intervals and recordings were discontinued following changes of >15%.

Synaptic responses were evoked at 0.33Hz by low-intensity microstimulation (100 μsec duration; 20-40 μA intensity) via a constant-current isolation unit (A360, World Precision Instruments, Sarasota, FL) connected to a patch electrode filled with oxygenated extracellular solution. For MF-PYR evoked synaptic recordings the stimulating electrode was placed in either the dentate gyrus or stratum lucidum. MF-origin of EPSCs was always confirmed by perfusion of slices with the group II mGluR agonist DCGIV at the end of recordings (1 μM) (Kamiya et al., 1996). For collateral fiber stimulation, the stimulating electrode was placed in CA3 stratum radiatum and evoked events did not exhibit DCGIV sensitivity.

To induce PYR BF, cell recordings were switched to current clamp mode. Depolarizing current pulses to evoke PYR BF were produced via the recording electrode in the absence of presynaptic stimulation for 5 minutes. Three distinct protocols were used: (1) PYRs were held at a control potential -60 mV in current clamp mode and a square-wave current pulse (0.5nA,125ms) was injected at 1Hz for 5'. This was the standard "Long pulse protocol"; (2) Alternatively, PYRs were held at a control potential (V_h=-60 mV) and a train of brief current pulses (5 pulses of 0.8nA, 5ms duration, 40Hz) was delivered at 1 Hz for 5' i.e. "short pulses protocol"; (3) CA3 PYR cells were held at their resting potential without current injection and BF was triggered by elevating $[K^+]_o$ from 3.5mM to 8.5 mM (Traynelis & Dingledine, 1988; Aradi & Maccaferri, 2004) for 5'. Following a 5' induction protocol $[K^+]_o$ was returned to 3.5mM. In all cases, synaptic events were measure at -60mV in voltage clamp mode after the induction protocol.

3.2.3 Data Analysis

For each recording, EPSC amplitudes from individual sweeps were measured during a 1-2 ms window around the peak of the EPSC waveform. For incorporation into group data the EPSC amplitudes for a given recording were binned in 1 minute running averages and normalized to the mean amplitude obtained during the base-line period. Data are presented as means ± SEMs. All data sets were subjected to the Shapiro-Wilk normality test. For data found to be normally distributed statistical significance was assessed with paired and un-paired t-tests as appropriate. For data sets not normally distributed the non-parametric Mann-Whitney U test was used to assess statistical significance. PPRs were obtained by calculating mean P2/mean P1, where P1 represents the amplitude of the first

evoked current and P2 the amplitude of the second for an average obtained from 20 consecutive individual traces. CV of synaptic currents was calculated as the SD of current amplitude divided by mean (x) of the current amplitude (CV=SD/x) for sequential (40-60) EPSCs.

3.2.4 Ca^{2+} -imaging of pyramidal cell dendrites

Recording pipettes (4–5 MΩ) were filled with a solution containing (in mM): 130 $KMeSO_3$, 2 $MgCl_2$, 10 diNa-phosphocreatine, 10 HEPES, 2 ATPTris, 0.4 GTPTris, and 0.2 Ca^{2+}-sensitive indicator Oregon green-488-BAPTA-1- hexapotassium salt (OGB-1; Molecular Probes, Eugene, OR, USA). After obtaining the whole-cell configuration, 20–30 min were allowed for intracellular diffusion of the fluorophore. Imaging was performed using a two-photon laser scanning microscope LSM 510 (Carl Zeiss, Kirkland, Quebec, Canada) based on a mode-locked Ti:sapphire laser operating at 800 nm, 76 MHz pulse repeat, <200 fs pulse width, and pumped by a solid-state source (Mira 900 and 5 W Verdi argon ion laser; Coherent, Santa Clara, CA). A long-range water-immersion objective (40x; numerical aperture, 0.8) was used. Fluorescence was detected through a short-pass filter (cutoff, 680 nm) in non-descanned detection mode and images were acquired using the LSM 510 software (Carl Zeiss). Ca^{2+} transients (average of three responses) evoked by the somatic depolarization protocols were measured at 30-50 µm from the soma by scanning a line through the dendrite. Depolarization protocols were randomized to rule out possible presentation order biases. Changes in fluorescence were

calculated relative to the baseline and expressed as $\%\Delta F/F = [(F - F_{rest})/F_{rest}] \times 100$. Summary data are expressed as mean ± SE.

3.3 Results

3.3.1 DiLTD of MF synaptic transmission is triggered by phasic AP-dependent L-VGCC activation.

CA3 PYR intrinsic bursts consist of four to six APs riding on a depolarizing potential with duration of ~100-125ms both in vivo and in vitro yielding an intra-burst frequency in the gamma range of approximately 30-60Hz (Kandel & Spencer, 1961; Wong & Prince, 1978; Miles & Wong, 1986). As the aim of this study is to examine the ability of PYR BF to induce DiLTD and our acute slices did not exhibit significant spontaneous BF, I first developed current injection protocols to drive PYR responses that mimic intrinsic BF. In current-clamp mode a suprathreshold 125ms depolarizing square-wave current pulse of either 0.25nA or 0.5nA to individual CA3 PYRs (Fig. 3.1A) was repetitively injected. Of these two protocols only the larger current (125ms, 0.5nA) yielded a consistent response producing 4-6 APs with intraburst frequency of 46.8$\pm$3.1Hz when provided at regular intervals; this protocol was named the "long pulse" protocol (Fig. 3.1A). To have absolute control over the number of spikes generated a brief train protocol was developed by applying a series of suprathreshold current pulses (5x5ms pulses of 0.8nA, 40Hz) to mimic intrinsic PYR BF (Fig. 3.1B). This "train" protocol reliably generated 5 APs with spike frequency of 40Hz when given at regular intervals (Fig 3.1C).

As the critical trigger for DiLTD induction is L-VGCC activation, whether the PYR BF produced by the long pulse and train protocols drives L-VGCC activity using two-photon Ca^{2+} imaging in PYRs filled with OGB-1 through the whole-cell recording electrode

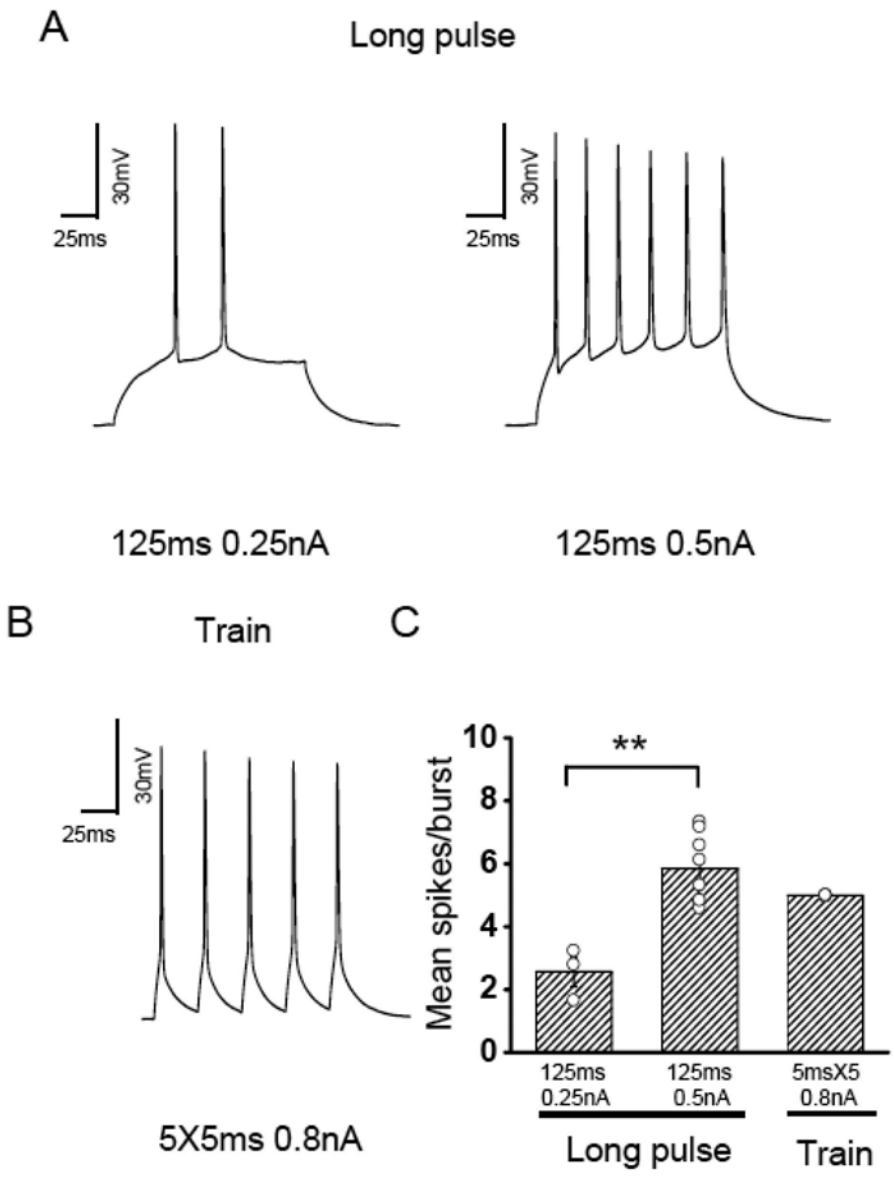

Figure 3.1 PYR BF generated by repetitive current injection. A, Sample traces obtained from representative PYR recordings in response to "long pulse" protocols consisting of a 125ms duration square wave current injection of 0.25nA (left panel) or 0.5nA (right panel). **B,** Sample trace illustrating a representative PYR membrane response to the "train" protocol consisting of a series of brief current pulses (5 pulses of 0.8nA, 5ms duration, 40Hz). **C,** Bar graph showing the average number of spikes observed during repetitive application (1Hz for 5 minutes) of 0.5nA long-pulse protocol or train protocol remains stable. *$p<0.05$,**$p<0.01$, for indicated comparison.

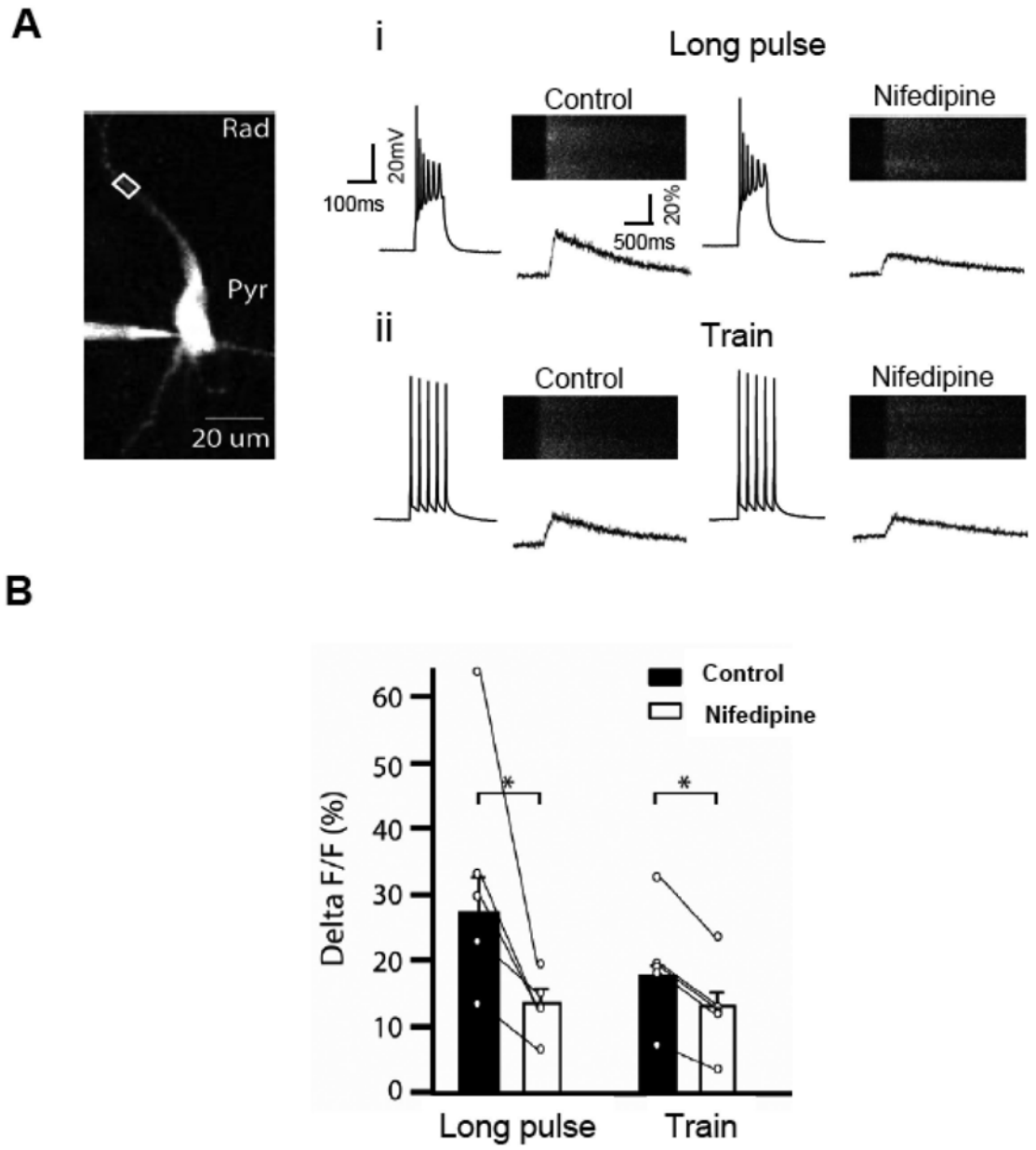

Figure 3.2 PYR BF generated by repetitive current injection activates L-VGCCs. A, Image of a PYR filled with OGB-1 through the recording pipette showing the region of the proximal apical dendrite (box) where BF driven CaTs were monitored by two-photon microscopy. Right panel: PYR firing patterns and associated CaTs observed in response to the long pulse (i) or train (ii) protocols before (Control) and after nifedipine (Nifedipine, 10 μM) treatment for the representative PYR illustrated in the left panel. **B,** Group data bar graph summary of the effects of nifedipine on CaTs elicited with the long pulse and train protocols (n=5) *$p<0.05$,**$p<0.01$, for indicated comparison.

(Fig. 3.2A) was examined. Thus we collaborated with Dr. Jean Claude Lacaille's laboratory where his postdoctoral fellow Dr. Joe Guillaume Pelletier performed the following experiment. CaTs within PYR proximal dendrites were monitored while driving PYR BF with either the long pulse or train protocol (Fig. 3.1A&B). Both protocols reliably produced a transient increase in intracellular Ca^{2+} within PYR proximal dendrites. Importantly, the CaTs driven by both protocols were significantly attenuated by treatment with the L-VGCC antagonist nifedipine revealing that PYR BF initiated by current injection protocols does indeed promote Ca^{2+} influx through L-VGCCs (Fig. 3.2A-B).

Given that the current injection protocols promote Ca^{2+} influx through L-VGCCs, I next tested whether a transient period of repetitive PYR BF produced by the long pulse and train protocols triggers DiLTD. After monitoring pharmacologically isolated AMPAR-mediated MF-PYR EPSCs for a control baseline period of 5-6 minutes in voltage-clamp mode (V_h=-60mV), I switched to current-clamp and repetitively subjected the recorded cells to either the long pulse (125ms, 0.5nA) or train protocol (5x5ms, 0.8nA) at 1Hz for 5' before switching back to voltage-clamp mode to examine the impact of BF on synaptic efficacy. Consistent with the observation that the protocols effectively drive L-VGCC activation, both protocols successfully depressed MF-PYR EPSCs to 54.0$\pm$4.2% (n=8) and 44.0$\pm$4.4% of control (n=4) for the long pulse and train protocols respectively (Fig.3.3A&B). As influx of Ca^{2+} through L-VGCCs is the critical trigger for DiLTD induction (Lei et al., 2003; Ho et al., 2007), I tested whether activation of L-VGCCs is required to trigger LTD. Application of the L-VGCC antagonist nifedipine successfully

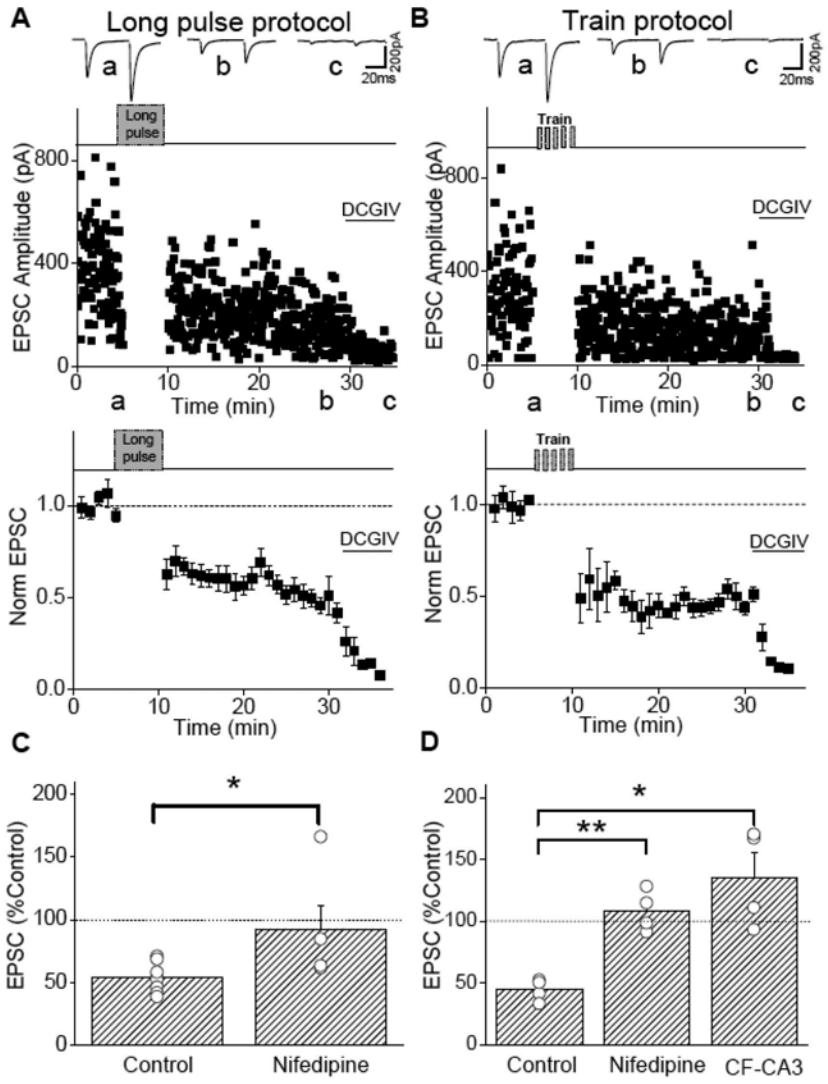

Figure 3.3 Repetitive PYR BF induces MF-PYR LTD. A, Representative MF-PYR EPSC amplitude time course plot (upper panel) and normalized group data (lower panel, n=8) illustrating LTD observed in slices from young mice (<P16) induced by repetitive application of the long pulse protocol (125ms, 0.5nA) at 1Hz for 5' in current-clamp mode (long pulse protocol indicated by grey box) to promote PYR BF. Traces above in A (and throughout) are the average of 20 consecutive EPSC pairs (20 Hz) obtained at the times indicated. **B,** Representative EPSC amplitude time course plot (upper panel) and normalized group data (lower panel, n=4) illustrating LTD in slices from young mice (<P16) induced by BF elicited by repetitive application of the train protocol (5 pulses of 0.8nA, 5ms duration, 25ms apart) at 1 Hz for 5' in current-clamp mode (train protocol indicated by grey bars). For group data timecourse plots here and throughout EPSC

amplitudes for each recording were binned in 1 minute intervals and normalized to the first 5 minutes of recording. **C,** Group data bar graph summary comparing long-pulse protocol induced MF-PYR LTD for interleaved recordings performed in the absence (Control; n=8) and presence (Nifedipine; n=5) of the L-VGCC blocker nifedipine (20 μM). **D,** Bar graph summary comparing train protocol induced MF-PYR LTD for interleaved recordings from control and nifedipine treated slices. Also shown is the effect of the train protocol on recurrent collateral fiber-PYR synapses (CF-CA3; n=4). Data plotted here an throughout represent EPSC amplitudes measured at 14-15 minutes post-induction expressed as a percentage of control responses (4-5 minutes) obtained prior to induction. *$p<0.05$, **$p<0.01$, for indicated comparisons.

blocked LTD induced by both the long pulse (92.6±19.1% of control, n=5; Fig. 3.3C) and train (118.4±15.3% of control, n=4; Fig.3.3D) protocols, indicating that the LTD triggered by both protocols depends on L-VGCC activation. To determine the site of LTD expression PPR was analyzed and CV of synaptic events obtained before and after LTD induction. Consistent with our previous description of DiLTD, the long pulse protocol induced LTD resulted in no change in PPR (1.6±0.1 vs. 1.6±0.1; p=0.09; n=5) and CV (0.39±0.03 vs. 0.46±0.04; p=0.14; n=5). Similar results were obtained with train-induced LTD [PPR (1.4±0.1 vs. 1.4±0.1; p=0.63; n=4) and CV (0.57±0.06 vs. 0.56±0.06; p=0.59; n=4)]. Taken together these results indicate that repetitive injection of suprathreshold depolarizing current pulses to postsynaptic PYRs can induce L-VGCC dependent postsynaptic LTD at MF-PYR synapses.

A transient period of intense PYR BF can induce NMDAR-dependent plasticity within the CA3 recurrent and perforant path networks (Bains et al., 1999; Smith & Swann, 1999; Stoop et al., 2003). In contrast NMDAR-independent DiLTD is specific for MF-PYR synapses (Lei et al., 2003; Ho et al., 2007). To determine whether the newly discovered NMDAR-independent plasticity is similarly specific to MF-PYR synapses, the effects of the train induction protocol at CF-CA3 of young mice (P10-15) in the absence of NMDAR-mediated signaling was examined. As a result, the train protocol did not produce LTD at CF-CA3 synapses (135.3±39.2%, n=4; Fig. 3.3D), demonstrating that, like DiLTD, NMDAR-independent LTD induced by phasic L-VGCC activation driven by repetitive PYR BF is specific for MF-PYR synapses.

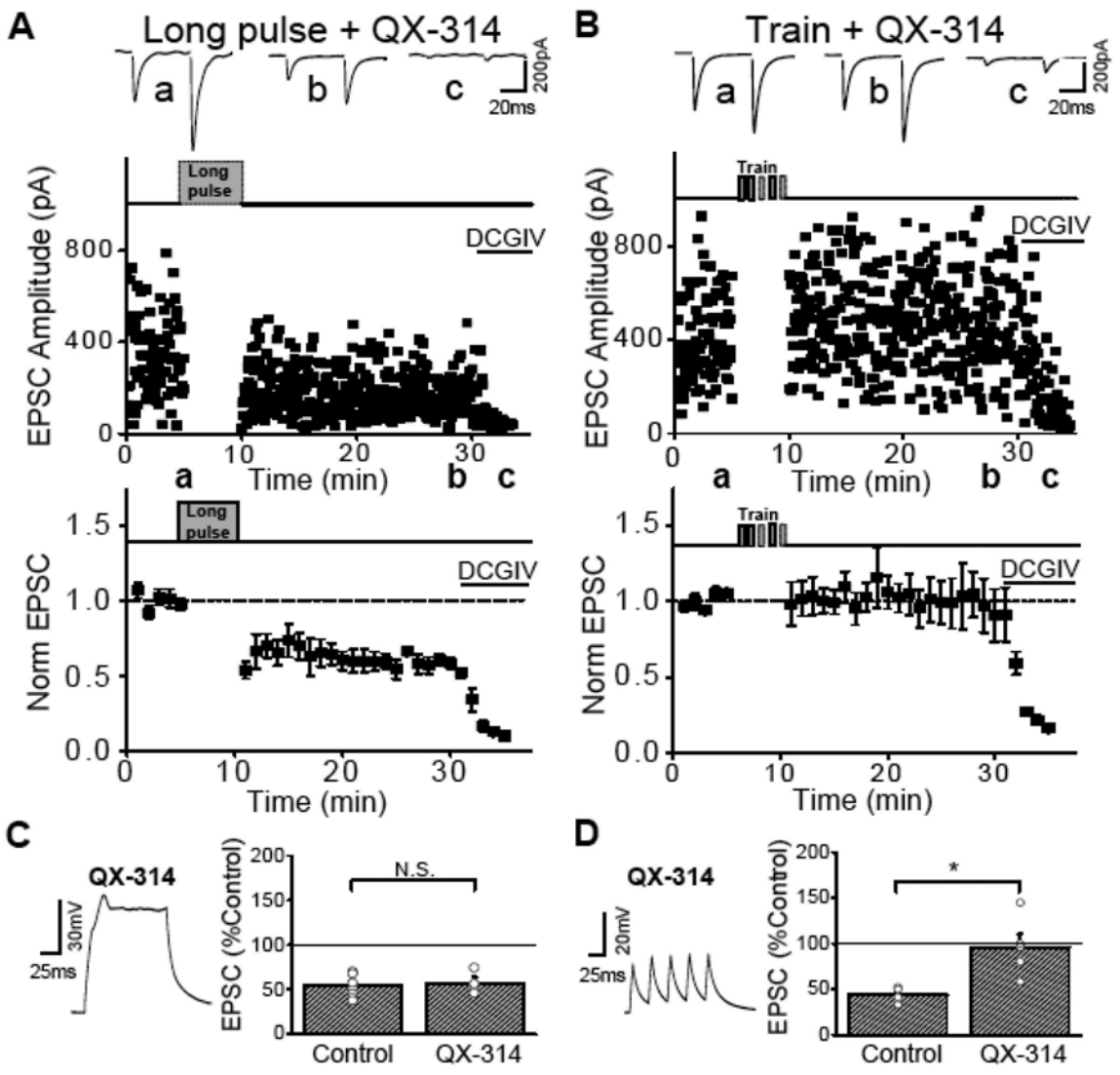

Figure 3.4 The role of AP generation in BF-induced MF-PYR LTD. A,B Representative EPSC amplitude time course plots (upper panels) and normalized group data (lower panels) for recordings in which the long pulse (A, n=4) or train (B, n=5) induction protocols were attempted in slices from young mice (<P16) using QX-314 (1mM)-supplemented intracellular solution to prevent AP firing. **C,D** Group data bar chart summary comparing LTD obtained using either the long pulse (C) or train (D) protocols for control MF-PYR recordings (Control, re-plotted from Fig. 2C&D) and recordings performed in the presence of QX-314. Also shown are sample traces of PYR responses to individual episodes of current injection in the presence of QX-314 during the long pulse (C) and train (D) induction periods. *$p<0.05$ for indicated comparisons.

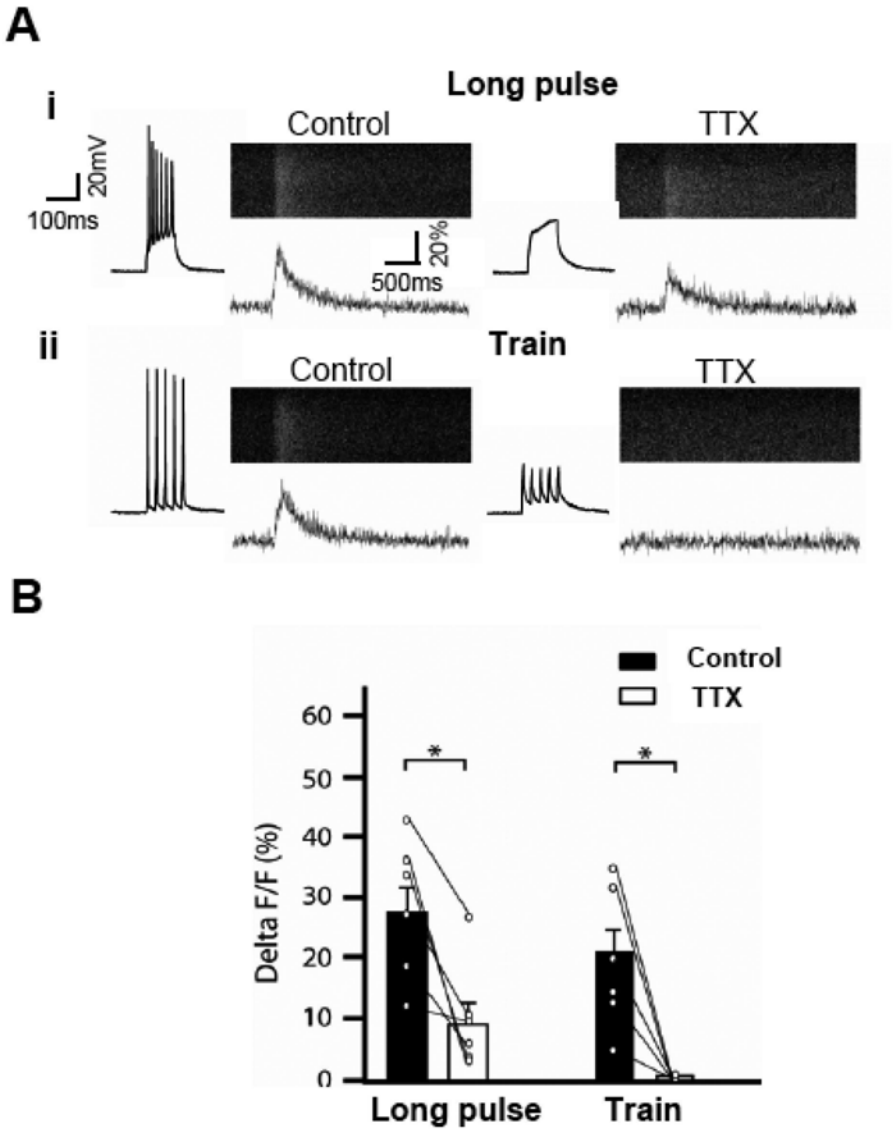

Figure 3.5 The role of AP generation associated with observed CaTs. A, PYR firing patterns and associated proximal apical dendrite CaTs observed in a representative recording with either the long pulse (i) or train (ii) protocols before and after TTX application. **B**, Bar graph summary of the effects of TTX on CaTs elicited with the long pulse and train protocols. *$p<0.05$ for indicated comparisons.

The results thus far indicate that both the long pulse and train protocols are able to promote L-VGCC dependent Ca^{2+} influx to trigger DiLTD, suggesting that natural patterns of PYR AP firing may be the physiological trigger for MF-PYR synapse depression. To confirm that AP BF serves as the critical trigger for LTD during our long pulse and train protocols, I examined whether APs are necessary to promote LTD by intracellularlly applying QX-314 to prevent PYR AP generation (Fig. 3.4). Interestingly, while intracellular application of QX-314 fully prevented LTD associated with the train protocol (96.1±14.3% of control 14-15 min after induction, n=5; Fig. 3.4B&D), it did not prevent LTD induced by the long pulse protocol (57.6±6.3% of control, n=4; Fig. 3.4A&C). A critical difference in the PYR voltage response observed with the long pulse vs. train protocol is the existence of a large plateau depolarization elicited with the long pulse protocol (cf. Fig. 3.1A). Thus, the lack of spiking requirement for the long pulse protocol in triggering DiLTD could reflect direct L-VGCC activation independent of AP generation. Indeed in Ca^{2+} imaging experiments while TTX application completely blocked CaTs associated with the train protocol (5.7±2.0% of control; Fig 3.5A&B), a significant CaT could still be elicited with the long pulse protocol (36.8±12.8% of control; Fig 3E&F), indicating that in the long pulse protocol, the increase in intracellular Ca^{2+} is contributed by both the APs and the plateau potential while the intracellular Ca^{2+} increase triggered by the train protocol is predominantly driven by APs. Because L-VGCC-dependent plasticity induced by the train protocol is AP-dependent this plasticity was named Burst Firing induced LTD (BF-LTD).

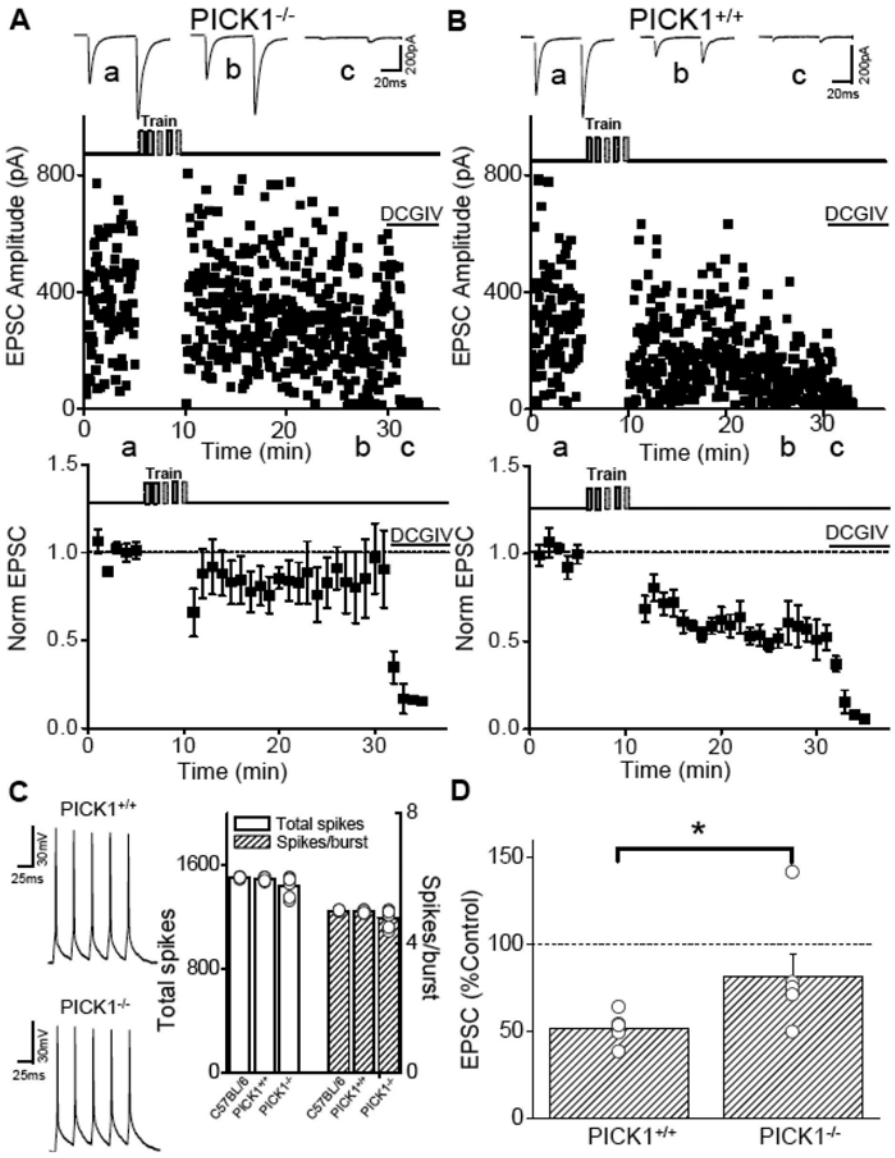

Figure 3.6 BF-driven LTD is inhibited in PICK1$^{-/-}$ mice. A,B Representative MF-PYR EPSC amplitude time course plots (upper panels) and normalized group data (lower panels) showing deficient BF-induced LTD in slices from young (<P16) PICK1$^{-/-}$ mice (A, n=6) compared to slices from littermate control PICK1$^{+/+}$ mice (B, n=6). **C** Left panel: Sample traces of PYR AP firing elicited with the train protocol in PICK1$^{+/+}$ and PICK1$^{-/-}$ mice as indicated. Right panel: Summary bar graph of total number of spikes observed during the BF-induction periods as well as the number of spikes obtained per burst in C57BL/6, PICK1$^{+/+}$ and PICK1$^{-/-}$ littermates as indicated. **D** Bar graph summary comparing BF-induced MF-PYR LTD for interleaved recordings from PICK1$^{-/-}$ and PICK1$^{+/+}$ mice. *$p<0.05$ for indicated comparison.

3.3.2 BF-driven LTD is inhibited in PICK1 KO mice

The PDZ domain-containing protein PICK1 regulates the levels of CP-AMPARs at various central synapses (Terashima et al., 2004; Bellone & Luscher, 2005; Gardner et al., 2005; Liu & Cull-Candy, 2005). Previously, we have demonstrated that PICK1 also participates in controlling the levels of CP-AMPARs at developing MF–PYR synapses, rendering them competent for DiLTD induction (Ho et al., 2007). Thus, to further confirm that BF-LTD is mechanistically related to DiLTD, we examined BF-LTD in PICK1$^{-/-}$ mice. Consistent with our previous observations for DiLTD, PICK1$^{-/-}$ mice exhibited suppressed BF-LTD: 14-15 min after induction, EPSCs were 81.6±12.7% of control responses (n = 6; Fig. 3.6A&D). In contrast, slices from age-matched wild-type (PICK1$^{+/+}$) littermates exhibited robust BF-LTD with EPSCs depressing to 52.0±3.4% of control (n = 6; Fig. 3.6B&D), while PPR and CV remained unchanged (PPR: 1.5±0.1 vs. 1.5±0.1; p=0.96; n=6, CV: 0.61±0.04 vs. 0.67±0.01; p=0.13; n=6). Results obtained from PICK1$^{+/+}$ mice were comparable to those observed in young C57BL/6 mice used throughout the study to this point (cf. Fig. 3.3B&D). Importantly, the number of APs triggered in PYRs from PICK1$^{-/-}$ and PICK1$^{+/+}$ mice was not significantly different indicating that the BF-LTD deficit in PICK1$^{-/-}$ mice is not related to an inability to reliably follow train protocol stimulation throughout the induction period (Fig. 3.6C). All these results indicate that BF-LTD and DiLTD share a similar requirement for PICK1.

3.3.3 Spontaneous AP firing by elevated $[K^+]_o$ induces DiLTD

We have demonstrated PYR BF driven by repetitively injected brief depolarizing electrotonic current pulses can sufficiently activate L-VGCCs for DiLTD induction (Fig.

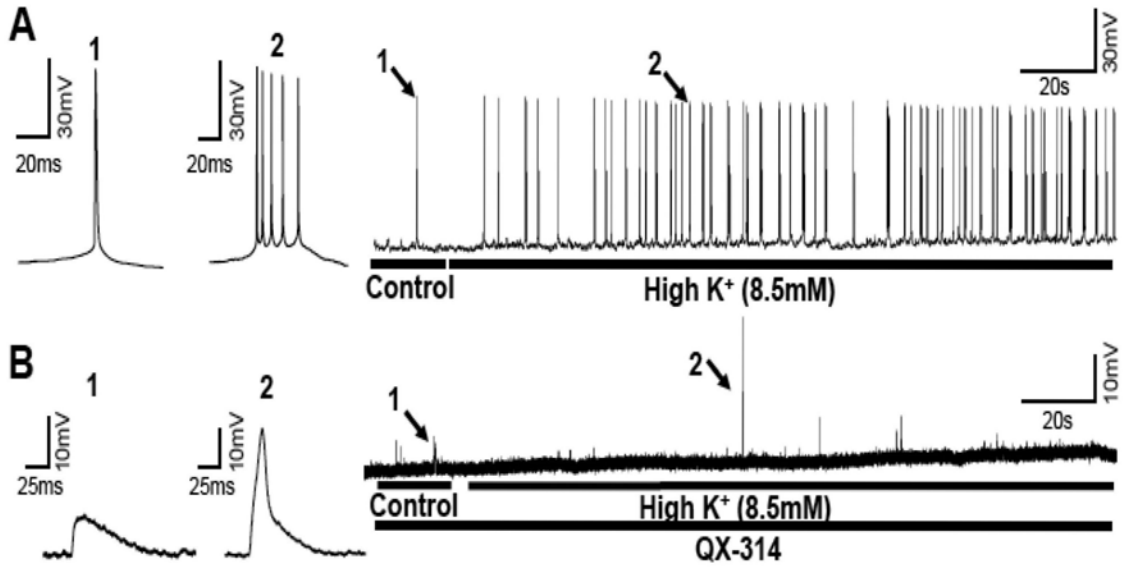

Figure 3.7 BF promoted by a transient elevation of $[K^+]_o$. **A,** Representative PYR recording in current clamp mode shows that transiently increasing $[K^+]_o$ (from 3.5 to 8.5mM) promotes BF in acute slices from young mice (<P16). **B,** In the presence of QX-314 BF firing is prevented.

3.3). However, it is still not known whether network driven BF can engage this type of plasticity. During in vivo seizure activity, interictal bursting events are accompanied by an increase in $[K^+]_o$ (Moody et al., 1974; Heinemann et al., 1977; Somjen & Giacchino, 1985) and similar interictal bursting events can be induced in vitro by modest elevation of $[K^+]_o$ from 3.5mM to 8.5mM (Rutecki et al., 1985; Traynelis & Dingledine, 1988; McBain, 1995; Aradi & Maccaferri, 2004). To examine whether intrinsically generated PYR network BF is also capable of inducing LTD, the effects of increased $[K^+]_o$ induced BF on MF-PYR synaptic transmission was examined. For these experiments, modest elevation of $[K^+]_o$ from 3.5mM to 8.5mM promoted bursting activity without the need for direct current injection. In control $[K^+]_o$ (i.e. 3.5mM), infrequent bursting was observed in 4 out of 5 cells with inter-burst frequency ranging from 0.03-0.16Hz, consistent with previous observations (Korn et al., 1987; Traynelis & Dingledine, 1988). However, within 2-3 minutes of elevated $[K^+]_o$ (i.e. 8.5mM), inter-burst frequency increased in all cells to frequencies ranging from 0.08-0.63 Hz (e.g. Fig. 3.7A). Consistent with the ability of PYR BF to drive LTD, following exposure to elevated $[K^+]_o$, MF-PYR evoked EPSCs depressed to 42.1$\pm$10.1% of control (n=5; Fig. 3.8A). Prolonged incubation of hippocampal cultured neurons in highly elevated $[K^+]_o$ (35mM) has been reported to alter presynaptic release probability (Moulder et al., 2004). However, the LTD induced by 5 minutes of modest $[K^+]_o$ elevation to 8.5mM to induce BF was not accompanied by changes in PPR (1.6$\pm$0.1 vs. 1.6$\pm$0.1; p=0.93; n=5) and CV (0.42$\pm$0.03 vs. 0.50$\pm$0.03; p=0.06; n=5) indicating that the reduced transmission observed following high $[K^+]_o$ treatment likely results from postsynaptic changes rather than alterations in presynaptic

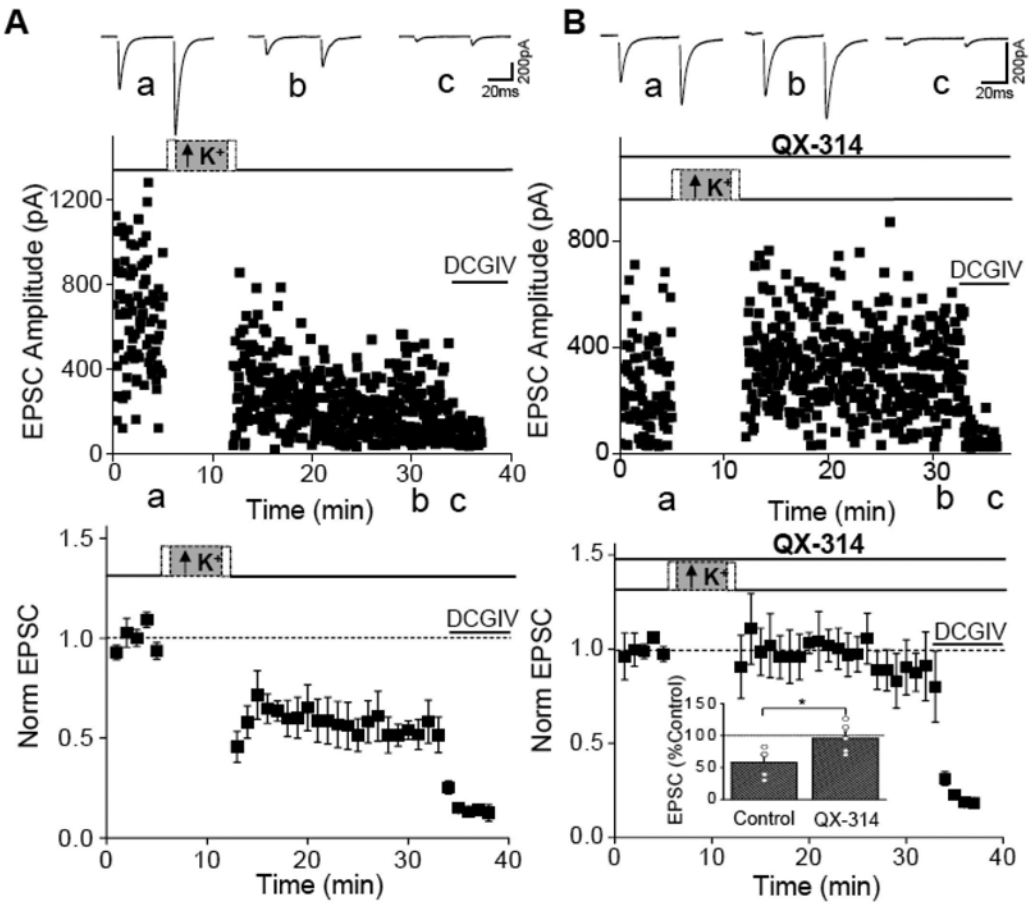

Figure 3.8 BF promoted by a transient elevation of $[K^+]_o$ induces MF-PYR LTD. A, Representative MF-PYR EPSC amplitude time course plot (upper panel) and normalized group data (lower panel, n=5) showing that 5 min of high $[K^+]_o$-induced BF generates LTD in slices from young mice (<P16). **B,** Representative EPSC amplitude time course plot (upper panel) and normalized group data (lower panel, n=5) for recordings in which the high $[K^+]_o$ LTD induction protocol was attempted in the presence of QX-314. Inset (D, lower panel) bar graph compares LTD observed using the high $[K^+]_o$ induction protocol for interleaved control and QX-314 recordings. *p<0.05 for indicated comparison.

release properties. Inclusion of intracellular QX-314 eliminated bursting events although the occasional plateau potential was still observed (Fig. 3.7B). Importantly, BF-driven LTD was blocked in recordings with QX-314 (95.6±10.7% of control; n=5, Fig. 3.8B) demonstrating the importance of AP generation in triggering BF-LTD. Interestingly, unlike the plateau potentials that occur with the long pulse protocol the "naturally" driven plateau potentials are incapable of triggering DiLTD demonstrating a requirement for AP generation to trigger LTD during network driven BF.

Chapter 4
Final Discussion

I. Developmental expression of Ca^{2+}-permeable AMPA receptors underlies depolarization-induced long-term depression at mossy fiber CA3 pyramid synapses.

In the mature CNS, excitatory transmission between principal neurons is dominated by CI-AMPARs because of prominent expression of edited GluR2 subunits within postsynaptic AMPARs. However, GluR2-lacking, CP-AMPARs participate at principal cell synapses early in development in various central structures (Pellegrini-Giampietro *et al.*, 1992b; Pickard *et al.*, 2000; Zhu *et al.*, 2000; Aizenman *et al.*, 2002; Kumar *et al.*, 2002; Eybalin *et al.*, 2004; Migues *et al.*, 2007). Here, I examined whether CP-AMPARs contribute at developing MF–PYR synapses using imaging and electrophysiological approaches. I found that MF–PYR transmission within the first 2–3 postnatal weeks uses a mixed population of CP- and CI-AMPARs. CP-AMPAR participation at MF–PYR synapses is developmentally regulated as CI-AMPARs dominate beyond P17. This temporal profile parallels the period during which MF–PYR synapses are DiLTD competent, and our findings suggest that CP-AMPARs are selectively targeted during DiLTD. Consistent with preferential removal of CP-AMPARs during DiLTD, young MF–PYR synapses lacking CP-AMPARs because of PICK1 disruption were DiLTD deficient. These data also revealed that PICK1 regulates the GluR2 content of MF–PYR synapses as reported previously (Terashima *et al.*, 2004; Gardner *et al.*, 2005; Liu & Cull-Candy, 2005; Bellone & Luscher, 2006). I conclude that expression of CP-AMPARs dictates the developmental window for DiLTD and additionally propose that DiLTD proceeds as the PICK1-dependent exchange of CI-AMPARs for CP-AMPARs reminiscent of plasticity in cerebellar stellate cells and VTA neurons (Gardner *et al.*, 2005; Liu & Cull-Candy, 2005; Bellone & Luscher, 2006).

Previous studies did not observe rectifying I–V curves or PhTx sensitivity of MF–PYR synaptic events in P15–P25 rat slices (Jonas et al., 1993; Toth et al., 2000). This age range biases toward developmental stages where MF–PYR transmission is entirely supported by CI-AMPARs, likely explaining the differences with our findings. Additionally, (Jonas et al., 1993) performed their study before the discovery that CP-AMPAR rectification results from intracellular polyamines, and so it was not common practice to supplement intracellular solutions with polyamines. Because spermine supplementation is critical for MF–PYR rectification (Fig. 1D), this may have also contributed to the lack of rectification in the previous investigation. Subsequently, Jonas and colleagues examined rectification properties of PYR somatic membrane patches from P13–P15 rat slices and again observed linear I–V relationships even with spermine present (Koh et al., 1995). This difference with our findings cannot be attributed to age differences or lack of spermine supplementation and, thus, indicates that young PYR extrasynaptic membranes are rich in CI-AMPARs. Similarly, CI-AMPARs dominate extrasynaptic membranes of cerebellar stellate cells and developing layer 5 pyramids despite synaptic expression of CP-AMPARs (Liu & Cull-Candy, 2000; Kumar & Huguenard, 2001; Kumar *et al.*, 2002; Gardner *et al.*, 2005). Additionally, I found that associational/commissural-PYR transmission is mediated solely by CI-AMPARs during early development. Considered together, the evidence indicates that during the first 2–3 postnatal weeks PYRs express CP-AMPARs in a synapse-specific manner. Species-dependent differences in synaptic expression of CP-AMPARs also exist (Bellone & Luscher, 2005, 2006); therefore, whether our observations in mouse differed from previous reports because of choice of experimental animal is a concern. However, both imaging and electrophysiological

recordings confirmed participation of CP-AMPARs at developing rat MF–PYR synapses. The imaging experiments also provided direct evidence for Ca^{2+} permeability of MF–PYR AMPARs, an important consideration because Ca^{2+} permeability is more sensitive to GluR2 content than is rectification or PhTx sensitivity (Dingledine et al., 1992; Washburn et al., 1997). A previous study in slice culture found that MF evoked CaTs in PYR spines were insensitive to the CP-AMPAR antagonist HPP-spermine [N-(4-hydroxyphenylpropanoyl)-spermine] (Reid et al., 2001). Again, this discrepancy with the findings likely reflects the limited developmental expression of CP-AMPARs at MF–PYR synapses as slices were obtained at P8 and cultured for 10–21 days.

CP-AMPARs impart distinct short- and long-term plasticity to various central synapses (Rozov *et al.*, 1998; Rozov & Burnashev, 1999; Liu & Cull-Candy, 2000; Toth *et al.*, 2000; Lei & McBain, 2002; Bellone & Luscher, 2005; Gardner *et al.*, 2005; Pelkey *et al.*, 2005; Shin *et al.*, 2005; Pelkey *et al.*, 2006). The loss of CaTs and decreased rectification after DiLTD induction indicate that CP-AMPARs are selectively depressed during DiLTD. Accordingly, MF–PYR synapses devoid of CP-AMPARs, in slices from older animals or after PICK1 disruption, do not exhibit DiLTD. The CI-AMPARs that support transmission after DiLTD appear to principally reflect the population initially present at naive synapses. However, the occasionally observed EPSC growth at +40 mV, particularly for the second EPSC in pairs of events (Fig. 2.5A, traces), suggests that CI-AMPARs may also be exchanged for CP-AMPARs after DiLTD, similar to LTD in cerebellar stellate cells and dopaminergic VTA neurons (Liu & Cull-Candy, 2000; Bellone & Luscher, 2005; Gardner *et al.*, 2005). The initial wide range of RIs at naive

MF–PYR synapses combined with the large variability in presynaptic release and low number of events collected at +40 mV in the recordings may have confounded reliable detection of EPSC growth at positive potentials. The greater success in observing such growth on the second EPSC of evoked pairs could reflect increased release probability combined with perisynaptic localization of new CI-AMPARs that will diffuse laterally to postsynaptic sites.

PICK1 as an important regulator of synaptic GluR2

The loss of CP-AMPAR-mediated MF–PYR transmission after PICK1 disruption was surprising because cerebellar stellate cells maintain, or even increase, the synaptic complement of CP-AMPARs after EVKI treatment or PICK1 knock-out (Gardner *et al.*, 2005; Liu & Cull-Candy, 2005). However, our findings are consistent with observations in CA1 pyramids in which PICK1 overexpression promotes CP-AMPAR accumulation at synapses, whereas EVKI overexpression increases GluR2 content (Terashima et al., 2004). Similarly, small interfering RNA knockdown of PICK1 promotes membrane insertion of GluR2-containing receptors (Sossa et al., 2006). Development of a unified model for PICK1 in regulating synaptic AMPAR composition is hampered by conflicting findings at distinct synapses, suggesting that PICK1 functions in a cell- and synapse-specific manner. For example, a well defined role for PICK1 in GluR2-containing AMPAR internalization exists at cerebellar parallel fiber–Purkinje neuron synapses (Xia *et al.*, 2000; Steinberg *et al.*, 2006), whereas stellate cells require PICK1 for synaptic delivery of GluR2-containing AMPARs (Gardner *et al.*, 2005; Liu & Cull-Candy, 2005).

Thus, evidence supports roles for PICK1 in AMPAR internalization and surface delivery. Indeed, PICK1 supports bidirectional changes in surface AMPARs (Sossa et al., 2006). This duality of function likely reflects the Ca^{2+} binding properties of PICK1, which yield bimodal regulation of PICK1–GluR2 interactions (Hanley & Henley, 2005; Sossa *et al.*, 2006). Our findings suggest a model in which PICK1 maintains intracellular pools of GluR2-containing AMPARs (Jin et al., 2006), which are trafficked to the surface after appropriate stimuli like increased intracellular Ca^{2+}. Loss of PICK1–GluR2 interactions by highly elevated intracellular Ca^{2+}, EVKI treatment, or PICK1 knock-out could promote mobilization of this CI-AMPAR intracellular pool to the surface, which subsequently may trigger removal of synaptic CP-AMPARs, allowing for synaptic incorporation of the CI-AMPARs through lateral diffusion. Although additional investigation is needed to characterize molecular events controlling AMPAR trafficking at MF–PYR synapses, the findings in this thesis further implicate PICK1 as an important regulator of synaptic GluR2 (Terashima *et al.*, 2004; Bellone & Luscher, 2005; Gardner *et al.*, 2005; Liu & Cull-Candy, 2005).

The critical trigger for DiLTD induction is an increase in postsynaptic Ca^{2+} by influx through L-type VGCCs and release from intracellular stores (Lei et al., 2003). Similarly, loss of synaptic CP-AMPARs in cerebellar stellate cells and VTA dopaminergic neurons is triggered by increased intracellular Ca^{2+} (Liu & Cull-Candy, 2000; Bellone & Luscher, 2005). CP-AMPAR removal may serve a protective feedback mechanism to combat additional cytosolic Ca^{2+} increases that can be deleterious for the postsynaptic cell (Sattler & Tymianski, 2000; Arundine & Tymianski, 2003). Alternatively, excess Ca^{2+} influx

through the CP-AMPARs themselves could provide a self-regulating mechanism triggering CP-AMPAR removal (Liu & Cull-Candy, 2000).

II. Burst firing induces postsynaptic LTD at developing mossy fiber-CA3 pyramid synapses

CA3 PYRs display intense synchronized network bursting behavior during the second and third postnatal weeks (Swann et al., 1993 Smith et al., 1995) coincident with the period of MF-synapse development (Amaral & Dent, 1981) and the emergence of functional L-VGCCs along PYR proximal apical dendrites in close proximity to MF inputs (Westenbroek et al., 1990; Glazewski et al., 1993; Hell et al., 1993; Elliott et al., 1995). This period also coincides with the developmental window of DiLTD competence at MF-PYR synapses, an NMDAR-independent form of postsynaptic plasticity driven by PYR L-VGCC activation (Lei et al., 2003; Ho et al., 2007). Based on this temporal overlap of BF emergence, L-VGCC upregulation, and DiLTD competence combined with the implicit role of L-VGCC activity in triggering DiLTD we reasoned that L-VGCC activation promoted by network bursting could serve as a physiologically relevant stimulus for DiLTD induction. Our imaging experiments directly revealed that BF does indeed activate L-VGCCs promoting Ca^{2+} influx within PYR proximal apical dendrites, confirming previous electrophysiological findings that PYR BF allows Ca^{2+} entry through L-VGCCs to regulate spike after-potentials (Aicardi & Schwartzkroin, 1990; Empson & Jefferys, 2001). Moreover, consistent with the hypothesis a transient period of PYR BF is capable of inducing LTD of MF-PYR transmission. Like DiLTD the

newly discovered BF-LTD is NMDAR-independent, L-VGCC-dependent, specific to MF-PYR synapses, expressed postsynaptically, and compromised in PICK1$^{-/-}$ mice. Based on these findings we conclude that PYR BF and tonic depolarization ultimately lead to the same form of MF-PYR plasticity suggesting a previously unsuspected role for the engagement of naturally occurring CA3 network BF patterns in MF synapse maturation.

BF as a common induction mechanism for activity-dependent development and plasticity

PYR network BF also triggers NMDAR-dependent postsynaptically expressed long-term plasticity at mature and immature collateral fiber- and perforant path-PYR synapses respectively (Smith et al., 1995; Bains et al., 1999; Stoop et al., 2003). Additionaly, a recent study revealed that PYR BF can promote long-term changes in PYR intrinsic excitability by persistently enhancing Kv7 channel function to inhibit spike after-depolarization potentials (Brown & Randall, 2009). Thus, PYR network BF may serve as a common induction mechanism to critically regulate diverse forms of activity-dependent development and plasticity within the hippocampal CA3 circuit.

PICK1 serves as a point of convergence for the regulation of surface GluR2 during synapse maturation

L-VGCC driven LTD in the developing MF system results in part from the loss of GluR2-lacking AMPARs present at nascent MF-PYR synapses converting them into GluR2-containing AMPAR dominated synapses that prevail at fully developed MF-PYR

contacts (Ho et al., 2007). A similar transient developmental period of GluR2-lacking AMPAR expression occurs at diverse central synapses and these receptors may provide a postsynaptic Ca^{2+} signal important for synapse maturation (Pellegrini-Giampietro et al., 1992; Pickard et al., 2000; Zhu et al., 2000; Kumar et al., 2002; Migues et al., 2007; Brill & Huguenard, 2008). While a canonical developmental trigger for the loss of GluR2-lacking AMPARs at immature synapses has not emerged, abundant evidence supports roles for intracellular Ca^{2+} and PICK1 in regulating surface GluR2 levels (Liu & Cull-Candy, 2000, 2002, 2005; Gardner et al., 2005; Terashima et al., 2004, 2008; Bellone & Luscher, 2005, 2006; Sossa et al., 2006, 2007). Similarly, BF-LTD was found to rely on increased intracellular Ca^{2+} and PICK1 signaling. Thus, although the route of Ca^{2+} entry may differ (eg. Liu and Cull-Candy, 2000; Bellone and Luscher, 2005), it seems likely that PICK1 serves as a point of convergence for the regulation of surface GluR2 during synapse maturation within diverse central circuits **(Fig. 4).** Whether developmental alterations in AP firing patterns serve to promote Ca^{2+} influx and loss of GluR2-lacking AMPARs at other immature central synapses remains to be determined. However, it is interesting to note that cerebellar granule cell AP firing has the capacity to regulate surface levels of GluR2-containing and lacking AMPARs at extrasynaptic sites (Liu & Cull-Candy, 2000, 2002).

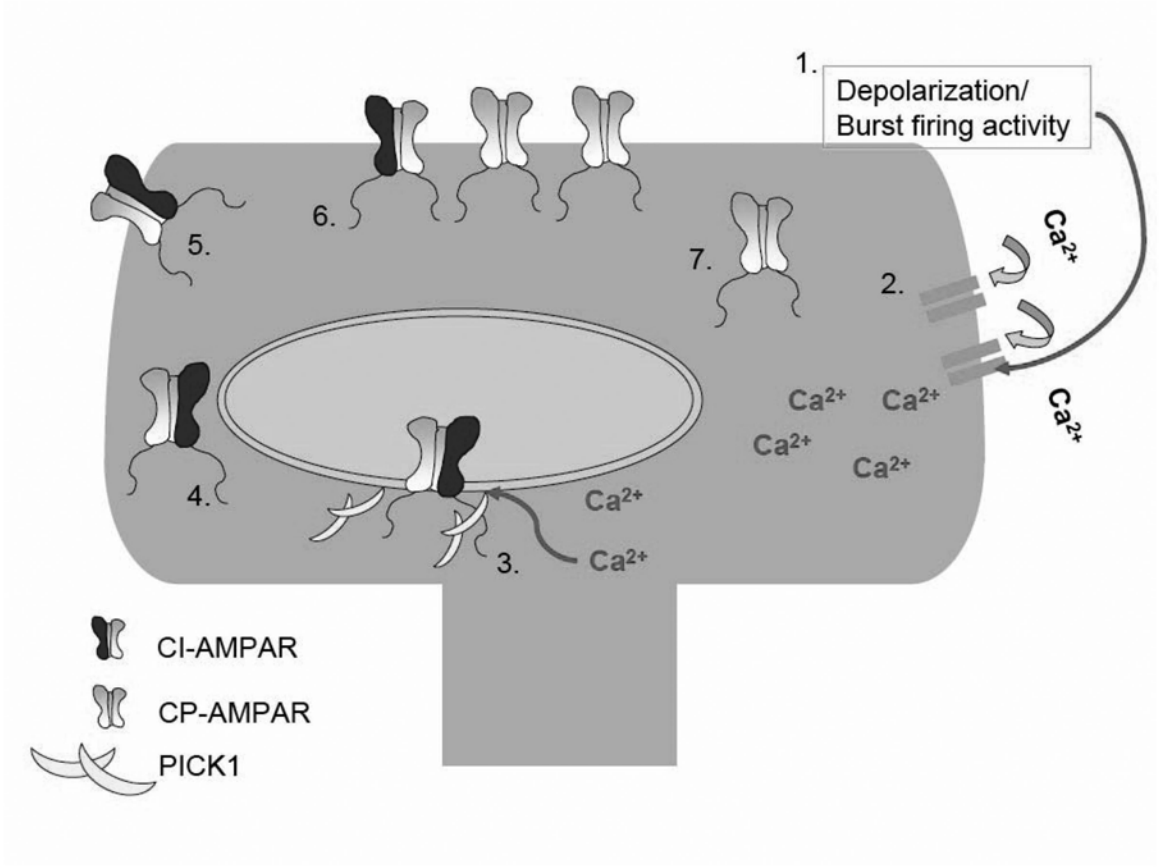

Figure 4 Schematic showing PICK1 as an important regulator of synaptic GluR2. Intense neuronal activity like depolarization or burst firing results in influx of Ca^{2+} through L-VGCCs (1 & 2). Loss of PICK1–GluR2 interactions by the increase in Ca^{2+} (3). GluR2 containing AMPARs moved into the extrasynaptic area (4 & 5). GluR2 containing AMPARs moved into synaptic area through lateral diffusion (6). Subsequent removal of GluR2 lacking AMPARs from the synaptic area (7).

Conclusion

In conclusion, I found that CP-AMPARs contribute to nascent MF–PYR transmission within the first 3 postnatal weeks. This early participation of CP-AMPARs likely provides a postsynaptic Ca^{2+} signal important for synapse maturation. I also demonstrate that the CP-AMPARs express in immature MF-PYR synapses can be removed from synapses during DiLTD. Interestingly, recent findings suggest that similar phenomenon may occur during various forms of synaptic plasticity in the mature CNS, although on more rapid timescales (Thiagarajan *et al.*, 2005; Clem & Barth, 2006; McCormack *et al.*, 2006; Plant *et al.*, 2006; Sutton *et al.*, 2006), further linking the processes of synapse development and plasticity.

What can be the natural process that drives the removal of CP-AMPARs from the immature synapses? Developing synapses are believed to proceed from silent, with transmission solely mediated by NMDARs, to functional by the stepwise acquisition of AMPARs (Isaac, 2003; Poncer, 2003). The conversion from silent to functional synapses is suggested to result from NMDAR activation during synchronized network activity driven by GABAergic mediated GDPs (Ben-Ari et al., 1997; Leinekugel, 2003). My findings in the previous section, along with other reports (Pellegrini-Giampietro *et al.*, 1992b; Pickard *et al.*, 2000; Zhu *et al.*, 2000; Aizenman *et al.*, 2002; Kumar *et al.*, 2002; Eybalin *et al.*, 2004; Migues *et al.*, 2007) indicate the transient incorporation of CP-AMPARs may represent a previously unappreciated step at many central synapses in this model. In the second part of my thesis research, further evidence was provided that the emergence of PYR BF has the capacity to serve as the developmental trigger for nascent

functional MF-PYR synapses to exit this transient immature form and adopt a mature phenotype with transmission dominated by GluR2-containing AMPARs. Thus, it appears that synchronized PYR network activity driven by distinct circuit mechanisms differentially shapes MF-PYR synaptic AMPAR profiles throughout synapse development from silent to fully mature connections.

References

1. Acsady L, Kamondi A, Sik A, Freund T & Buzsaki G. (1998). GABAergic cells are the major postsynaptic targets of mossy fibers in the rat hippocampus. Journal of Neuroscience **18,** 3386-3403.

2. Aicardi G & Schwartzkroin PA. (1990). Suppression of epileptiform burst discharges in CA3 neurons of rat hippocampal slices by the organic calcium channel blocker, verapamil. Experimental Brain Research Experimentelle Hirnforschung **81,** 288-296.

3. Aizenman CD, Munoz-Elias G & Cline HT. (2002). Visually driven modulation of glutamatergic synaptic transmission is mediated by the regulation of intracellular polyamines. Neuron **34,** 623-634.

4. Altman J & Das GD. (1967). Postnatal neurogenesis in the guinea-pig. Nature **214,** 1098-1101.

5. Amaral DG & Dent JA. (1981). Development of the mossy fibers of the dentate gyrus: I. A light and electron microscopic study of the mossy fibers and their expansions. The Journal of Comparative Neurology **195,** 51-86.

6. Aradi I & Maccaferri G. (2004). Cell type-specific synaptic dynamics of synchronized bursting in the juvenile CA3 rat hippocampus. Journal of Neuroscience **24,** 9681-9692.

7. Arundine M & Tymianski M. (2003). Molecular mechanisms of calcium-dependent neurodegeneration in excitotoxicity. Cell Calcium **34,** 325-337.

8. Ayalon G & Stern-Bach Y. (2001). Functional assembly of AMPA and kainate receptors is mediated by several discrete protein-protein interactions. Neuron **31,** 103-113.

9. Babb TL, Brown WJ, Pretorius J, Davenport C, Lieb JP & Crandall PH. (1984). Temporal lobe volumetric cell densities in temporal lobe epilepsy. Epilepsia **25,** 729-740.

10. Babb TL, Kupfer WR, Pretorius JK, Crandall PH & Levesque MF. (1991). Synaptic reorganization by mossy fibers in human epileptic fascia dentata. Neuroscience **42,** 351-363.

11. Bagal AA, Kao JP, Tang CM & Thompson SM. (2005). Long-term potentiation of exogenous glutamate responses at single dendritic spines. Proceedings of the National Academy of Sciences of the United States of America **102,** 14434-14439.

12. Bahn S, Volk B & Wisden W. (1994). Kainate receptor gene expression in the developing rat brain. Journal of Neuroscience **14,** 5525-5547.

13. Baier H & Bonhoeffer F. (1992). Axon guidance by gradients of a target-derived component. Science **255,** 472-475.

14. Bains JS, Longacher JM & Staley KJ. (1999). Reciprocal interactions between CA3 network activity and strength of recurrent collateral synapses. Nature Neuroscience **2,** 720-726.

15. Barria A, Derkach V & Soderling T. (1997a). Identification of the Ca2+/calmodulin-dependent protein kinase II regulatory phosphorylation site in the alpha-amino-3-hydroxyl-5-methyl-4-isoxazole-propionate-type glutamate receptor. Journal of Biological Chemistry **272,** 32727-32730.

16. Barria A, Muller D, Derkach V, Griffith LC & Soderling TR. (1997b). Regulatory phosphorylation of AMPA-type glutamate receptors by CaM-KII during long-term potentiation. Science **276,** 2042-2045.

17. Battistin T & Cherubini E. (1994). Developmental shift from long-term depression to long-term potentiation at the mossy fibre synapses in the rat hippocampus. European Journal of Neuroscience **6,** 1750-1755.

18. Bellone C & Luscher C. (2005). mGluRs induce a long-term depression in the ventral tegmental area that involves a switch of the subunit composition of AMPA receptors. European Journal of Neuroscience **21,** 1280-1288.

19. Bellone C & Luscher C. (2006). Cocaine triggered AMPA receptor redistribution is reversed in vivo by mGluR-dependent long-term depression. Nature Neuroscience **9,** 636-641.

20. Ben-Ari Y, Cherubini E, Corradetti R & Gaiarsa JL. (1989). Giant synaptic potentials in immature rat CA3 hippocampal neurones. The Journal of physiology **416,** 303-325.

21. Ben-Ari Y & Gho M. (1988). Long-lasting modification of the synaptic properties of rat CA3 hippocampal neurones induced by kainic acid. The Journal of Physiology **404,** 365-384.

22. Bennett JA & Dingledine R. (1995). Topology profile for a glutamate receptor: three transmembrane domains and a channel-lining reentrant membrane loop. Neuron **14,** 373-384.

23. Berretta N, Rossokhin AV, Cherubini E, Astrelin AV & Voronin LL. (1999). Long-term synaptic changes induced by intracellular tetanization of CA3 pyramidal neurons in hippocampal slices from juvenile rats. Neuroscience **93,** 469-477.

24. Berzhanskaya J, Urban NN & Barrionuevo G. (1998). Electrophysiological and pharmacological characterization of the direct perforant path input to hippocampal area CA3. Journal of neurophysiology **79,** 2111-2118.

25. Bettler B, Boulter J, Hermans-Borgmeyer I, O'Shea-Greenfield A, Deneris ES, Moll C, Borgmeyer U, Hollmann M & Heinemann S. (1990). Cloning of a novel glutamate receptor subunit, GluR5: expression in the nervous system during development. Neuron **5,** 583-595.

26. Bilkey DK & Schwartzkroin PA. (1990). Variation in electrophysiology and morphology of hippocampal CA3 pyramidal cells. Brain research **514,** 77-83.

27. Birtoli B & Ulrich D. (2004). Firing mode-dependent synaptic plasticity in rat neocortical pyramidal neurons. Journal of Neuroscience **24,** 4935-4940.

28. Blackstad TW, Brink K, Hem J & Jeune B. (1970). Distribution of hippocampal mossy fibers in the rat. An experimental study with silver impregnation methods. The Journal of Comparative Neurology **138,** 433-449.

29. Bladt F, Tafuri A, Gelkop S, Langille L & Pawson T. (2002). Epidermolysis bullosa and embryonic lethality in mice lacking the multi-PDZ domain protein GRIP1. Proceedings of the National Academy of Sciences of the United States of America **99,** 6816-6821.

30. Bolea S, Avignone E, Berretta N, Sanchez-Andres JV & Cherubini E. (1999). Glutamate controls the induction of GABA-mediated giant depolarizing potentials through AMPA receptors in neonatal rat hippocampal slices. Journal of Neurophysiology **81,** 2095-2102.

31. Bortolotto ZA, Clarke VR, Delany CM, Parry MC, Smolders I, Vignes M, Ho KH, Miu P, Brinton BT, Fantaske R, Ogden A, Gates M, Ornstein PL, Lodge D,

Bleakman D & Collingridge GL. (1999). Kainate receptors are involved in synaptic plasticity. Nature **402,** 297-301.

32. Boulter J, Hollmann M, O'Shea-Greenfield A, Hartley M, Deneris E, Maron C & Heinemann S. (1990). Molecular cloning and functional expression of glutamate receptor subunit genes. Science **249,** 1033-1037.

33. Bowie D & Mayer ML. (1995). Inward rectification of both AMPA and kainate subtype glutamate receptors generated by polyamine-mediated ion channel block. Neuron **15,** 453-462.

34. Breustedt J & Schmitz D. (2004). Assessing the role of GLUK5 and GLUK6 at hippocampal mossy fiber synapses. Journal of Neuroscience **24,** 10093-10098.

35. Bronner-Fraser M. (1986). An antibody to a receptor for fibronectin and laminin perturbs cranial neural crest development in vivo. Developmental Biology **117,** 528-536.

36. Buckmaster PS & Dudek FE. (1997). Neuron loss, granule cell axon reorganization, and functional changes in the dentate gyrus of epileptic kainate-treated rats. The Journal of Comparative Neurology **385,** 385-404.

37. Burette A, Wyszynski M, Valtschanoff JG, Sheng M & Weinberg RJ. (1999). Characterization of glutamate receptor interacting protein-immunopositive neurons in cerebellum and cerebral cortex of the albino rat. The Journal of Comparative Neurology **411,** 601-612.

38. Burnashev N, Khodorova A, Jonas P, Helm PJ, Wisden W, Monyer H, Seeburg PH & Sakmann B. (1992a). Calcium-permeable AMPA-kainate receptors in fusiform cerebellar glial cells. Science **256,** 1566-1570.

39. Burnashev N, Monyer H, Seeburg PH & Sakmann B. (1992b). Divalent ion permeability of AMPA receptor channels is dominated by the edited form of a single subunit. Neuron **8,** 189-198.

40. Burrone J & Murthy VN. (2003). Synaptic gain control and homeostasis. Current Opinion in Neurobiology **13,** 560-567.

41. Busetto G, Higley MJ & Sabatini BL. (2008). Developmental presence and disappearance of postsynaptically silent synapses on dendritic spines of rat layer 2/3 pyramidal neurons. The Journal of Physiology **586,** 1519-1527.

42. Castillo PE, Janz R, Sudhof TC, Tzounopoulos T, Malenka RC & Nicoll RA. (1997a). Rab3A is essential for mossy fibre long-term potentiation in the hippocampus. Nature **388,** 590-593.

43. Castillo PE, Malenka RC & Nicoll RA. (1997b). Kainate receptors mediate a slow postsynaptic current in hippocampal CA3 neurons. Nature **388,** 182-186.

44. Castillo PE, Schoch S, Schmitz F, Sudhof TC & Malenka RC. (2002). RIM1alpha is required for presynaptic long-term potentiation. Nature **415,** 327-330.

45. Castillo PE, Weisskopf MG & Nicoll RA. (1994). The role of Ca2+ channels in hippocampal mossy fiber synaptic transmission and long-term potentiation. Neuron **12,** 261-269.

46. Chapman B & Stryker MP. (1992). Origin of orientation tuning in the visual cortex. Current Opinion in Neurobiology **2,** 498-501.

47. Chapman B & Stryker MP. (1993). Development of orientation selectivity in ferret visual cortex and effects of deprivation. Journal of Neuroscience **13,** 5251-5262.

48. Chen L, Chetkovich DM, Petralia RS, Sweeney NT, Kawasaki Y, Wenthold RJ, Bredt DS & Nicoll RA. (2000). Stargazin regulates synaptic targeting of AMPA receptors by two distinct mechanisms. Nature **408,** 936-943.

49. Chen L, El-Husseini A, Tomita S, Bredt DS & Nicoll RA. (2003). Stargazin differentially controls the trafficking of alpha-amino-3-hydroxyl-5-methyl-4-isoxazolepropionate and kainate receptors. Molecular Pharmacology **64,** 703-706.

50. Chicurel ME & Harris KM. (1992). Three-dimensional analysis of the structure and composition of CA3 branched dendritic spines and their synaptic relationships with mossy fiber boutons in the rat hippocampus. The Journal of Comparative Neurology **325,** 169-182.

51. Cherubini E, Gaiarsa JL & Ben-Ari Y. (1991). GABA: an excitatory transmitter in early postnatal life. Trends in Neurosciences **14,** 515-519.

52. Chittajallu R, Vignes M, Dev KK, Barnes JM, Collingridge GL & Henley JM. (1996). Regulation of glutamate release by presynaptic kainate receptors in the hippocampus. Nature **379,** 78-81.

53. Chung HJ, Xia J, Scannevin RH, Zhang X & Huganir RL. (2000). Phosphorylation of the AMPA receptor subunit GluR2 differentially regulates its interaction with PDZ domain-containing proteins. Journal of Neuroscience **20,** 7258-7267.

54. Claiborne BJ, Amaral DG & Cowan WM. (1986). A light and electron microscopic analysis of the mossy fibers of the rat dentate gyrus. The Journal of Comparative neurology **246,** 435-458.

55. Clark BA & Cull-Candy SG. (2002). Activity-dependent recruitment of extrasynaptic NMDA receptor activation at an AMPA receptor-only synapse. Journal of Neuroscience **22,** 4428-4436.

56. Clem RL & Barth A. (2006). Pathway-specific trafficking of native AMPARs by in vivo experience. Neuron **49,** 663-670.

57. Cohan CS. (1990). Frequency-dependent and cell-specific effects of electrical activity on growth cone movements of cultured Helisoma neurons. Journal of Neurobiology **21,** 400-413.

58. Collingridge GL, Isaac JT & Wang YT. (2004). Receptor trafficking and synaptic plasticity. Nature Review Neuroscience **5,** 952-962.

59. Contractor A, Sailer AW, Darstein M, Maron C, Xu J, Swanson GT & Heinemann SF. (2003). Loss of kainate receptor-mediated heterosynaptic facilitation of mossy-fiber synapses in $KA2^{-/-}$ mice. Journal of Neuroscience **23,** 422-429.

60. Contractor A, Swanson G & Heinemann SF. (2001). Kainate receptors are involved in short- and long-term plasticity at mossy fiber synapses in the hippocampus. Neuron **29,** 209-216.

61. Contractor A, Swanson GT, Sailer A, O'Gorman S & Heinemann SF. (2000). Identification of the kainate receptor subunits underlying modulation of excitatory synaptic transmission in the CA3 region of the hippocampus. Journal of Neuroscencei **20,** 8269-8278.

62. Cronin J & Dudek FE. (1988). Chronic seizures and collateral sprouting of dentate mossy fibers after kainic acid treatment in rats. Brain Research **474,** 181-184.

63. Cull-Candy S, Brickley S & Farrant M. (2001). NMDA receptor subunits: diversity, development and disease. Current Opinion in Neurobiology **11,** 327-335.

64. Cull-Candy S, Kelly L & Farrant M. (2006). Regulation of Ca2+-permeable AMPA receptors: synaptic plasticity and beyond. Current Opinion in Neurobiology **16,** 288-297.

65. Czarnecki A, Birtoli B & Ulrich D. (2007). Cellular mechanisms of burst firing-mediated long-term depression in rat neocortical pyramidal cells. The Journal of Physiology **578,** 471-479.

66. Darstein M, Petralia RS, Swanson GT, Wenthold RJ & Heinemann SF. (2003). Distribution of kainate receptor subunits at hippocampal mossy fiber synapses. Journal of Neuroscience **23,** 8013-8019.

67. Daw MI, Chittajallu R, Bortolotto ZA, Dev KK, Duprat F, Henley JM, Collingridge GL & Isaac JT. (2000). PDZ proteins interacting with C-terminal GluR2/3 are involved in a PKC-dependent regulation of AMPA receptors at hippocampal synapses. Neuron **28,** 873-886.

68. Derkach V, Barria A & Soderling TR. (1999). Ca2+/calmodulin-kinase II enhances channel conductance of alpha-amino-3-hydroxy-5-methyl-4-isoxazolepropionate type glutamate receptors. The Proceedings of the National Academy of Sciences of the United States of America **96,** 3269-3274.

69. Dev KK, Nakanishi S & Henley JM. (2004). The PDZ domain of PICK1 differentially accepts protein kinase C-alpha and GluR2 as interacting ligands. Journal of Biological Chemistry **279,** 41393-41397.

70. Dev KK, Nishimune A, Henley JM & Nakanishi S. (1999). The protein kinase C alpha binding protein PICK1 interacts with short but not long form alternative splice variants of AMPA receptor subunits. Neuropharmacology **38,** 635-644.

71. Dingledine R, Borges K, Bowie D & Traynelis SF. (1999). The glutamate receptor ion channels. Pharmacological Reviews **51,** 7-61.

72. Dingledine R, Hume RI & Heinemann SF. (1992). Structural determinants of barium permeation and rectification in non-NMDA glutamate receptor channels. Journal of Neuroscience **12,** 4080-4087.

73. Dobrunz LE & Stevens CF. (1999). Response of hippocampal synapses to natural stimulation patterns. Neuron **22,** 157-166.

74. Dodd J & Jessell TM. (1988). Axon guidance and the patterning of neuronal projections in vertebrates. Science **242,** 692-699.

75. Domenici MR, Berretta N & Cherubini E. (1998). Two distinct forms of long-term depression coexist at the mossy fiber-CA3 synapse in the hippocampus during development. The Proceedings of the National Academy of Sciences of the United States of America **95,** 8310-8315.

76. Donevan SD & Rogawski MA. (1995). Intracellular polyamines mediate inward rectification of Ca(2+)-permeable alpha-amino-3-hydroxy-5-methyl-4-isoxazolepropionic acid receptors. The Proceedings of the National Academy of Sciences of the United States of America **92,** 9298-9302.

77. Dong H, O'Brien RJ, Fung ET, Lanahan AA, Worley PF & Huganir RL. (1997). GRIP: a synaptic PDZ domain-containing protein that interacts with AMPA receptors. Nature **386,** 279-284.

78. Dawson JC, Legg JA & Machesky LM. (2006). Bar domain proteins: a role in tubulation, scission and actin assembly in clathrin-mediated endocytosis. Trends in Cell Biology **16,** 493-498.

79. Dudek FE & Shao LR. (2004). Mossy fiber sprouting and recurrent excitation: direct electrophysiologic evidence and potential implications. Epilepsy Currents **4,** 184-187.

80. Eckenhoff MF & Rakic P. (1988). Nature and fate of proliferative cells in the hippocampal dentate gyrus during the life span of the rhesus monkey. Journal of Neuroscience **8,** 2729-2747.

81. Elliott EM, Malouf AT & Catterall WA. (1995). Role of calcium channel subtypes in calcium transients in hippocampal CA3 neurons. Journal of Neuroscience **15,** 6433-6444.

82. Empson RM & Jefferys JG. (2001). Ca(2+) entry through L-type Ca(2+) channels helps terminate epileptiform activity by activation of a Ca(2+) dependent afterhyperpolarisation in hippocampal CA3. Neuroscience **102,** 297-306.

83. Eybalin M, Caicedo A, Renard N, Ruel J & Puel JL. (2004). Transient Ca2+-permeable AMPA receptors in postnatal rat primary auditory neurons. European Journal of Neuroscience **20,** 2981-2989.

84. Fedele DE, Gouder N, Guttinger M, Gabernet L, Scheurer L, Rulicke T, Crestani F & Boison D. (2005). Astrogliosis in epilepsy leads to overexpression of adenosine kinase, resulting in seizure aggravation. Brain **128,** 2383-2395.

85. Fields RD, Neale EA & Nelson PG. (1990). Effects of patterned electrical activity on neurite outgrowth from mouse sensory neurons. Journal of Neuroscience **10,** 2950-2964.

86. Fraser SE & Perkel DH. (1990). Competitive and positional cues in the patterning of nerve connections. Journal of neurobiology **21,** 51-72.

87. Frotscher M, Jonas P & Sloviter RS. (2006). Synapses formed by normal and abnormal hippocampal mossy fibers. Cell and tissue research **326,** 361-367.

88. Garaschuk O, Hanse E & Konnerth A. (1998). Developmental profile and synaptic origin of early network oscillations in the CA1 region of rat neonatal hippocampus. The Journal of Physiology **507 (Pt 1),** 219-236.

89. Gardner SM, Takamiya K, Xia J, Suh JG, Johnson R, Yu S & Huganir RL. (2005). Calcium-permeable AMPA receptor plasticity is mediated by subunit-specific interactions with PICK1 and NSF. Neuron **45,** 903-915.

90. Garyantes TK & Regehr WG. (1992). Electrical activity increases growth cone calcium but fails to inhibit neurite outgrowth from rat sympathetic neurons. Journal of Neuroscience **12,** 96-103.

91. Gasic GP & Hollmann M. (1992). Molecular neurobiology of glutamate receptors. Annual Review of Physiology **54,** 507-536.

92. Gierer A. (1983). Model for the retino-tectal projection. Proceedings of the Royal Society of London Series B, Containing Papers of a Biological Character **218,** 77-93.

93. Glazewski S, Skangiel-Kramska J & Kossut M. (1993). Development of NMDA receptor-channel complex and L-type calcium channels in mouse hippocampus. Journal of Neuroscience Research **35,** 199-206.

94. Goodman CS & Shatz CJ. (1993). Developmental mechanisms that generate precise patterns of neuronal connectivity. Cell **72 Suppl,** 77-98.

95. Greger IH, Khatri L, Kong X & Ziff EB. (2003). AMPA receptor tetramerization is mediated by Q/R editing. Neuron **40,** 763-774.

96. Greger IH, Khatri L & Ziff EB. (2002). RNA editing at arg607 controls AMPA receptor exit from the endoplasmic reticulum. Neuron **34,** 759-772.

97. Gundersen RW & Barrett JN. (1979). Neuronal chemotaxis: chick dorsal-root axons turn toward high concentrations of nerve growth factor. Science **206,** 1079-1080.

98. Gundersen RW & Barrett JN. (1980). Characterization of the turning response of dorsal root neurites toward nerve growth factor. The Journal of Cell Biology **87,** 546-554.

99. Gyori J, Atzori M & Cherubini E. (1996). Postsynaptic induction of mossy fibre long term depression in developing rat hippocampus. Neuroreport **7,** 1660-1664.

100. Hanley JG & Henley JM. (2005). PICK1 is a calcium-sensor for NMDA-induced AMPA receptor trafficking. The EMBO Journal **24,** 3266-3278.

101. Hanse E, Durand GM, Garaschuk O & Konnerth A. (1997). Activity-dependent wiring of the developing hippocampal neuronal circuit. Seminars in Cell & Developmental Biology **8,** 35-42.

102. Harms KJ, Tovar KR & Craig AM. (2005). Synapse-specific regulation of AMPA receptor subunit composition by activity. Journal of Neuroscience **25,** 6379-6388.

103. Haydon PG, McCobb DP & Kater SB. (1984). Serotonin selectively inhibits growth cone motility and synaptogenesis of specific identified neurons. Science **226,** 561-564.

104. Hell JW, Westenbroek RE, Warner C, Ahlijanian MK, Prystay W, Gilbert MM, Snutch TP & Catterall WA. (1993). Identification and differential subcellular localization of the neuronal class C and class D L-type calcium channel alpha 1 subunits. Journal of Cell Biology **123,** 949-962.

105. Hemond P, Epstein D, Boley A, Migliore M, Ascoli GA & Jaffe DB. (2008). Distinct classes of pyramidal cells exhibit mutually exclusive firing patterns in hippocampal area CA3b. Hippocampus **18,** 411-424

106. Henze DA, Urban NN & Barrionuevo G. (2000). The multifarious hippocampal mossy fiber pathway: a review. Neuroscience **98,** 407-427.

107. Higuchi M, Single FN, Kohler M, Sommer B, Sprengel R & Seeburg PH. (1993). RNA editing of AMPA receptor subunit GluR-B: a base-paired intron-exon structure determines position and efficiency. Cell **75,** 1361-1370.

108. Ho MT, Pelkey KA, Topolnik L, Petralia RS, Takamiya K, Xia J, Huganir RL, Lacaille JC & McBain CJ. (2007). Developmental expression of Ca2+-permeable AMPA receptors underlies depolarization-induced long-term depression at mossy fiber CA3 pyramid synapses. Journal of Neuroscience **27,** 11651-11662.

109. Hollmann M, Hartley M & Heinemann S. (1991). Ca2+ permeability of KA-AMPA--gated glutamate receptor channels depends on subunit composition. Science **252,** 851-853.

110. Hollmann M & Heinemann S. (1994). Cloned glutamate receptors. Annual Review of Neuroscience **17,** 31-108.

111. Hollmann M, O'Shea-Greenfield A, Rogers SW & Heinemann S. (1989). Cloning by functional expression of a member of the glutamate receptor family. Nature **342,** 643-648.

112. Isaac JT. (2003). Postsynaptic silent synapses: evidence and mechanisms. Neuropharmacology **45,** 450-460.

113. Isaac JT, Ashby M & McBain CJ. (2007). The role of the GluR2 subunit in AMPA receptor function and synaptic plasticity. Neuron **54,** 859-871.

114. Isaac JT, Crair MC, Nicoll RA & Malenka RC. (1997). Silent synapses during development of thalamocortical inputs. Neuron **18,** 269-280.

115. Isaac JT, Nicoll RA & Malenka RC. (1995). Evidence for silent synapses: implications for the expression of LTP. Neuron **15,** 427-434.

116. Jia Z, Agopyan N, Miu P, Xiong Z, Henderson J, Gerlai R, Taverna FA, Velumian A, MacDonald J, Carlen P, Abramow-Newerly W & Roder J. (1996). Enhanced LTP in mice deficient in the AMPA receptor GluR2. Neuron **17,** 945-956.

117. Jin W, Ge WP, Xu J, Cao M, Peng L, Yung W, Liao D, Duan S, Zhang M & Xia J. (2006). Lipid binding regulates synaptic targeting of PICK1, AMPA receptor trafficking, and synaptic plasticity. Journal of Neuroscience **26,** 2380-2390.

118. Jonas P, Major G & Sakmann B. (1993). Quantal components of unitary EPSCs at the mossy fibre synapse on CA3 pyramidal cells of rat hippocampus. Journal of Physiology **472,** 615-663.

119. Ju W, Morishita W, Tsui J, Gaietta G, Deerinck TJ, Adams SR, Garner CC, Tsien RY, Ellisman MH & Malenka RC. (2004). Activity-dependent regulation of dendritic synthesis and trafficking of AMPA receptors. Nature Neuroscience **7,** 244-253.

120. Kakegawa W, Tsuzuki K, Yoshida Y, Kameyama K & Ozawa S. (2004). Input- and subunit-specific AMPA receptor trafficking underlying long-term potentiation at hippocampal CA3 synapses. European Journal of Neuroscience **20,** 101-110.

121. Kamboj SK, Swanson GT & Cull-Candy SG. (1995). Intracellular spermine confers rectification on rat calcium-permeable AMPA and kainate receptors. Journal of Physiology **486 (Pt 2),** 297-303.

122. Kamiya H & Ozawa S. (2000). Kainate receptor-mediated presynaptic inhibition at the mouse hippocampal mossy fibre synapse. The Journal of Physiology **523 Pt 3,** 653-665.

123. Kamiya H, Shinozaki H & Yamamoto C. (1996). Activation of metabotropic glutamate receptor type 2/3 suppresses transmission at rat hippocampal mossy fibre synapses. The Journal of Physiology **493 (Pt 2),** 447-455.

124. Kandel ER, Spencer WA & Brinley FJ, Jr. (1960). Transient and long-lasting electrical responses to direct hippocampal stimulation. The American journal of physiology **198,** 687-692.

125. Kapur A, Yeckel MF, Gray R & Johnston D. (1998). L-Type calcium channels are required for one form of hippocampal mossy fiber LTP. Journal of Neurophysiology **79,** 2181-2190.

126. Kasyanov AM, Safiulina VF, Voronin LL & Cherubini E. (2004). GABA-mediated giant depolarizing potentials as coincidence detectors for enhancing synaptic efficacy in the developing hippocampus. Proceedings of the National Academy of Sciences of the United States of America **101,** 3967-3972.

127. Keinanen K, Wisden W, Sommer B, Werner P, Herb A, Verdoorn TA, Sakmann B & Seeburg PH. (1990). A family of AMPA-selective glutamate receptors. Science **249,** 556-560.

128. Kim CH, Chung HJ, Lee HK & Huganir RL. (2001). Interaction of the AMPA receptor subunit GluR2/3 with PDZ domains regulates hippocampal long-term depression. Proceedings of the National Academy of Sciences of the United States of America **98,** 11725-11730.

129. Klausnitzer J & Manahan-Vaughan D. (2008). Frequency facilitation at mossy fiber-CA3 synapses of freely behaving rats is regulated by adenosine A1 receptors. Journal of Neuroscience **28,** 4836-4840.

130. Kobayashi K, Manabe T & Takahashi T. (1996). Presynaptic long-term depression at the hippocampal mossy fiber-CA3 synapse. Science **273,** 648-650.

131. Koh DS, Burnashev N & Jonas P. (1995). Block of native Ca(2+)-permeable AMPA receptors in rat brain by intracellular polyamines generates double rectification. Journal of Physiology **486 (Pt 2),** 305-312.

132. Kott S, Werner M, Korber C & Hollmann M. (2007). Electrophysiological properties of AMPA receptors are differentially modulated depending on the associated member of the TARP family. Journal of Neuroscience **27,** 3780-3789.

133. Kotti T, Riekkinen PJ, Sr. & Miettinen R. (1997). Characterization of target cells for aberrant mossy fiber collaterals in the dentate gyrus of epileptic rat. Experimental Neurology **146,** 323-330.

134. Kumar SS & Huguenard JR. (2001). Properties of excitatory synaptic connections mediated by the corpus callosum in the developing rat neocortex. Journal of Neurophysiology **86,** 2973-2985.

135. Kumar SS, Bacci A, Kharazia V & Huguenard JR. (2002). A developmental switch of AMPA receptor subunits in neocortical pyramidal neurons. Journal of Neuroscience **22,** 3005-3015.

136. Kwon HB & Castillo PE. (2008a). Long-term potentiation selectively expressed by NMDA receptors at hippocampal mossy fiber synapses. Neuron **57,** 108-120.

137. Kwon HB & Castillo PE. (2008b). Role of glutamate autoreceptors at hippocampal mossy fiber synapses. Neuron **60,** 1082-1094.

138. Langdon RB, Johnson JW & Barrionuevo G. (1995). Posttetanic potentiation and presynaptically induced long-term potentiation at the mossy fiber synapse in rat hippocampus. Journal of Neurobiology **26,** 370-385.

139. Lawrence JJ, Grinspan ZM & McBain CJ. (2004). Quantal transmission at mossy fibre targets in the CA3 region of the rat hippocampus. The Journal of Physiology **554,** 175-193.

140. Lei S & McBain CJ. (2002). Distinct NMDA receptors provide differential modes of transmission at mossy fiber-interneuron synapses. Neuron **33,** 921-933.

141. Lei S & McBain CJ. (2004). Two Loci of expression for long-term depression at hippocampal mossy fiber-interneuron synapses. Journal of Neuroscience **24,** 2112-2121.

142. Lei S, Pelkey KA, Topolnik L, Congar P, Lacaille JC & McBain CJ. (2003). Depolarization-induced long-term depression at hippocampal mossy fiber-CA3 pyramidal neuron synapses. Journal of Neuroscience **23,** 9786-9795.

143. Leinekugel X, Medina I, Khalilov I, Ben-Ari Y & Khazipov R. (1997). Ca2+ oscillations mediated by the synergistic excitatory actions of GABA(A) and NMDA receptors in the neonatal hippocampus. Neuron **18,** 243-255.

144. Letourneau PC. (1978). Chemotactic response of nerve fiber elongation to nerve growth factor. Developmental Biology **66,** 183-196.

145. Li P, Kerchner GA, Sala C, Wei F, Huettner JE, Sheng M & Zhuo M. (1999). AMPA receptor-PDZ interactions in facilitation of spinal sensory synapses. Nature Neuroscience **2,** 972-977.

146. Li P & Zhuo M. (1998). Silent glutamatergic synapses and nociception in mammalian spinal cord. Nature **393,** 695-698.

147. Liao D, Hessler NA & Malinow R. (1995). Activation of postsynaptically silent synapses during pairing-induced LTP in CA1 region of hippocampal slice. Nature **375,** 400-404.

148. Liao D, Zhang X, O'Brien R, Ehlers MD & Huganir RL. (1999). Regulation of morphological postsynaptic silent synapses in developing hippocampal neurons. Nature Neuroscience **2,** 37-43.

149. Liu SJ & Cull-Candy SG. (2002). Activity-dependent change in AMPA receptor properties in cerebellar stellate cells. Journal of Neuroscience **22,** 3881-3889.

150. Liu SJ & Cull-Candy SG. (2005). Subunit interaction with PICK and GRIP controls Ca2+ permeability of AMPARs at cerebellar synapses. Nature Neuroscience **8,** 768-775.

151. Liu SQ & Cull-Candy SG. (2000). Synaptic activity at calcium-permeable AMPA receptors induces a switch in receptor subtype. Nature **405,** 454-458.

152. Lombardi R & Riezman H. (2001). Rvs161p and Rvs167p, the two yeast amphiphysin homologs, function together in vivo. Journal of Biological Chemistry **276,** 6016-6022.

153. Lomeli H, Wisden W, Kohler M, Keinanen K, Sommer B & Seeburg PH. (1992). High-affinity kainate and domoate receptors in rat brain. FEBS Letters **307,** 139-143.

154. Lu T & Trussell LO. (2007). Development and elimination of endbulb synapses in the chick cochlear nucleus. Journal of Neuroscience **27,** 808-817.

155. Lumsden AG & Davies AM. (1983). Earliest sensory nerve fibres are guided to peripheral targets by attractants other than nerve growth factor. Nature **306,** 786-788.

156. Lynch M & Sutula T. (2000). Recurrent excitatory connectivity in the dentate gyrus of kindled and kainic acid-treated rats. Journal of Neurophysiology **83,** 693-704.

157. Maccaferri G, Toth K & McBain CJ. (1998). Target-specific expression of presynaptic mossy fiber plasticity. Science **279,** 1368-1370.

158. Mack V, Burnashev N, Kaiser KM, Rozov A, Jensen V, Hvalby O, Seeburg PH, Sakmann B & Sprengel R. (2001). Conditional restoration of hippocampal synaptic potentiation in Glur-A-deficient mice. Science **292,** 2501-2504.

159. Mackie EJ, Tucker RP, Halfter W, Chiquet-Ehrismann R & Epperlein HH. (1988). The distribution of tenascin coincides with pathways of neural crest cell migration. Development (Cambridge, England) **102,** 237-250.

160. Mammen AL, Kameyama K, Roche KW & Huganir RL. (1997). Phosphorylation of the alpha-amino-3-hydroxy-5-methylisoxazole4-propionic acid receptor GluR1 subunit by calcium/calmodulin-dependent kinase II. Journal of Biology Chemistry **272,** 32528-32533.

161. Mansour M, Nagarajan N, Nehring RB, Clements JD & Rosenmund C. (2001). Heteromeric AMPA receptors assemble with a preferred subunit stoichiometry and spatial arrangement. Neuron **32,** 841-853.

162. Matsuda S, Launey T, Mikawa S & Hirai H. (2000). Disruption of AMPA receptor GluR2 clusters following long-term depression induction in cerebellar Purkinje neurons. The EMBO Journal **19,** 2765-2774.

163. Matsuda S, Mikawa S & Hirai H. (1999). Phosphorylation of serine-880 in GluR2 by protein kinase C prevents its C terminus from binding with glutamate receptor-interacting protein. Journal of Neurochemistry **73,** 1765-1768

164. McBain CJ. (2008). Differential mechanisms of transmission and plasticity at mossy fiber synapses. Progress in Brain Research **169,** 225-240.

165. McBain CJ & Dingledine R. (1993). Heterogeneity of synaptic glutamate receptors on CA3 stratum radiatum interneurones of rat hippocampus. The Journal of Physiology **462,** 373-392.

166. McCormack SG, Stornetta RL & Zhu JJ. (2006). Synaptic AMPA receptor exchange maintains bidirectional plasticity. Neuron **50,** 75-88.

167. McMahon LL & Kauer JA. (1997). Hippocampal interneurons express a novel form of synaptic plasticity. Neuron **18,** 295-305.

168. Melcher T, Maas S, Higuchi M, Keller W & Seeburg PH. (1995). Editing of alpha-amino-3-hydroxy-5-methylisoxazole-4-propionic acid receptor GluR-B pre-

mRNA in vitro reveals site-selective adenosine to inosine conversion. Journal of Biological Chemistry **270,** 8566-8570.

169. Meng Y, Zhang Y & Jia Z. (2003). Synaptic transmission and plasticity in the absence of AMPA glutamate receptor GluR2 and GluR3. Neuron **39,** 163-176.

170. Merlin LR & Wong RK. (1993). Synaptic modifications accompanying epileptogenesis in vitro: long-term depression of GABA-mediated inhibition. Brain Research **627,** 330-340.

171. Meyer RL. (1982). Tetrodotoxin blocks the formation of ocular dominance columns in goldfish. Science **218,** 589-591.

172. Migues PV, Cammarota M, Kavanagh J, Atkinson R, Powis DA & Rostas JA. (2007). Maturational changes in the subunit composition of AMPA receptors and the functional consequences of their activation in chicken forebrain. Developmental Neuroscience **29,** 232-240.

173. Miles R & Wong RK. (1983). Single neurones can initiate synchronized population discharge in the hippocampus. Nature **306,** 371-373.

174. Ming G, Henley J, Tessier-Lavigne M, Song H & Poo M. (2001). Electrical activity modulates growth cone guidance by diffusible factors. Neuron **29,** 441-452.

175. Mohajerani MH & Cherubini E. (2006). Role of giant depolarizing potentials in shaping synaptic currents in the developing hippocampus. Critical Reviews in Neurobiology **18,** 13-23.

176. Molnar E, McIlhinney RA, Baude A, Nusser Z & Somogyi P. (1994). Membrane topology of the GluR1 glutamate receptor subunit: epitope mapping by site-directed antipeptide antibodies. Journal of Neurochemistry **63,** 683-693.

177. Molnar P & Nadler JV. (1999). Mossy fiber-granule cell synapses in the normal and epileptic rat dentate gyrus studied with minimal laser photostimulation. Journal of Neurophysiology **82,** 1883-1894.

178. Monaghan DT & Cotman CW. (1985). Distribution of N-methyl-D-aspartate-sensitive L-[3H]glutamate-binding sites in rat brain. Journal of Neuroscience **5,** 2909-2919.

179. Monyer H, Seeburg PH & Wisden W. (1991). Glutamate-operated channels: developmentally early and mature forms arise by alternative splicing. Neuron **6,** 799-810.

180. Moore KA, Nicoll RA & Schmitz D. (2003). Adenosine gates synaptic plasticity at hippocampal mossy fiber synapses. Proceedings of the National Academy of Sciences of the United States of America **100,** 14397-14402.

181. Moore SD, Barr DS & Wilson WA. (1993). Seizure-like activity disrupts LTP in vitro. Neuroscience Letters **163,** 117-119.

182. Moriyoshi K, Masu M, Ishii T, Shigemoto R, Mizuno N & Nakanishi S. (1991). Molecular cloning and characterization of the rat NMDA receptor. Nature **354,** 31-37.

183. Mosbacher J, Schoepfer R, Monyer H, Burnashev N, Seeburg PH & Ruppersberg JP. (1994). A molecular determinant for submillisecond desensitization in glutamate receptors. Science **266,** 1059-1062.

184. Moulder KL, Meeks JP, Shute AA, Hamilton CK, de Erausquin G & Mennerick S. (2004). Plastic elimination of functional glutamate release sites by depolarization. Neuron **42,** 423-435.

185. Mulle C, Sailer A, Perez-Otano I, Dickinson-Anson H, Castillo PE, Bureau I, Maron C, Gage FH, Mann JR, Bettler B & Heinemann SF. (1998). Altered synaptic physiology and reduced susceptibility to kainate-induced seizures in GluR6-deficient mice. Nature **392,** 601-605.

186. Muller T, Moller T, Berger T, Schnitzer J & Kettenmann H. (1992). Calcium entry through kainate receptors and resulting potassium-channel blockade in Bergmann glial cells. Science **256,** 1563-1566.

187. Nagy A, Rossant J, Nagy R, Abramow-Newerly W & Roder JC. (1993). Derivation of completely cell culture-derived mice from early-passage embryonic stem cells. Proceedings of the National Academy of Sciences of the United States of America **90,** 8424-8428.

188. Negrete-Diaz JV, Sihra TS, Delgado-Garcia JM & Rodriguez-Moreno A. (2007). Kainate receptor-mediated presynaptic inhibition converges with presynaptic inhibition mediated by Group II mGluRs and long-term depression at the hippocampal mossy fiber-CA3 synapse. Journal of Neural Transmission **114,** 1425-1431.

189. Nicoll RA & Malenka RC. (1995). Contrasting properties of two forms of long-term potentiation in the hippocampus. Nature **377,** 115-118.

190. Nicoll RA & Schmitz D. (2005). Synaptic plasticity at hippocampal mossy fibre synapses. Nature Reviews **6,** 863-876.

191. Obenaus A, Esclapez M & Houser CR. (1993). Loss of glutamate decarboxylase mRNA-containing neurons in the rat dentate gyrus following pilocarpine-induced seizures. Journal of Neuroscience **13,** 4470-4485.

192. Ogoshi F, Yin HZ, Kuppumbatti Y, Song B, Amindari S & Weiss JH. (2005). Tumor necrosis-factor-alpha (TNF-alpha) induces rapid insertion of Ca2+-permeable alpha-amino-3-hydroxyl-5-methyl-4-isoxazole-propionate (AMPA)/kainate (Ca-A/K) channels in a subset of hippocampal pyramidal neurons. Experimental Neurology **193,** 384-393.

193. Parent JM, Tada E, Fike JR & Lowenstein DH. (1999). Inhibition of dentate granule cell neurogenesis with brain irradiation does not prevent seizure-induced mossy fiber synaptic reorganization in the rat. Journal of Neuroscience **19,** 4508-4519.

194. Parent JM, Yu TW, Leibowitz RT, Geschwind DH, Sloviter RS & Lowenstein DH. (1997). Dentate granule cell neurogenesis is increased by seizures and contributes to aberrant network reorganization in the adult rat hippocampus. Journal of Neuroscience **17,** 3727-3738.

195. Paternain AV, Herrera MT, Nieto MA & Lerma J. (2000). GluR5 and GluR6 kainate receptor subunits coexist in hippocampal neurons and coassemble to form functional receptors. J Neurosci **20,** 196-205.

196. Pelkey KA, Lavezzari G, Racca C, Roche KW & McBain CJ. (2005). mGluR7 is a metaplastic switch controlling bidirectional plasticity of feedforward inhibition. Neuron **46,** 89-102.

197. Pelkey KA & McBain CJ. (2008). Target-cell-dependent plasticity within the mossy fibre-CA3 circuit reveals compartmentalized regulation of presynaptic function at divergent release sites. The Journal of physiology **586,** 1495-1502.

198. Pelkey KA, Topolnik L, Lacaille JC & McBain CJ. (2006). Compartmentalized Ca(2+) channel regulation at divergent mossy-fiber release sites underlies target cell-dependent plasticity. Neuron **52,** 497-510.

199. Pellegrini-Giampietro DE, Bennett MV & Zukin RS. (1992a). Are Ca(2+)-permeable kainate/AMPA receptors more abundant in immature brain? Neuroscience Letters **144,** 65-69.

200. Pellegrini-Giampietro DE, Zukin RS, Bennett MV, Cho S & Pulsinelli WA. (1992b). Switch in glutamate receptor subunit gene expression in CA1 subfield of hippocampus following global ischemia in rats. Proceedings of the National Academy of Sciences of the United States of America **89,** 10499-10503.

201. Peter BJ, Kent HM, Mills IG, Vallis Y, Butler PJ, Evans PR & McMahon HT. (2004). BAR domains as sensors of membrane curvature: the amphiphysin BAR structure. Science **303,** 495-499.

202. Petralia RS, Esteban JA, Wang YX, Partridge JG, Zhao HM, Wenthold RJ & Malinow R. (1999). Selective acquisition of AMPA receptors over postnatal development suggests a molecular basis for silent synapses. Nature Neuroscience **2,** 31-36.

203. Petralia RS & Wenthold RJ. (1992). Light and electron immunocytochemical localization of AMPA-selective glutamate receptors in the rat brain. The Journal of Comparative Neurology **318,** 329-354.

204. Petralia RS & Wenthold RJ. (1999). Immunocytochemistry of NMDA receptors. Methods in Molecular Biology **128,** 73-92.

205. Pickard L, Noel J, Henley JM, Collingridge GL & Molnar E. (2000). Developmental changes in synaptic AMPA and NMDA receptor distribution and AMPA receptor subunit composition in living hippocampal neurons. Journal of Neuroscience **20,** 7922-7931.

206. Pinheiro PS, Perrais D, Coussen F, Barhanin J, Bettler B, Mann JR, Malva JO, Heinemann SF & Mulle C. (2007). GluR7 is an essential subunit of presynaptic kainate autoreceptors at hippocampal mossy fiber synapses. Proceedings of the National Academy of Sciences of the United States of America **104,** 12181-12186.

207. Plant K, Pelkey KA, Bortolotto ZA, Morita D, Terashima A, McBain CJ, Collingridge GL & Isaac JT. (2006). Transient incorporation of native GluR2-lacking AMPA receptors during hippocampal long-term potentiation. Nature Neuroscience **9,** 602-604.

208. Poncer JC. (2003). Hippocampal long term potentiation: silent synapses and beyond. Journal of Physiology, Paris **97,** 415-422.

209. Priel A, Kolleker A, Ayalon G, Gillor M, Osten P & Stern-Bach Y. (2005). Stargazin reduces desensitization and slows deactivation of the AMPA-type glutamate receptors. Journal of Neuroscience **25,** 2682-2686.

210. Prince DA & Connors BW. (1986). Mechanisms of interictal epileptogenesis. Advances in Neurology **44,** 275-299.

211. Raymond CR & Redman SJ. (2002). Different calcium sources are narrowly tuned to the induction of different forms of LTP. Journal of Neurophysiology **88,** 249-255.

212. Rebola N, Lujan R, Cunha RA & Mulle C. (2008). Adenosine A2A receptors are essential for long-term potentiation of NMDA-EPSCs at hippocampal mossy fiber synapses. Neuron **57,** 121-134.

213. Regehr WG, Delaney KR & Tank DW. (1994). The role of presynaptic calcium in short-term enhancement at the hippocampal mossy fiber synapse. Journal of Neuroscience **14,** 523-537.

214. Reid CA, Dixon DB, Takahashi M, Bliss TV & Fine A. (2004). Optical quantal analysis indicates that long-term potentiation at single hippocampal mossy fiber synapses is expressed through increased release probability, recruitment of new release sites, and activation of silent synapses. Journal of Neuroscience **24,** 3618-3626.

215. Reid CA, Fabian-Fine R & Fine A. (2001). Postsynaptic calcium transients evoked by activation of individual hippocampal mossy fiber synapses. Journal of Neuroscience **21,** 2206-2214.

216. Represa A, Tremblay E & Ben-Ari Y. (1987). Kainate binding sites in the hippocampal mossy fibers: localization and plasticity. Neuroscience **20,** 739-748.

217. Riccio RV & Matthews MA. (1985). The postnatal development of the rat primary visual cortex during optic nerve impulse blockade by intraocular tetrodotoxin: a quantitative electron microscopic analysis. Brain Research **352,** 55-68.

218. Rivera C, Voipio J, Payne JA, Ruusuvuori E, Lahtinen H, Lamsa K, Pirvola U, Saarma M & Kaila K. (1999). The K+/Cl- co-transporter KCC2 renders GABA hyperpolarizing during neuronal maturation. Nature **397,** 251-255.

219. Roche KW, O'Brien RJ, Mammen AL, Bernhardt J & Huganir RL. (1996). Characterization of multiple phosphorylation sites on the AMPA receptor GluR1 subunit. Neuron **16,** 1179-1188.

220. Rogers SL, Letourneau PC, Palm SL, McCarthy J & Furcht LT. (1983). Neurite extension by peripheral and central nervous system neurons in response to substratum-bound fibronectin and laminin. Developmental Biology **98,** 212-220.

221. Rosenmund C, Stern-Bach Y & Stevens CF. (1998). The tetrameric structure of a glutamate receptor channel. Science **280,** 1596-1599.

222. Rouach N, Byrd K, Petralia RS, Elias GM, Adesnik H, Tomita S, Karimzadegan S, Kealey C, Bredt DS & Nicoll RA. (2005). TARP gamma-8 controls hippocampal AMPA receptor number, distribution and synaptic plasticity. Nature Neuroscience **8,** 1525-1533.

223. Rozov A & Burnashev N. (1999). Polyamine-dependent facilitation of postsynaptic AMPA receptors counteracts paired-pulse depression. Nature **401,** 594-598.

224. Rozov A, Zilberter Y, Wollmuth LP & Burnashev N. (1998). Facilitation of currents through rat Ca2+-permeable AMPA receptor channels by activity-dependent relief from polyamine block. Journal of Physiology **511 (Pt 2),** 361-377.

225. Rueter SM, Burns CM, Coode SA, Mookherjee P & Emeson RB. (1995). Glutamate receptor RNA editing in vitro by enzymatic conversion of adenosine to inosine. Science **267,** 1491-1494.

226. Sanes JR & Lichtman JW. (1999). Development of the vertebrate neuromuscular junction. Annual Review of Neuroscience **22,** 389-442.

227. Salin PA, Scanziani M, Malenka RC & Nicoll RA. (1996). Distinct short-term plasticity at two excitatory synapses in the hippocampus. Proceedings of the National Academy of Sciences of the United States of America **93,** 13304-13309.

228. Sattler R & Tymianski M. (2000). Molecular mechanisms of calcium-dependent excitotoxicity. Journal of Molecular Medicine (Berlin, Germany) **78,** 3-13.

229. Scharfman HE, Sollas AL, Berger RE & Goodman JH. (2003). Electrophysiological evidence of monosynaptic excitatory transmission between granule cells after seizure-induced mossy fiber sprouting. Journal of Neurophysiology **90,** 2536-2547.

230. Schmidt JT. (1985a). Formation of retinotopic connections: selective stabilization by an activity-dependent mechanism. Cellular and Molecular Neurobiology **5,** 65-84.

231. Schmidt JT. (1985b). Selective stabilization of retinotectal synapses by an activity-dependent mechanism. Federation Proceedings **44,** 2767-2772.

232. Schmitz D, Mellor J, Breustedt J & Nicoll RA. (2003). Presynaptic kainate receptors impart an associative property to hippocampal mossy fiber long-term potentiation. Nature Neuroscience **6,** 1058-1063.

233. Schneiderman JH, Sterling CA & Luo R. (1994). Hippocampal plasticity following epileptiform bursting produced by GABAA antagonists. Neuroscience **59,** 259-273.

234. Schoch S, Castillo PE, Jo T, Mukherjee K, Geppert M, Wang Y, Schmitz F, Malenka RC & Sudhof TC. (2002). RIM1alpha forms a protein scaffold for regulating neurotransmitter release at the active zone. Nature **415,** 321-326.

235. Schwartzkroin PA & Prince DA. (1977). Penicillin-induced epileptiform activity in the hippocampal in vitro prepatation. Annals of Neurology **1,** 463-469.

236. Seeburg PH. (1996). The role of RNA editing in controlling glutamate receptor channel properties. Journal of Neurochemistry **66,** 1-5.

237. Seeburg PH, Higuchi M & Sprengel R. (1998). RNA editing of brain glutamate receptor channels: mechanism and physiology. Brain Research Review **26,** 217-229.

238. Seki T & Arai Y. (1993). Highly polysialylated neural cell adhesion molecule (NCAM-H) is expressed by newly generated granule cells in the dentate gyrus of the adult rat. Journal of Neuroscience **13,** 2351-2358.

239. Shin J, Shen F & Huguenard JR. (2005). Polyamines modulate AMPA receptor-dependent synaptic responses in immature layer v pyramidal neurons. Journal of Neurophysiology **93,** 2634-2643.

240. Siegel SJ, Brose N, Janssen WG, Gasic GP, Jahn R, Heinemann SF & Morrison JH. (1994). Regional, cellular, and ultrastructural distribution of N-methyl-D-aspartate receptor subunit 1 in monkey hippocampus. Proceedings of the National Academy of Sciences of the United States of America **91,** 564-568.

241. Sipila ST, Huttu K, Soltesz I, Voipio J & Kaila K. (2005). Depolarizing GABA acts on intrinsically bursting pyramidal neurons to drive giant depolarizing potentials in the immature hippocampus. Journal of Neuroscience **25,** 5280-5289.

242. Sivakumaran S, Mohajerani MH & Cherubini E. (2009). At immature mossy-fiber-CA3 synapses, correlated presynaptic and postsynaptic activity persistently enhances GABA release and network excitability via BDNF and cAMP-dependent PKA. Journal of Neuroscience **29,** 2637-2647.

243. Smith KL & Swann JW. (1999). Long-term depression of perforant path excitatory postsynaptic potentials following synchronous network bursting in area CA3 of immature hippocampus. Neuroscience **89,** 625-630.

244. Smith KL, Szarowski DH, Turner JN & Swann JW. (1995). Diverse neuronal populations mediate local circuit excitation in area CA3 of developing hippocampus. Journal of Neurophysiology **74,** 650-672.

245. Sommer B, Keinanen K, Verdoorn TA, Wisden W, Burnashev N, Herb A, Kohler M, Takagi T, Sakmann B & Seeburg PH. (1990). Flip and flop: a cell-specific functional switch in glutamate-operated channels of the CNS. Science **249,** 1580-1585.

246. Sommer B, Kohler M, Sprengel R & Seeburg PH. (1991). RNA editing in brain controls a determinant of ion flow in glutamate-gated channels. Cell **67,** 11-19.

247. Sossa KG, Court BL & Carroll RC. (2006). NMDA receptors mediate calcium-dependent, bidirectional changes in dendritic PICK1 clustering. Molecular and Cellular Neurosciences **31,** 574-585.

248. Soto D, Coombs ID, Kelly L, Farrant M & Cull-Candy SG. (2007). Stargazin attenuates intracellular polyamine block of calcium-permeable AMPA receptors. Nature Neuroscience **10,** 1260-1267.

249. Sperry RW. (1963). Chemoaffinity in the Orderly Growth of Nerve Fiber Patterns and Connections. Proceedings of the National Academy of Sciences of the United States of America **50,** 703-710.

250. Spruston N, Jonas P & Sakmann B. (1995). Dendritic glutamate receptor channels in rat hippocampal CA3 and CA1 pyramidal neurons. The Journal of Physiology **482 (Pt 2),** 325-352.

251. Srivastava S, Osten P, Vilim FS, Khatri L, Inman G, States B, Daly C, DeSouza S, Abagyan R, Valtschanoff JG, Weinberg RJ & Ziff EB. (1998). Novel anchorage of GluR2/3 to the postsynaptic density by the AMPA receptor-binding protein ABP. Neuron **21,** 581-591.

252. Staley K, Smith R, Schaack J, Wilcox C & Jentsch TJ. (1996). Alteration of GABAA receptor function following gene transfer of the CLC-2 chloride channel. Neuron **17,** 543-551.

253. Staley K, Smith R, Schaack J, Wilcox C & Jentsch TJ. (1996). Alteration of GABAA receptor function following gene transfer of the CLC-2 chloride channel. Neuron **17,** 543-551.

254. Stanfield BB & Trice JE. (1988). Evidence that granule cells generated in the dentate gyrus of adult rats extend axonal projections. Experimental Brain Research Experimentelle Hirnforschung **72,** 399-406.

255. Staudinger J, Lu J & Olson EN. (1997). Specific interaction of the PDZ domain protein PICK1 with the COOH terminus of protein kinase C-alpha. Journal of Biological Chemistry **272,** 32019-32024.

256. Staudinger J, Zhou J, Burgess R, Elledge SJ & Olson EN. (1995). PICK1: a perinuclear binding protein and substrate for protein kinase C isolated by the yeast two-hybrid system. The Journal of Cell Biology **128,** 263-271.

257. Steinberg JP, Takamiya K, Shen Y, Xia J, Rubio ME, Yu S, Jin W, Thomas GM, Linden DJ & Huganir RL. (2006). Targeted in vivo mutations of the AMPA receptor subunit GluR2 and its interacting protein PICK1 eliminate cerebellar long-term depression. Neuron **49,** 845-860.

258. Stoop R, Conquet F, Zuber B, Voronin LL & Pralong E. (2003). Activation of metabotropic glutamate 5 and NMDA receptors underlies the induction of persistent bursting and associated long-lasting changes in CA3 recurrent connections. Journal of Neuroscience **23,** 5634-5644.

259. Straub H, Hohling JM, Kohling R, Lucke A, Tuxhorn I, Ebner A, Wolf P, Pannek H, Oppel F & Speckmann EJ. (2000). Effects of nifedipine on rhythmic synchronous activity of human neocortical slices. Neuroscience **100,** 445-452.

260. Sugihara H, Moriyoshi K, Ishii T, Masu M & Nakanishi S. (1992). Structures and properties of seven isoforms of the NMDA receptor generated by alternative splicing. Biochemical and biophysical research communications **185,** 826-832.

261. Sutton MA, Ito HT, Cressy P, Kempf C, Woo JC & Schuman EM. (2006). Miniature neurotransmission stabilizes synaptic function via tonic suppression of local dendritic protein synthesis. Cell **125,** 785-799.

262. Sutula T. (2002). Seizure-Induced Axonal Sprouting: Assessing Connections Between Injury, Local Circuits, and Epileptogenesis. Epilepsy Currents **2,** 86-91.

263. Sutton MA, Ito HT, Cressy P, Kempf C, Woo JC & Schuman EM. (2006). Miniature neurotransmission stabilizes synaptic function via tonic suppression of local dendritic protein synthesis. Cell **125,** 785-799.

264. Sutula T, Cascino G, Cavazos J, Parada I & Ramirez L. (1989). Mossy fiber synaptic reorganization in the epileptic human temporal lobe. Annals of Neurology **26,** 321-330.

265. Swann JW, Smith KL & Brady RJ. (1993). Localized excitatory synaptic interactions mediate the sustained depolarization of electrographic seizures in developing hippocampus. Journal of Neuroscience **13,** 4680-4689.

266. Tauck DL & Nadler JV. (1985). Evidence of functional mossy fiber sprouting in hippocampal formation of kainic acid-treated rats. Journal of Neuroscience **5,** 1016-1022.

267. Tanabe Y, Masu M, Ishii T, Shigemoto R & Nakanishi S. (1992). A family of metabotropic glutamate receptors. Neuron **8,** 169-179.

268. Tauck DL & Nadler JV. (1985). Evidence of functional mossy fiber sprouting in hippocampal formation of kainic acid-treated rats. Journal of Neuroscience **5,** 1016-1022.

269. Tessier-Lavigne M, Placzek M, Lumsden AG, Dodd J & Jessell TM. (1988). Chemotropic guidance of developing axons in the mammalian central nervous system. Nature **336,** 775-778.

270. Terashima A, Cotton L, Dev KK, Meyer G, Zaman S, Duprat F, Henley JM, Collingridge GL & Isaac JT. (2004). Regulation of synaptic strength and AMPA receptor subunit composition by PICK1. Journal of Neuroscience **24,** 5381-5390.

271. Thiagarajan TC, Lindskog M & Tsien RW. (2005). Adaptation to synaptic inactivity in hippocampal neurons. Neuron **47,** 725-737.

272. Tomita S, Adesnik H, Sekiguchi M, Zhang W, Wada K, Howe JR, Nicoll RA & Bredt DS. (2005). Stargazin modulates AMPA receptor gating and trafficking by distinct domains. Nature **435,** 1052-1058.

273. Tomita S, Chen L, Kawasaki Y, Petralia RS, Wenthold RJ, Nicoll RA & Bredt DS. (2003). Functional studies and distribution define a family of transmembrane AMPA receptor regulatory proteins. The Journal of Cell Biology **161,** 805-816.

274. Toni N, Laplagne DA, Zhao C, Lombardi G, Ribak CE, Gage FH & Schinder AF. (2008). Neurons born in the adult dentate gyrus form functional synapses with target cells. Nature Neuroscience **11,** 901-907.

275. Topolnik L, Congar P & Lacaille JC. (2005). Differential regulation of metabotropic glutamate receptor- and AMPA receptor-mediated dendritic Ca2+ signals by presynaptic and postsynaptic activity in hippocampal interneurons. Journal of Neuroscience **25,** 990-1001.

276. Toth K & McBain CJ. (1998). Afferent-specific innervation of two distinct AMPA receptor subtypes on single hippocampal interneurons. Nature Neuroscience **1,** 572-578.

277. Toth K & McBain CJ. (2000). Target-specific expression of pre- and postsynaptic mechanisms. The Journal of Physiology **525 Pt 1,** 41-51.

278. Toth K, Suares G, Lawrence JJ, Philips-Tansey E & McBain CJ. (2000). Differential mechanisms of transmission at three types of mossy fiber synapse. Journal of Neuroscience **20,** 8279-8289.

279. Traub RD & Wong RK. (1982). Cellular mechanism of neuronal synchronization in epilepsy. Science **216,** 745-747.

280. Traynelis SF & Dingledine R. (1988). Potassium-induced spontaneous electrographic seizures in the rat hippocampal slice. Journal of Neurophysiology **59,** 259-276.

281. Tsuzuki K, Isa T & Ozawa S. (2000). Subunit composition of AMPA receptors expressed by single hippocampal neurons. Neuroreport **11,** 3583-3587.

282. Tzounopoulos T, Janz R, Sudhof TC, Nicoll RA & Malenka RC. (1998). A role for cAMP in long-term depression at hippocampal mossy fiber synapses. Neuron **21,** 837-845.

283. Urban NN & Barrionuevo G. (1996). Induction of hebbian and non-hebbian mossy fiber long-term potentiation by distinct patterns of high-frequency stimulation. Journal of Neuroscience **16,** 4293-4299.

284. Verdoorn TA, Burnashev N, Monyer H, Seeburg PH & Sakmann B. (1991). Structural determinants of ion flow through recombinant glutamate receptor channels. Science **252,** 1715-1718.

285. Vignes M, Clarke VR, Parry MJ, Bleakman D, Lodge D, Ornstein PL & Collingridge GL. (1998). The GluR5 subtype of kainate receptor regulates excitatory synaptic transmission in areas CA1 and CA3 of the rat hippocampus. Neuropharmacology **37,** 1269-1277.

286. Vignes M & Collingridge GL. (1997). The synaptic activation of kainate receptors. Nature **388,** 179-182.

287. Wallace DJ, Zum Alten Borgloh SM, Astori S, Yang Y, Bausen M, Kugler S, Palmer AE, Tsien RY, Sprengel R, Kerr JN, Denk W & Hasan MT. (2008). Single-spike detection in vitro and in vivo with a genetic Ca(2+) sensor. Nature Methods **5,** 797-804.

288. Walter J, Kern-Veits B, Huf J, Stolze B & Bonhoeffer F. (1987). Recognition of position-specific properties of tectal cell membranes by retinal axons in vitro. Development (Cambridge, England) **101,** 685-696.

289. Washburn MS, Numberger M, Zhang S & Dingledine R. (1997). Differential dependence on GluR2 expression of three characteristic features of AMPA receptors. Journal of Neuroscience **17,** 9393-9406.

290. Watanabe M, Fukaya M, Sakimura K, Manabe T, Mishina M & Inoue Y. (1998). Selective scarcity of NMDA receptor channel subunits in the stratum lucidum (mossy fibre-recipient layer) of the mouse hippocampal CA3 subfield. The European Journal of Neuroscience **10,** 478-487.

291. Weisskopf MG, Castillo PE, Zalutsky RA & Nicoll RA. (1994). Mediation of hippocampal mossy fiber long-term potentiation by cyclic AMP. Science **265,** 1878-1882.

292. Wenthold RJ, Petralia RS, Blahos J, II & Niedzielski AS. (1996). Evidence for multiple AMPA receptor complexes in hippocampal CA1/CA2 neurons. Journal of Neuroscience **16,** 1982-1989.

293. Westenbroek RE, Ahlijanian MK & Catterall WA. (1990). Clustering of L-type Ca2+ channels at the base of major dendrites in hippocampal pyramidal neurons. Nature **347,** 281-284.

294. Wiesel TN & Hubel DH. (1974). Ordered arrangement of orientation columns in monkeys lacking visual experience. The Journal of Comparative Neurology **158,** 307-318.

295. Williams S & Johnston D. (1989). Long-term potentiation of hippocampal mossy fiber synapses is blocked by postsynaptic injection of calcium chelators. Neuron **3,** 583-588.

296. Wong RK & Prince DA. (1978). Participation of calcium spikes during intrinsic burst firing in hippocampal neurons. Brain Research **159,** 385-390.

297. Wong RK & Traub RD. (1983). Synchronized burst discharge in disinhibited hippocampal slice. I. Initiation in CA2-CA3 region. Journal of Neurophysiology **49,** 442-458.

298. Wu J & Fisher RS. (2000). Hyperthermic spreading depressions in the immature rat hippocampal slice. Journal of Neurophysiology **84,** 1355-1360.

299. Wyszynski M, Kim E, Yang FC & Sheng M. (1998). Biochemical and immunocytochemical characterization of GRIP, a putative AMPA receptor anchoring protein, in rat brain. Neuropharmacology **37,** 1335-1344.

300. Xia J, Chung HJ, Wihler C, Huganir RL & Linden DJ. (2000). Cerebellar long-term depression requires PKC-regulated interactions between GluR2/3 and PDZ domain-containing proteins. Neuron **28,** 499-510.

301. Xia J, Zhang X, Staudinger J & Huganir RL. (1999). Clustering of AMPA receptors by the synaptic PDZ domain-containing protein PICK1. Neuron **22,** 179-187.

302. Xiang Z, Greenwood AC, Kairiss EW & Brown TH. (1994). Quantal mechanism of long-term potentiation in hippocampal mossy-fiber synapses. Journal of Neurophysiology **71,** 2552-2556.

303. Xie ZP & Poo MM. (1986). Initial events in the formation of neuromuscular synapse: rapid induction of acetylcholine release from embryonic neuron. Proceedings of the National Academy of Sciences of the United States of America **83,** 7069-7073.

304. Xu J & Xia J. (2006). Structure and function of PICK1. Neuro-Signals **15,** 190-201.

305. Yaari Y, Konnerth A & Heinemann U. (1986). Nonsynaptic epileptogenesis in the mammalian hippocampus in vitro. II. Role of extracellular potassium. Journal of Neurophysiology **56,** 424-438.

306. Yamada J, Okabe A, Toyoda H, Kilb W, Luhmann HJ & Fukuda A. (2004). Cl- uptake promoting depolarizing GABA actions in immature rat neocortical neurones is mediated by NKCC1. The Journal of Physiology **557,** 829-841.

307. Yamamoto C, Sawada S & Takada S. (1983). Suppressing action of 2-amino-4-phosphonobutyric acid on mossy fiber-induced excitation in the guinea pig hippocampus. Experimental Brain Research Experimentelle Hirnforschung **51,** 128-134.

308. Yang JH, Sklar P, Axel R & Maniatis T. (1995). Editing of glutamate receptor subunit B pre-mRNA in vitro by site-specific deamination of adenosine. Nature **374,** 77-81.

309. Yeckel MF, Kapur A & Johnston D. (1999). Multiple forms of LTP in hippocampal CA3 neurons use a common postsynaptic mechanism. *Nat Neurosci* **2,** 625-633.

310. Yeckel MF & Berger TW. (1990). Feedforward excitation of the hippocampus by afferents from the entorhinal cortex: redefinition of the role of the trisynaptic pathway. Proceedings of the National Academy of Sciences of the United States of America **87,** 5832-5836.

311. Yokoi M, Kobayashi K, Manabe T, Takahashi T, Sakaguchi I, Katsuura G, Shigemoto R, Ohishi H, Nomura S, Nakamura K, Nakao K, Katsuki M & Nakanishi S. (1996). Impairment of hippocampal mossy fiber LTD in mice lacking mGluR2. Science **273,** 645-647.

312. Yuen EY, Gu Z & Yan Z. (2007a). Calpain regulation of AMPA receptor channels in cortical pyramidal neurons. Journal of Physiology **580,** 241-254.

313. Yuen EY, Liu W & Yan Z. (2007b). The phosphorylation state of GluR1 subunits determines the susceptibility of AMPA receptors to calpain cleavage. Journal of Biological Chemistry **282,** 16434-16440.

314. Zalutsky RA & Nicoll RA. (1991). Comparison of two forms of long-term potentiation in single hippocampus neurons. Correction. Science **251,** 856.

315. Zamanillo D, Sprengel R, Hvalby O, Jensen V, Burnashev N, Rozov A, Kaiser KM, Koster HJ, Borchardt T, Worley P, Lubke J, Frotscher M, Kelly PH, Sommer B, Andersen P, Seeburg PH & Sakmann B. (1999). Importance of AMPA receptors for hippocampal synaptic plasticity but not for spatial learning. Science **284,** 1805-1811.

316. Zhu JJ, Esteban JA, Hayashi Y & Malinow R. (2000). Postnatal synaptic potentiation: delivery of GluR4-containing AMPA receptors by spontaneous activity. Nature Neuroscience **3,** 1098-1106.

317. Zucker RS. (1989). Short-term synaptic plasticity. Annual Review of Neuroscience **12,** 13-31.